Improved Methods for Gridding, Stochastic Modeling, and Compact Characterization of Terrain Surfaces

Jacob N. Lambeth

Thesis submitted to the faculty of the Virginia Polytechnic Institute and State University in partial fulfillment of the requirements for the degree of

Master of Science

In

Mechanical Engineering

John B. Ferris

Saied Taheri

Tana Tjhung

April 20, 2013

Blacksburg, VA

Keywords: Terrain, Surfaces, Gridding, Modeling, Characterization, Markov Chains

Improved Methods for Gridding, Stochastic Modeling, and Compact Characterization of Terrain Surfaces

Jacob N. Lambeth

Abstract

Accurate terrain models provide the chassis designer with a powerful tool to make informed design decisions early in the design process. During this stage, engineers are challenged with predicting vehicle loads through modeling and simulation. The accuracy of these simulation results depends not only on the fidelity of the model, but also on the excitation to the model. It is clear that the terrain is the main excitation to the vehicle [1]. The inputs to these models are often based directly on physical measurements (terrain profiles); therefore, the terrain measurements must be as accurate as possible. A collection of novel methods can be developed to aid in the study and application of 3D terrain measurements, which are dense and non-uniform, including efficient gridding, stochastic modeling, and compact characterization.

Terrain measurements are not collected with uniform spacing, which is necessary for efficient data storage and simulation. Many techniques are developed to help effectively grid dense terrain point clouds in a curved regular grid (CRG) format, including center and random vehicle paths, sorted gridding methods, and software implementation. In addition, it is beneficial to characterize the terrain as a realization of an underlying stochastic process and to develop a mathematical model of that process. A method is developed to represent a continuous-state Markov chain as a collection of univariate distributions, to be applied to terrain road profiles. The resulting form is extremely customizable and significantly more compact than a discrete-state Markov chain, yet it still provides a viable alternative for stochastically modeling terrain. Many new simulation techniques take advantage of 3D gridded roads along with traditional 2D terrain profiles. A technique is developed to model and synthesize 3D terrain surfaces by applying a variety of 2D stochastic models to the topological components of terrain, which are also decomposed into frequency bandwidths and down-sampled. The quality of the synthetic surface is determined using many statistical tests, and the entire work is implemented into a powerful software suite. Engineers from many disciplines who work with terrain surfaces need to describe the overall physical characteristics compactly and consistently. A method is developed to characterize terrain surfaces with a few coefficients by performing a principal component analysis, via singular value decomposition (SVD), to the parameter sets that define a collection of surface models.

Acknowledgements

I would like to thank my advisor and committee-chair, Dr. John Ferris, for continuous support and insight throughout my research in the Vehicle Terrain Performance Lab. By always challenging me to perform at my best, I have gained more knowledge and skills than I could have anticipated. I would also like to thank Dr. Tana Tjhung and Dr. Saied Taheri for providing great feedback with respect to this thesis and my research as a whole.

This research would not have been possible without the generous sponsorships of TARDEC and Chrysler. I am very grateful for the opportunity to work on each project.

Lastly, I would like to thank my family and friends for their support throughout my time at Virginia Tech.

Table of Contents

List of Figures

List of Tables

Chapter 1. Introduction

Accurate terrain models provide the chassis designer with a powerful tool to make informed design decisions early in the design process. During this stage, engineers are challenged with predicting vehicle loads through modeling and simulation. The accuracy of these simulation results depends not only on the fidelity of the model, but also on the excitation to the model. It is clear that the terrain is the main excitation to the vehicle [1]. These models are often based directly on physical measurements; therefore, the terrain measurements must be as accurate as possible.

Terrain measurement systems, such as the Vehicle Terrain Measurement System (VTMS), developed by the Vehicle Terrain Performance Laboratory (VTPL), are an enabling technology, creating a new level of fidelity and resolution in terrain measurement. However, these terrain measurements are not collected with regular spacing, which is necessary for efficient data storage and simulation. It is therefore common practice to grid this dense, non-uniform data. The process of accurately gridding the data requires extensive search algorithms that can be computationally inefficient. The grid is also largely dependent on a coordinate transformation known as a Curved Regular Grid (CRG), where the grid is defined relative to a path in the horizontal plane (typically taken to be the center of the road).

Once the data have been gridded, the relevant terrain points used for simulations can quickly be extracted from the data. Depending on the simulation type, this may be one 2D profile, a 3D wheel-path strip, or the entire 3D grid. Regardless of the format of the terrain data used for simulation, it is beneficial to characterize the terrain as a realization of an underlying stochastic process and to develop a mathematical model of that process (e.g., an autoregressive model or a Markov chain). The model would be parameterized to best fit the measured terrain, preferably with a few parameters. The values for each of the parameters would then indicate the type of terrain being modeled. The resulting stochastic model could then be used to generate as much synthetic terrain of that terrain type as required.

The advantage to using synthetic terrain with the same physical properties as the original measured terrain is that some variation in the simulation results can be achieved. Consider a simple example in which a vehicle/tire model is simulated over some measured terrain and the peak load is identified. Each time that vehicle/tire is simulated on that same measured section of road the exact same peak load will be calculated. Using different realizations of the stochastic model (different synthetic terrain) the variation in the peak load can be simulated, so that, for example, the variation in the range of possible peak loads can be estimated.

In addition to having the ability to create unique, synthetic terrain, engineers from many disciplines who work with terrain surfaces need to describe the overall physical characteristics compactly and consistently. Well established scalar characteristics, such as International Roughness Index (IRI) and Root-Mean-Square (RMS), are the most compact representation,

providing insight into the surface character, but limited because they are a single number and do not provide a means by which synthetic surfaces with the same statistical properties can be generated. Alternatively, surfaces can be represented precisely by mathematical models defined by many parameters. Greater insight is gained and synthetic surfaces can be generated, but the representation is not compact.

Thesis Statement:

A collection of novel methods can be developed to aid in the study and application of 3D terrain measurements, which are dense and non-uniform, including efficient gridding, stochastic modeling, and compact characterization.

Scope of Thesis

This work focuses on measured terrain, primarily taken from a 3D terrain measurement system. The terrain is assumed to be non-deformable and anisotropic in nature. For example, open fields, beaches, mud, or soft soil measurements are outside the scope. This work, however, can be applied to paved asphalt and concrete roads, gravel roads, or rough trails. Any modeling, synthesis, or characterization is performed on terrain that has been gridded using the techniques discussed in Chapter 2. The necessary modeling and decompositions cannot be applied to the original, non-uniform, point cloud.

Contributions

The main contributions of this thesis are:

1) Multiple techniques to effectively and efficiently grid 3D terrain, including automatic center and alternate (random) vehicle path generation, application of sorted gridding methods, and software implementation.
2) A process to create a compact continuous-state Markov chain to be applied to terrain road profiles.
3) Methods to model and synthesize 3D terrain, determine the quality of a synthetic surface, and a software package to explore 3D terrain modeling.
4) A technique to characterize 3D terrain with only a few coefficients.

This thesis is organized as follows. Chapter 2 develops many techniques to help effectively grid dense terrain point clouds in a Curved Regular Grid (CRG) format, including center and random vehicle paths, sorted gridding methods, and software implementation. Chapter 3 develops a process to represent a continuous-state Markov chain as a collection of univariate distributions, to be applied to various components of terrain. The resulting form is extremely customizable and significantly more compact than a discrete-state Markov chain, yet it still provides a viable alternative for stochastically modeling terrain. A technique to model and

synthesize 3D terrain surfaces by applying a variety of 2D stochastic models to the topological components of terrain, which are also decomposed into frequency bandwidths and down-sampled is developed in Chapter 4. The quality of the synthetic surface is determined using many statistical tests, and the entire work is implemented into a powerful software suite. Next a method to characterize terrain surfaces in a compact form by performing a principal component analysis, via singular value decomposition (SVD), to the parameter sets that define a collection of surface models. The primary conclusions of this thesis are then presented, followed by references and some additional information contained in appendices.

Chapter 2. Gridding the Point Cloud

2.1 Introduction

Accurate terrain models provide the chassis designer with a powerful tool to make informed design decisions early in the design process. During this stage, engineers are challenged with predicting vehicle loads through modeling and simulation. The accuracy of these simulation results depends not only on the fidelity of the model, but also on the excitation to the model. It is clear that the terrain is the main excitation to the vehicle [1]. These models are often based directly on three dimensional measurements; therefore, the terrain measurements must be as accurate as possible.

Terrain measurement systems, such as the VTMS, are an enabling technology, creating a new level of fidelity and resolution in terrain measurement. However, these terrain measurements are not collected with regular spacing, which is necessary for efficient data storage and simulation. It is therefore common practice to grid this dense, irregularly spaced data. The process of accurately gridding the data requires extensive search algorithms that can be computationally inefficient. The grid is also largely dependent on a coordinate transformation known as a curved regular grid, where a path must be chosen to define the CRG (typically the center of the road).

This chapter examines alternate gridding methods to improve efficiency while maintaining accuracy. Additionally, a solution for automated path generation is developed. Algorithms for center path and alternate paths are proposed and implemented. First, background information on terrain surface measurements, curved regular grids, and a stochastic gridding method are presented. Next, a procedure for center and alternate path generation is developed. Then, a binning technique to improve gridding efficiency with small memory usage is developed. This chapter concludes with a discussion of software implementation, comparison of gridding algorithms, and conclusions.

2.2 Background

2.2.1 Terrain Measurement Non-Uniformity

Terrain measurement systems take advantage of a variety of sensors to obtain a dense and accurate measurement of the terrain. Measurements are taken with a 3D scanning laser that is mounted on a host vehicle. Variation in vehicle position and orientation are taken into account using an inertial navigation system (INS) and accelerometers. The laser collects data transversely using a rotating prism and time-of-flight calculations [2]. Data are collected at equal angles of rotation, θ, as shown in Figure 2-1. Because the distance of a flat surface from the laser increases towards the edge of a scan, adjacent measurements are further spaced apart. The irregularity is also affected by undulations in the surface. This can also be seen in Figure 2-1, as the height of the surface at locations x_1, x_2, and x_3 are all different. The combination of this and the equal

angle measurements result in the transverse spacing between x_1 and x_2 to be smaller than the transverse spacing between x_2 and x_3.

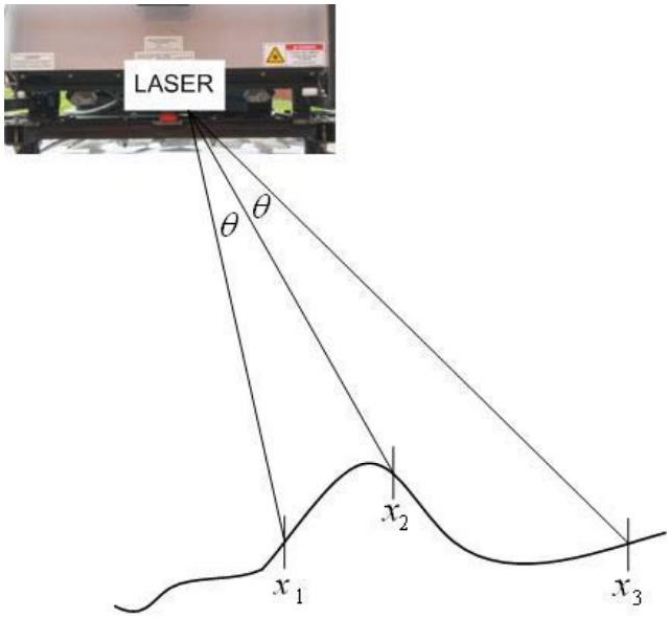

Figure 2-1. Equal angle laser collection.

The longitudinal spacing of the measurements is affected by a variety of things as well. Changes in speed of the host vehicle will immediately affect the longitudinal distance between laser scans. The shape of the surface will also result in irregularity in a manner similar to transverse spacing. Finally, the yaw and pitch of the host vehicle will affect the location of the measurements in both directions.

After processing the information from each sensor of a particular run, the data are represented by a 3D point cloud. That is, every measurement is characterized by an x, y, and z coordinate. The Vehicle Terrain Measurement System (VTMS), for example, collects nearly one million data points per second, corresponding to about one gigabyte of processed data per minute of acquisition time. The VTMS is the platform used to capture the data used for this research. The VTMS is shown in Figure 2-2. The gray box mounted onto the vehicle contains the sensors necessary to take measurements.

Figure 2-2. Vehicle Terrain Measurement System (VTMS).

To perform an accurate tire or vehicle simulation using an entire dataset is unrealistic. The act of simply determining which data points interact with the tire at any point in the simulation is a computationally intense task. It is much more efficient to represent the data in some uniform way, allowing the simulation software/algorithms to quickly find which points excite the vehicle at the appropriate time.

2.2.2 Curved Regular Grid (CRG)

One way to efficiently represent a dense road surface is with a Curved Regular Grid (CRG). The CRG consists of a path coordinate, u, and a perpendicular coordinate, v. Discrete longitudinal locations along coordinate u are defined as vector $\boldsymbol{u}$ and are indexed by i. Discrete transverse locations along coordinate v are defined as vector $\boldsymbol{v}$ and are indexed by j. These vectors are usually regularly spaced. The coordinate definition for a typical CRG is shown in Figure 2-3. An example of a uniform grid is shown in Figure 2-4 [3].

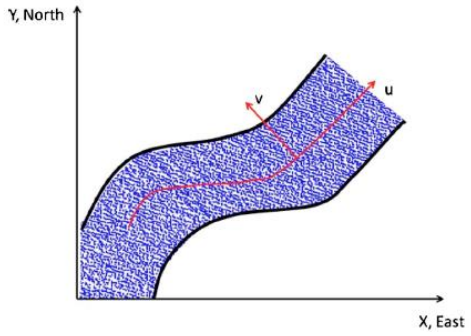

Figure 2-3. Curved regular grid (CRG) in horizontal plane with point cloud.

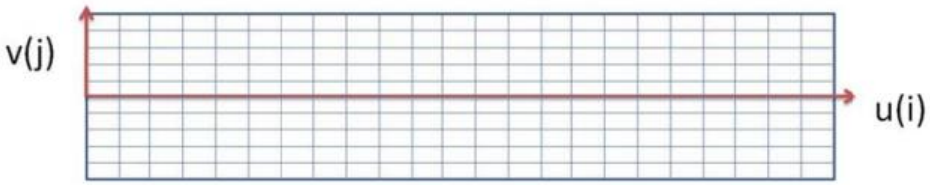

Figure 2-4. CRG example coordinates.

2.2.3 Weighting Function

The terrain height corresponding to each discrete point $(\boldsymbol{u}, \boldsymbol{v})$ in a CRG is determined by examining the vertical heights of the surrounding points. There are many spatial interpolation methods that may be used to weight this height value (e.g. mean, median, inverse-distance-to-a-power, or kriging). Traditionally, a search radius is introduced to perform the spatial interpolation. This search radius is applied to every grid node $(\boldsymbol{u}, \boldsymbol{v})$, and points that rest within the search radius are considered for the height of the corresponding node. That is, all data points that lie within an absolute horizontal distance of a grid node are used to determine the height of the node. This is shown in Figure 2-5 [4].

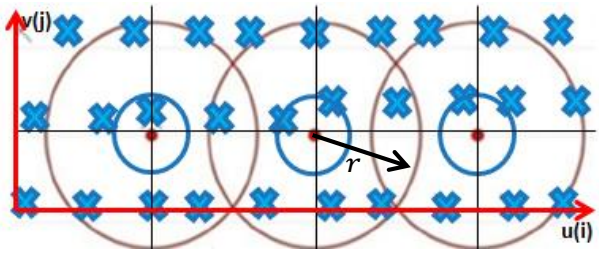

Figure 2-5. Grid nodes in CRG with nearby data points, search radius, and horizontal uncertainty.

A stochastic weighting function is used [5] to account for horizontal uncertainty of the terrain measurement system. The red dots in Figure 2-5 represent grid nodes in the CRG, while the blue x's represent actual data from the point cloud. The red circles are the search radii (magnitude of r), and the blue circles are the horizontal uncertainty of the grid nodes. With a

stochastic weighting function, the height of each grid node is determined by the inverse distance away of the surrounding data points, their vertical heights, and the horizontal uncertainty of the node measurement. This weighting function, as shown in Figure 2-6, weights all measurements that are within the horizontal uncertainty of the grid nodes (blue circles indicating the standard deviation of the error, σ) nearly the same. The weighting function applied to a particular data point, $\widetilde{w}(d/\sigma)$, decreases as the normalized distance from the grid node, d/σ increases.

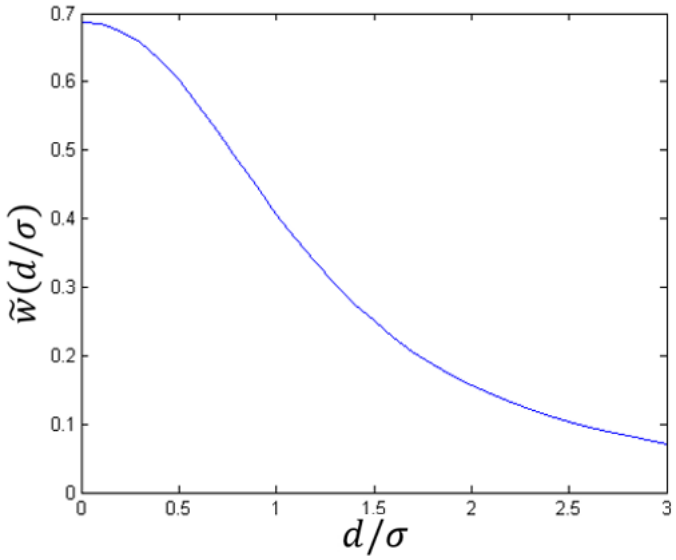

Figure 2-6. Stochastic weighting function.

2.3 Path Generation

2.3.1 Center Path Generation

The CRG representation of a road is dependent on the global location of the u-axis. This can be thought of as the "path" that the vehicle takes when traveling the road. This path is very important for vehicle and tire simulation. Any number of paths can be chosen to indicate a possible path that a driver may take to travel along the road. These paths do not have to be the *actual* path taken during the measurement of the road itself. In this way, the run-to-run variation found in physical driving can be simulated in virtual driving. This variability improves the understanding of the variation inherent in modeling driver paths. The development of alternate driving paths is one of the contributions of this research. Regardless of the path chosen, the v vector can be defined such that one point (or a cluster of points) are located at one-half of the track width on the left side of the path and a point (or a cluster) are located at one-half of the track width on the right side of the path. In this way, the wheel paths are easily identified in the gridded data and the resulting grid can be used for efficient simulation. The first automated implementation of path selection begins by examining the x and y locations of the data. Assuming data were taken using a vehicle measurement system, these locations will resemble a road with a width of about 4 meters. A top down view of an example road is shown in Figure 2-7. The road surface is approximated by a set of yellow dots, which when taken together, show

a clear representation of the road surface. It is clear from the figure that manually choosing the path from points that appear to lie in the center of the road is inefficient and unrepeatable.

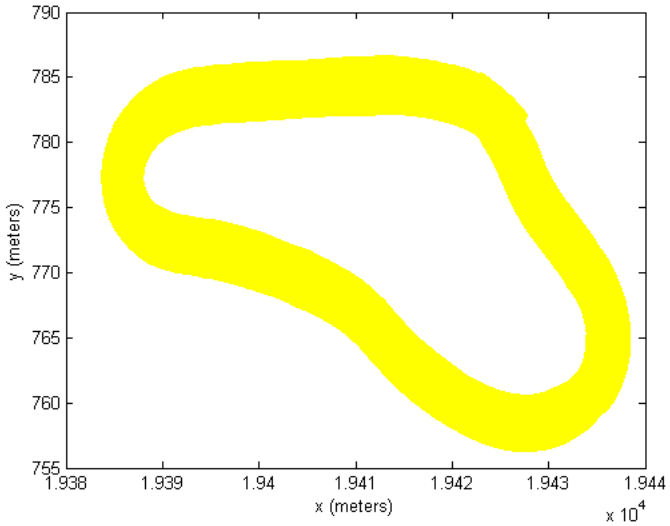

Figure 2-7. X-Y scatter plot of gravel track.

A method is developed to estimate a set of points that define the center of the road. These points are determined from the point cloud automatically. It is assumed that the data are arranged in the file in the same order in which they were collected. The center path can be constructed using a block-by-block median technique. Undesired frequency content must also be removed through filtering. The block size and filter cutoffs are chosen using the following reasoning.

A realistic estimate for the vehicle speed during measurement is 10 meters per second. The frequency responsible for wheel-hop (2nd mode) of a vehicle is about 1 Hz at this speed [6]. Wheel-hop occurs at a higher frequency than the primary ride frequency (1st mode) and roll frequency. To ensure the wheel-hop frequency is captured and aliasing does not occur, the data block size is set to 5 hundredths of a second (corresponding to about ½ meter longitudinal spacing). The median x and y point of each block is then calculated. The median is chosen to avoid the possibility of a skewed path from a bad measurement point. To guarantee path points do not overlap, they are merged together if they are deemed too close. This is to avoid a collection of path points that reside overtop one another if the host vehicle was close to stationary. The block-by-block median technique is shown in Figure 2-8. The point cloud is represented by yellow dots, and two data blocks are represented by blue rectangles. The median point of each data block is plotted as red circles. The median points are within 5 % of the actual center of each block. This is an acceptable tradeoff to ensure insensitivity to outliers.

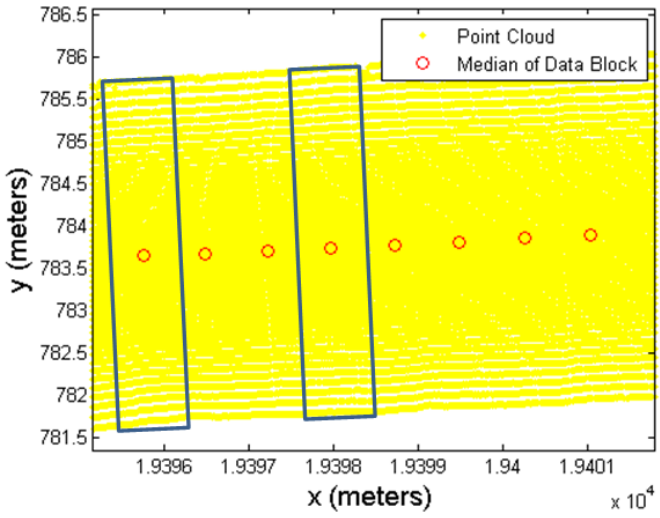

Figure 2-8. Block-by-block median calculation.

Next, the path points are low pass filtered with a cutoff frequency of 1 Hz to remove undesired frequency content, such as the modal responses. This method is quick, reliable, and requires no inputs from the user. Additionally, it does not use any GPS/INS data, making it usable for a wider audience. The resulting set of path points is generally a smooth curve located along the center of the road. An example of a suggested path is shown in Figure 2-9. The global position of the path points, defining a path along the center of a road, are shown as the red circles. The point cloud is represented with yellow dots. One can see in the figure that the path points created successfully represent the center of the road.

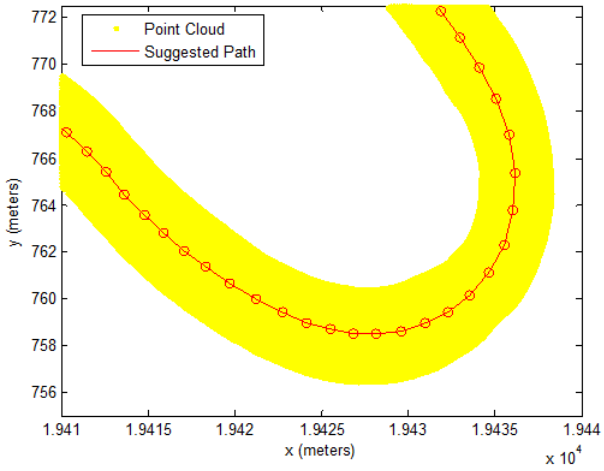

Figure 2-9. Center path automatically generated.

2.3.2 Alternate Path Generation

Although only one path ($\boldsymbol{u}$ vector) is needed to create a CRG, grids created from alternate paths can provide useful information as well. Randomly generated paths would emulate the driving paths that drivers may have taken along the terrain surface. These paths would be represented by different coordinates, $\boldsymbol{u}$, shown in Figure 2-10. For each different path $\boldsymbol{u}$, a new CRG can be generated. These paths would capture the inherent run-to-run variation that would result from driving different paths down the same baseline 3D surface. The set of profiles in a CRG also represents a set of possible 2D measurements that would have been measured at that point in time using a 2D profiler instead of a 3D surface measurement. Therefore, the randomly generated grids can be used as the run-to-run variation of measurement. If future measurements, with a 2D profiler, fall outside the bounds created from the multiple grids, road deterioration can be concluded.

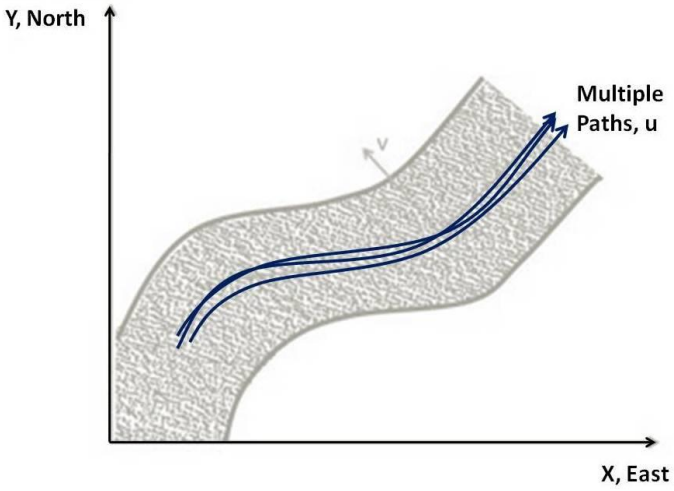

Figure 2-10. CRG based on multiple alternate paths.

Consider two vectors, $\boldsymbol{q_x}$ and $\boldsymbol{q_y}$, that contain the global position in the x and y coordinates respectively defining a path along the center of a road (e.g., the red circles in Figure 2-9). These path points are indexed by h and are irregularly spaced. Two continuous functions, $Q_x(h)$ and $Q_y(h)$ are derived by fitting a cubic spline the original path points. The angle of travel can be estimated as

$$\phi(h) = \tan^{-1}\frac{Q'_y(h)}{Q'_x(h)}, \qquad \text{Equation 2.1}$$

where $Q'_x(h)$ and $Q'_y(h)$ are first derivatives with respect to h. An alternate path point (p_x, p_y) is defined at a distance, d, extending from an original path point and perpendicular to the path. Consider the path point in question to be located at the origin, then the direction from the original path point to the alternative path point is $\phi + \frac{\pi}{2}$, and the location of the alternative path point is thus,

$$p_x = -d\cos\phi$$
$$p_y = d\cos\phi$$ Equation 2.2

Now consider vectors, $\boldsymbol{d}$, $\boldsymbol{p_x}$, and $\boldsymbol{p_y}$, each indexed by h. A set of alternate path points, affected by a random component, can be modeled as a Gaussian random walk with drift.

$$d_h = \frac{1}{2}d_{h-1} + \delta_h$$ Equation 2.3

$$\delta_h = \mathcal{N}(0, \sigma_p)$$ Equation 2.4

$$p_{xh} = -d_h \sin\phi(h) + q_{xh}$$ Equation 2.5

$$p_{yh} = d_h \cos\phi(h) + q_{yh}$$ Equation 2.6

The distance of the first alternate path point is a normally distributed random number centered on zero; $d_0 = \mathcal{N}(0, \sigma_p)$. Subsequent alternate path points are created based on the previous alternate path point. The result is a randomly generated alternate path that is a random walk process with a persistent drift toward the origin, emulating a real driver. As the alternate path deviates further from the center path, the drift component increases. An example is shown in Figure 2-11. The point cloud is yellow dots, the alternate path points are green squares, and the center path points are red circles. Each alternate path point is a function of the previous alternate path point's distance from the center path, d_{h-1}, the direction of travel, ϕ_h, and a user specified standard deviation, σ_p. Typically, the alternate path alternates between the left and right side of the center path.

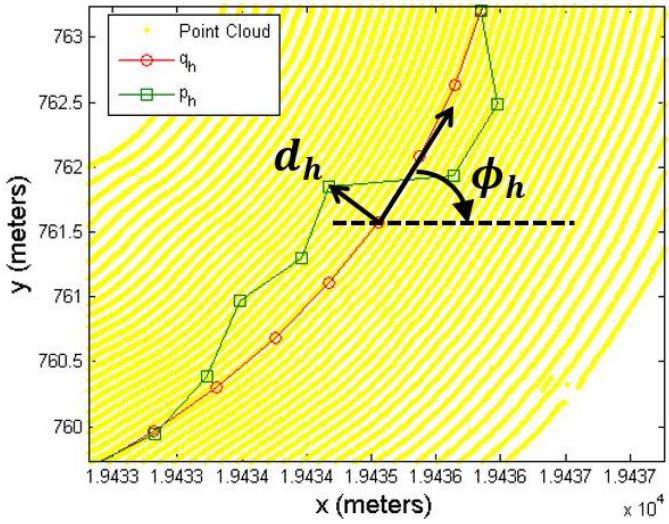

Figure 2-11. Alternate path point generation.

These alternate path points are low pass filtered after creation to ensure no frequency content above 1 Hz is present. An example is shown in Figure 2-12 where paths are generated for a curved road segment. In this example, the point cloud is yellow dots, the center path points are red circles, and the alternate path points are green squares and blue x's. Each alternate path takes the turn differently.

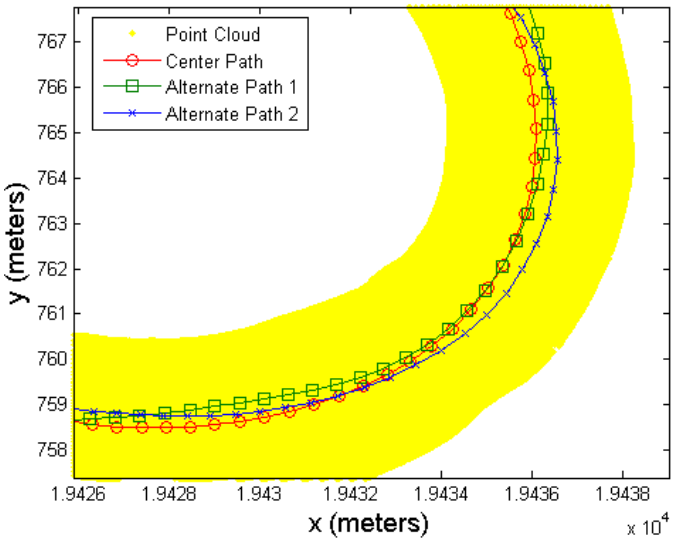

Figure 2-12. Center and alternate path automatically generated.

In addition to creating the alternate path points, the same geometry technique can be used to shift a path towards a particular side of the road. In this case, d would be constant and there would be no random component. This can prove to be useful to ensure an equally spaced wheel path, for example.

After the path points have been created (alternate or center), the u coordinate is created from these points such that the grid nodes at $v = 0$ are equally spaced by construction. This is done by fitting a smooth curve through the path points and calculating the necessary samples on this curve such that the absolute distance between nodes are equal. The distance between the nodes at $v = 0$ is based on the preferred grid density.

2.4 Efficient Gridding

The density of a point cloud created from a terrain measurement system affects both the accuracy and the density of the resulting grid. However, creating an accurate and dense grid can be a computationally intense. Consider a road that is 1 kilometer long and 3.5 meters wide and the required grid density has a spacing of 2.5 mm longitudinally and transversely. The result is a grid containing over 14 million nodes. Assuming the host vehicle took measurements with a traveling speed of 10 meters per second, the 1 kilometer point cloud would contain a total of 100 million points. Held in ASCII format, the file size would be about 3 gigabytes. If the nearest few points for each grid node must be used to accurately estimate the grid node's height, there are potentially 1.4×10^{15} distance calculations to be made (every grid node to every data point). Clearly this is not a very efficient method for finding nearby points.

The gridding techniques developed here assumes:

- The grid spacing is larger than the spot size of the laser.

- The precision of the height measurements are within the vertical resolution of the grid data being reported.

A search radius is defined for each grid node within which all the data points that affect the nodal height calculation must be located. That is, only points located within the search radius will be considered. There may be an additional limit placed on the maximum number of points considered for each grid node. For example, if the limit is 10 data points for each grid node and there are 100 points within the search radius of a grid node, only the 10 data points that are nearest to the grid node will be kept for stochastic weighting. Additionally, there may be a lower limit placed on the number of points for each grid node. If the number of points within the original search radius is less than this number, the search radius may increase until this number is met. This would, of course, require developing a new bin sizes for any grid nodes with an insufficient number of points within the current search radius.

2.4.1 KD Tree

One efficient method to grid data is with a KD (k-dimensional) tree. A KD tree is an algorithm whereby points are divided into bins based solely on their position relative to the other data points. It is a binary tree where the data are continuously split across alternating axes. The splitting axes are determined using the median of the remaining (un-binned) points. An example of the binning generated from a KD tree using MATLAB's built in function is shown in Figure 2-13. The divisions (black lines) creating the bins of the KD tree alternate between horizontal and vertical directions. To find the points within a particular grid node's search radius, the distances to points within the node's current bin and nearby bins are calculated.

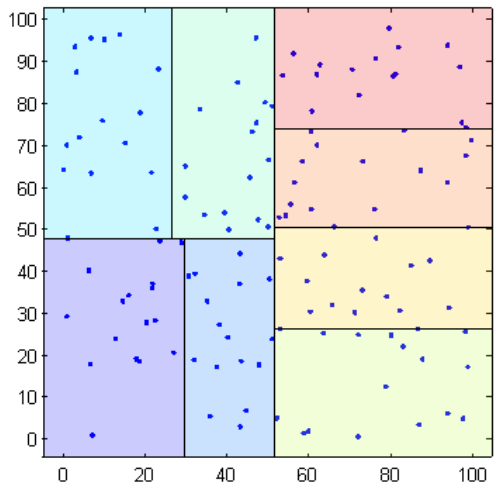

Figure 2-13. KD tree representation, 8 bins [7].

2.4.2 Cell Array Binning

Rectangular binning is also a common approach used to sort data. The method developed here, cell array binning, is an efficient application of binning to dense terrain point clouds, ultimately used for gridding. Like the KD tree, it is intended to pre-sort the data and grid nodes. It also ensures all points within a specified search radius, r, are accounted for while successfully ignoring distance calculations for the majority of points located outside a node's search radius.

First, a block of data is sorted into square bins. The boundaries of the outside bins are determined from the boundaries of the data block, while the height and width are set equal to the desired search radius. The sorting can be accomplished efficiently via histogram counting (in MATLAB, histc). After sorting each of the data points, they are accumulated into a MATLAB cell array equal in size to the total number of bins. Memory usage is relatively small because cell arrays are sparse. Next, the grid nodes (for the CRG) are sorted using the same method. Relevant points for any particular grid node are determined as points that lie within the current bin location of the node, and each of its adjacent bins. An example is shown in Figure 2-14. The red dot represents the location of the grid node under examination, while the black circle is the search radius. The blue x's are the locations of the data points in the surrounding bins. The bin boundaries are represented by the dashed lines on the plot. The current bin location of the grid node is represented in bold.

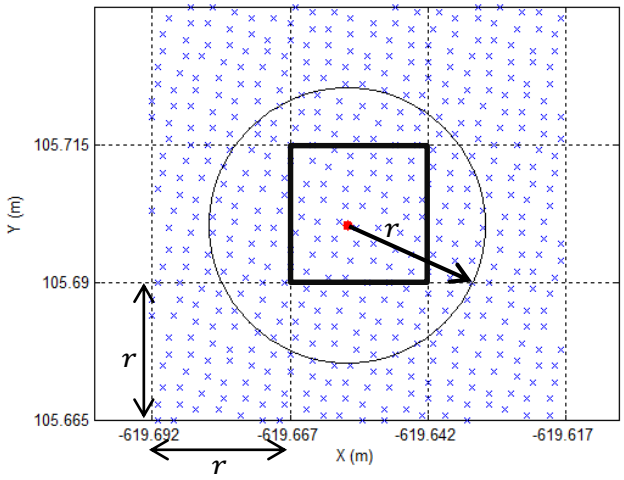

Figure 2-14. Cell array binning of one grid node and its nearby data points.

It is clear that all data points located within the node's search radius are also located within the surrounding bins regardless of the location of the grid node in the center bin. Therefore, given a grid node and a block of data, possibly separated into many thousands or millions of bins, the data can be very quickly reduced to only 9 bins that contain possible points that are within the node's search radius. This requires no calculations to determine nearby bins, as is the case with a KD tree.

Finally, before doing any distance calculations, relevant points for the grid node are reduced by comparing their locations to the edges of a square containing the grid node and its search radius, shown in Figure 2-15. Here, all points located outside the green square are no longer considered relevant. Once again, all points present in the search radius of the grid node are considered.

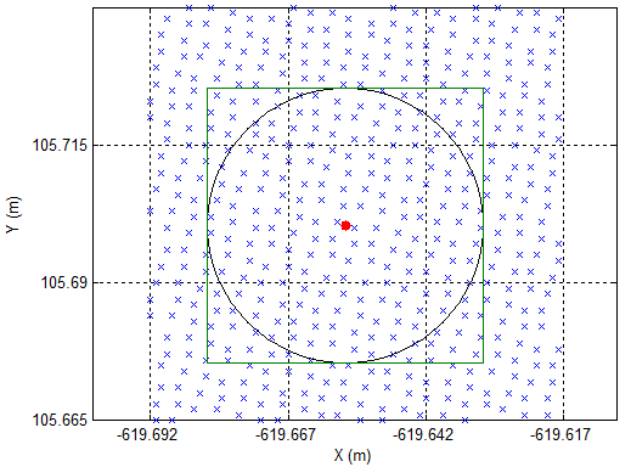

Figure 2-15. Point reduction after cell array binning.

Now that the number of relevant points has been greatly reduced, distance calculations are performed on all the remaining points. Data points that are located within the search radius are kept and sorted, while points located outside are ignored. If there is a limit on the total number of points used for a grid node, only the nearest ones are kept. These points are then weighted using the stochastic gridding method described previously to estimate the height of the grid node.

Recall the example of a road that is 1 kilometer long and 3.5 meters wide, and the required grid density has a spacing of 2.5 mm longitudinally and transversely. The resulting grid contains over 14 million nodes and the point cloud contains about 100 million points. An exhaustive search of nearby data points to grid nodes consists of 1.4×10^{15} distance calculations (every grid node to every data point). Using cell array binning, the number of distance calculations for the same scenario would be reduced to approximately 1.7×10^{10}, a significant 100,000 times improvement in processing speed. Additional processing time is added for the initial bin sorting, where the number of calculations is dependent on the sorting algorithm, number of bins, and number of data points; however, in general, this additional time is insignificant compared to the overall time-savings.

2.4.3 Search Algorithm Comparison

There are scenarios where each of the two gridding algorithms is more efficient than the other. The KD tree algorithm is a built-in MATLAB method that is very fast when most or all of the point cloud can be loaded into memory at one time. If this is the case and a predetermined

number of the nearest points are desired for each grid node, the KD tree is the fastest method for this calculation. If the number of points considered for each grid node is only dependent on a specified search radius (no limit on number of z values), or the road must be loaded in many blocks (due to memory limitations), cell array binning is usually faster. Additionally, because the cell array binning algorithm is built using an independent for-loop, parallel processing is also accessible. By taking advantage of one of these two methods, most dense point clouds, that may be many kilometers in length, can be gridded in a reasonable amount of time.

2.5 Software Implementation

The gridding techniques described in the previous sections have all been implemented into a software package called *CloudSurfer*. *CloudSurfer* has an easy to use interface that allows a user to quickly open a point cloud, create center and alternate paths, and choose from many options before efficiently gridding the data. The interface is shown in Figure 2-16. It is clear from the figure that options include longitudinal and transverse grid spacing, path offsets, number of alternate paths, and standard deviation used for creating the alternate paths. Additionally, the user can manually input path points or transverse grid points into the provided tables. Path points may also be selected from an overhead view of the road.

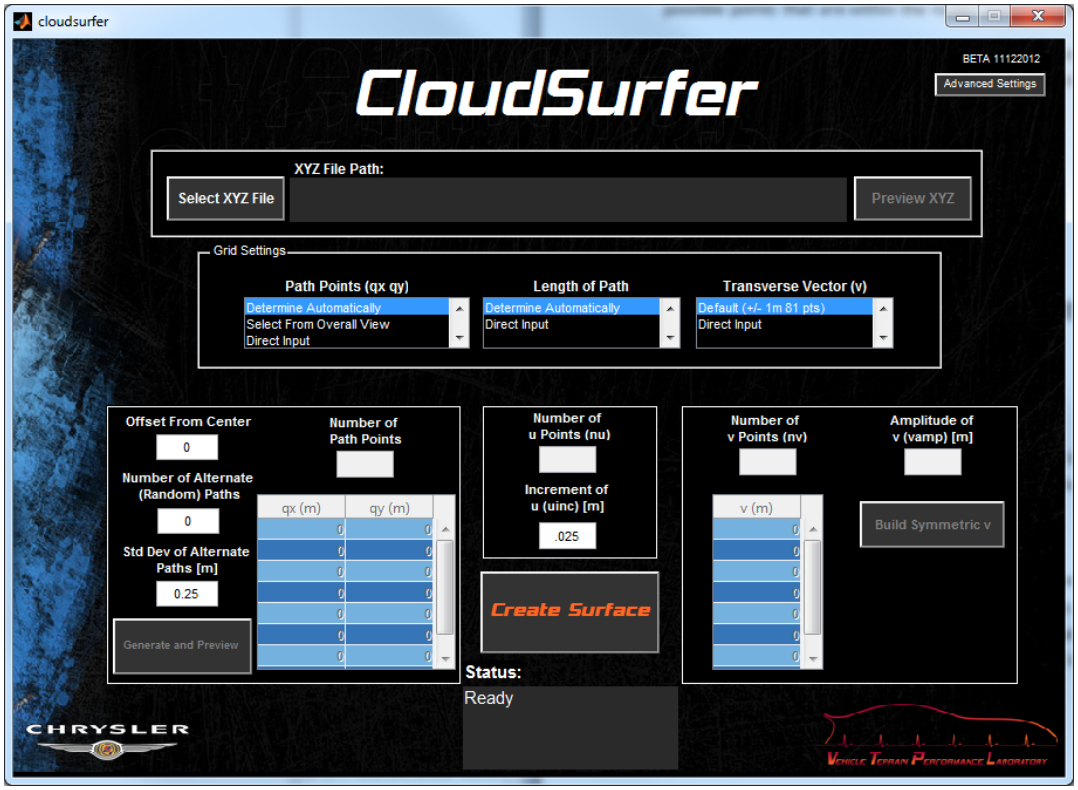

Figure 2-16. *CloudSurfer* graphical user interface

Advanced settings include the gridding algorithm (KD tree or cell array binning), block size (how much of the point cloud to load in at a time), stochastic weighting function parameters, minimum and maximum number of points per grid node, and search tolerance. The software grids the data and outputs it in a variety of formats. These include RGR, RDF, CRG, and MATLAB Surf Structure. This array of output formats allows compatibility with many other software packages, such as Adams and CarSim. Also, the software compiles important processing information, mesh images, and path images into an HTML report.

2.6 Conclusions

Many methods to improve the gridding process for high fidelity terrain measurements are developed in this chapter. Robust algorithms for path generation are developed, allowing curved regular grids to be created from center and alternate paths. The grids created from alternate paths provide a useful tool to determine the run-to-run variation of the measurements. Two different gridding methods are implemented and compared. The KD tree provides efficient searches for high memory computers. The second algorithm, cell array binning, improves memory usage, while maintaining high efficiency. Both algorithms retain the accuracy of an exhaustive search algorithm and show an improved computational speed of several orders of magnitude.

The improvements to the gridding process are realized in the software *CloudSurfer*. *CloudSurfer* allows a user to very easily grid a road, while delivering many options for customization and performance improvements. The software is regularly used in the lab to convert the point cloud terrain measurements into grids that can be decomposed, modeled, and analyzed. Some of the analysis that can be exploited with gridded terrain is explored in the following chapters.

Chapter 3. Developing a Compact Continuous-State Markov Chain for Terrain Road Profiles

3.1 Introduction

Chassis loads that represent severe customer usage are necessary throughout the vehicle design and development process in order to define design objectives. However, the true loads are available only at the conclusion of the program when the design is complete. Early in the design process, engineers are challenged with predicting these loads through vehicle modeling and simulation. The accuracy of these simulation results depends not only on the fidelity of the model, but also on the excitation to the model. It is clear that the terrain is the main excitation to the vehicle [1]. Non-deformable terrain imposes a unilateral geometric boundary constraint on rolling tires to which the chassis responds by generating loads, moments, motions, deformations, etc. The terrain profile remains a consistent excitation to the chassis, even as the chassis design changes. Knowledge of this excitation, when applied in conjunction with high fidelity tire and vehicle models, would allow chassis loads to be accurately predicted in vehicle simulations. Therefore, throughout the design process the system response to this consistent excitation can be calculated and compared for each chassis design considered. Accurate terrain models would then provide the chassis designer with a powerful tool to make informed design decisions early in the design process while changes are relatively inexpensive to implement. This will, in turn, shorten vehicle development time and reduce overall development costs.

The terrain profile is an indexed set of terrain profile heights that can be considered a discrete signal and represented in vector form. The current practice for durability analysis is to use these signals directly as excitations in vehicle simulation; however, simulating the vehicle responses for extensive terrain excitations is computationally impractical. It is critical to be able to group together measured terrains with similar physical properties, so that choices can be made regarding which terrain sections should be selected for simulation.

It is beneficial to characterize the terrain as a realization of an underlying stochastic process and to develop a mathematical model of that process (e.g., an autoregressive model or a Markov chain). The model would be parameterized to best fit the measured terrain, preferably with a few parameters. The values for each of the parameters would then indicate the type of terrain being modeled. The resulting stochastic model could then be used to generate as much synthetic terrain of that terrain type as required.

The advantage to using synthetic terrain with the same physical properties as the original measured terrain is that some variation in the simulation results can be achieved. Consider a simple example in which a vehicle/tire model is simulated over some measured terrain and the peak load is identified. Each time that vehicle/tire is simulated on that same section of road the exact same peak load will be calculated. Using different realizations of the stochastic model (different synthetic terrain) the variation in the peak load can be simulated, so that, for example, the variation in the range of possible peak loads can be estimated.

The goal of this work is to develop a compact set of coefficients that model the terrain such that the resulting synthesis has similar properties to the measured terrain. Although other stochastic models can be developed to achieve this goal, a first order, continuous-state Markov model is developed in this work. The objective is to represent the conditional transition probabilities from the current state (terrain height) to the next state. These transitions are typically quantized and binned to form a transition matrix.

Presently, a process is developed to represent this transition probability as a collection of univariate distributions. The distribution must be continuous and defined across the entire real axis. The location-scale family of distributions fit these criteria. The logistic distribution is chosen for a proof-of-concept. It is proposed that the location and scale parameters can be modeled with a simple polynomial function of the current state. Other functions are also possible. An initial estimate of the polynomial coefficients describing the n^{th} degree polynomial for each of these parameters (location and scale) is calculated using least squares. This initial estimate of the polynomial coefficients is refined by introducing the maximum likelihood estimate (MLE).

The remainder of the chapter is developed as follows. First, a brief background of Markov chains and MLE are discussed. Next, the model creation process is developed by assuming a first order Markov model for a given profile. The model represents a continuous manifold of cumulative conditional transition probabilities. A sliding window is developed to estimate the cumulative conditional transition probability for each transition from the current state to the next state. The logistic distribution is proposed to model the conditional transitions. The logistic distribution is defined by two parameters (location and scale) that are modeled with a polynomial and refined with MLE. An example demonstrates how this distribution can be applied to a particular terrain profile. The resulting transition function is characterized by only a few coefficients (8 for the example) and describes a first order continuous-state Markov chain for a terrain profile. A short case study is performed that compares the admissible distributions on a rough and smooth road. Expanding this case study, introducing frequency decomposition, addressing model instability, and three-dimensional applications are discussed as the focus of future work.

3.2 Background

Autoregressive (AR) models can compactly represent terrain profiles if it can be shown that the residual process is independent and identically distributed (i.i.d.). In this case, the AR model can be characterized solely by the model parameters and the parameters that describe the residual process [8, 9]. The stability of the AR models must be checked and, in some cases, enforced on the model [10]. Discrete-state Markov chains have also been proposed as a candidate to model terrain road profiles [11]. Road profiles are quantized before characterizing the chain with a transition matrix. The underlying process (terrain), however, is continuous.

Consider a discrete-time stochastic process

$$\{Z_i, i = 0, 1, 2, \dots\}, \qquad \text{Equation 3.1}$$

where Z_i are a family of continuous random variables defined on a common probability space. Each measurement (representing a realization of the process) is taken at a discrete moment in time, i. Let S represent the state space where all z_i are elements of S. It should be clear that z_i can take on any value within the continuous state space, *S*. Throughout the development of this technique, the distinction is explicitly made between the general case where all possible realizations (all possible collections of z_i), and the specific case of a particular realization (a particular measured terrain) is being considered.

The Markov property can be written as

$$f\left\{Z_{i+1} = z_{i+1} \middle| \begin{matrix} Z_0 = z_0, \dots, \\ Z_{i-1} = z_{i-1}, Z_i = z_i \end{matrix}\right\} = f\{Z_{i+1} = z_{i+1} | Z_i = z_i\}. \qquad \text{Equation 3.2}$$

where f denotes probability density and z_i represents the general case in which any z_i can take on any value within the continuous state space, *S*. That is, if a signal possesses the first order Markov property then, conditioned on the present, the future and past are independent. Of course the conditional probability must satisfy the axioms of probability, including

$$f\{Z_{i+1} = z_{i+1} | Z_i = z_i\} \geq 0, \forall z_i, z_{i+1} \in S, \qquad \text{Equation 3.3}$$

$$\lim_{z_{i+1} \to \infty} P\{Z_{i+1} < z_{i+1} | Z_i = z_i\} = 1\ , \qquad \text{Equation 3.4}$$

$$\lim_{z_{i+1} \to -\infty} P\{Z_{i+1} < z_{i+1} | Z_i = z_i\} = 0\ . \qquad \text{Equation 3.5}$$

Oftentimes, the state space is discrete and finite, and the transition properties are time invariant, in which case the process can be fully characterized by a transition matrix [12]. The issue with this representation is that the number of parameters necessary to characterize a transition matrix is equal to the square of the number of states, which becomes cumbersome for more than a few states. There is also error introduced in the quantization process by which the states are defined. The effect of various binning techniques applied to terrain profiles has been researched previously [13, 14]. The purpose of this work is to expand the application of Markov chains on terrain road profiles from discrete space [11, 13, 14] to continuous space.

If the first order Markov property holds, the state space is continuous, and the transitions are time-invariant, then this Markov chain can be fully described by its cumulative conditional probability function (transition function) for any current state z_i.

$$\mathrm{P}\{Z_{i+1} \leq z_{i+1} | Z_i = z_i\} = F(z_{i+1} | z_i)\ \forall z_i, z_{i+1} \in S, \forall i\ . \qquad \text{Equation 3.6}$$

This Markov conditional probability is a manifold that spans the Cartesian product of the state space, $S \times S \to F$. Differentiating the transition function with respect to z_{i+1} yields the Markov probability density function (PDF), or transition density, $f(z_{i+1} | z_i)$.

Recall that the joint probability of independent discrete events y_1, y_2, and y_3, that are all elements of the state space S and defined on the same probability space, is the product of the probability of each individual event:

$$P\{y_1 y_2 y_3\} = P\{y_1\}P\{y_2\}P\{y_3\}. \qquad \text{Equation 3.7}$$

If the events occur from a parameterized distribution (by vector $\boldsymbol{\theta}$), the likelihood of the parameter set given the outcomes is equal to the product of the probabilities of the outcomes given the parameter set. If events are elements of a continuous parameterized distribution, the likelihood of a set of parameters, $\boldsymbol{\theta}$, is the product of the probability densities of the independent outcomes, $\boldsymbol{y}$, given the parameter set:

$$L(\boldsymbol{\theta}|\boldsymbol{y}) = \prod_{i=1}^{m} f(y_i; \boldsymbol{\theta})\,. \qquad \text{Equation 3.8}$$

Because each *transition* in a Markov chain is independent (first order Markov Property), the conditional probability can be substituted for the independent outcomes, $y_i = z_{i+1}|z_i$, and the likelihood of a parameter set given the outcomes of the Markov chain is

$$L(\boldsymbol{\theta}|\boldsymbol{z}) = f(z_0)\prod_{i=1}^{m-1} f(z_{i+1}|z_i; \boldsymbol{\theta}), \qquad \text{Equation 3.9}$$

where $\boldsymbol{z}$ is a particular realization of the Markov chain, $\boldsymbol{\theta}$ is a vector of coefficients that describe the distribution, and m is the length of $\boldsymbol{z}$. In the case of terrain profiles, i is in terms of discrete locations (rather than time). To determine the best model for a realization, the coefficients that maximize the likelihood function must be found. Much research has been done on the behavior of MLE's for Markov processes. Under certain conditions, the MLE for a Markov process can be proved to be consistent and asymptotically normal [15].

Generally it is more efficient to work with the logarithm of the likelihood function. Assuming the initial state of the process is known, the log-likelihood function is

$$l(\boldsymbol{\theta}|\boldsymbol{z}) = \sum_{i=1}^{m-1} \ln f(z_{i+1}|z_i; \boldsymbol{\theta}). \qquad \text{Equation 3.10}$$

The maximum of the likelihood function occurs at the same location as the maximum of the log-likelihood function.

Maximization of the log-likelihood function is straightforward using optimization methods. If the parameter space is more than, say two or three, the initial guess for optimization is vital. Otherwise, the problem may become untraceable and alternatives to MLE are required. When the transition density is not known in closed form these alternatives have proved useful to model a Markov process [16-18]. Gaussian distributions have been applied to transition

functions for discrete diffusion processes [19]. MLE has been applied to multivariate elliptical distributions to estimate Markov chains as well [20].

3.3 Continuous-State Markov Chain Creation

The development of a continuous-state Markov chain (CMC) model begins by considering a first order Markov process representing a given profile. It should be clear that the measurements (realizations) for each terrain profile are acquired at discrete locations along a path, so that the horizontal locations are discretized, but the heights that correspond to each of these discrete horizontal locations are continuous and not binned or otherwise quantized in any way. It is assumed that the appropriateness of a first order Markov process is valid.

Consider a pair of sequential horizontal locations at which measurements are acquired, indexed i and $i+1$, and their corresponding heights, z_i and z_{i+1}. As the index i is increased, each pair of sequential heights can be plotted as a point in a transition plot, an example of which is shown in Figure 3-1. The conditional probability, $z_{i+1}|\, z_i$, is represented as horizontal lines in the figure and the conditional probability density can be estimated by the density of the points lying along that line. For example, consider an initial state of zero (a horizontal line at $z_i = 0$). The probability density for $z_{i+1}|\, z_i = 0$ is minimal for $z_{i+1} <$ -0.005, builds to a peak at $z_{i+1} =$ 0, and then decreases as z_{i+1} approaches 0.005. Similarly, the transition plot can be used to estimate the cumulative conditional probability density. In this way, the CMC represents a continuous manifold of cumulative conditional transition probabilities.

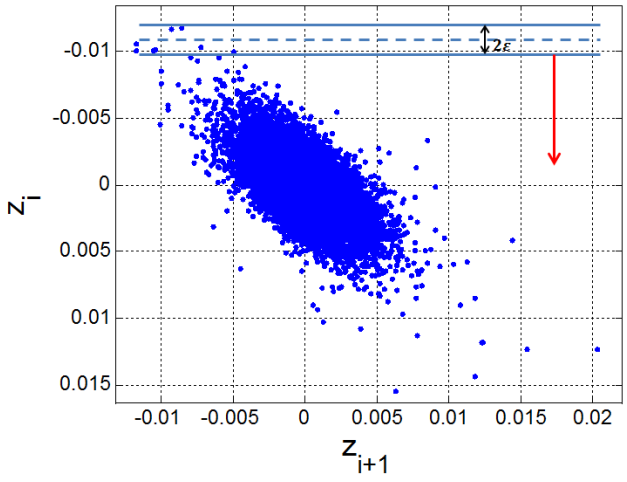

Figure 3-1. Example transition plot for road profile.

A sliding window is developed to estimate the cumulative conditional transition probability for each transition from the current state to the next state. Consider an initial state $z_i = 0.011$, shown as a dashed horizontal line in Figure 3-1. A narrow rectangular window of width 2ε, shown as two solid horizontal lines in Figure 3-1, is used to estimate the cumulative probability of transition from the given current state $z_i = 0.011$, to all other possible states z_{i+1}. This windowing method is only used to derive a first approximation of the cumulative

probability transition, so the somewhat arbitrary choice of the window width, ε, need not be made unnecessarily complicated. In general the resulting cumulative conditional probability is estimated by

$$F(z_{i+1}|z_i) \approx \mathrm{P}\{Z_{i+1} \leq z_{i+1}|z_i - \varepsilon < Z_i < z_i + \varepsilon\} \ \forall z_i, z_{i+1} \in S \ and \ \forall i \qquad \text{Equation 3.11}$$

Next a smooth, monotonically increasing function that satisfies the conditions in Equation 3.3-Equation 3.5 is used to represent the underlying cumulative probability transition function for which Equation 3.11 is an estimate. A distribution from the location-scale family with two parameters (representing location and scale) is selected. For this continuous-state first order Markov process, the cumulative conditional transition probability, given the current state, can be approximated by a location-scale distribution, $F(z_{i+1}|z_i; a, b)$, where the location parameter is a and the scale parameter is b. In this work, the logistic distribution is selected, which has the cumulative density function

$$F_{logistic}(Z; a, b) = \frac{1}{1 + e^{-\frac{Z-a}{b}}}, \qquad \text{Equation 3.12}$$

where Z is the random variable, a is the location parameter, and b is the scale parameter. The probability density function is

$$f_{logistic}(Z; a, b) = \frac{e^{-\frac{Z-a}{b}}}{b\left(1 + e^{-\frac{Z-a}{b}}\right)^2}. \qquad \text{Equation 3.13}$$

The location-scale parameters (a and b), however, are certainly dependent on the current state (else the process would be zeroth order). For a continuous-state Markov chain, the true underlying transition probability for any current state is unique, but expected to be smoothly varying with changes in the initial state. Therefore, the parameters defining the logistic distribution can be modulated to represent the range of possible initial states. That is, the entire manifold of possible transitions can be estimated by representing the location and scale parameters as functions of the initial state.

Initial estimates of the location-scale parameters (a and b) are made using the windowing technique defined in Equation 3.11 and shown in Figure 3-1, resulting in many discrete parameter estimations (vectors $\boldsymbol{a}$ and $\boldsymbol{b}$) corresponding to many different initial states, $\boldsymbol{z}_i$. These parameter vectors are plotted vs. the initial state in Figure 3-2, where the location parameter, a, is plotted as crosses, and the scale parameter, b, is plotted as points. In this work, two simple polynomial functions: $a(z_i)$ and $b(z_i)$, shown in Figure 3-2 as a solid line and a dashed line respectively, are chosen to estimate the parameters. Suppose p^{th} and q^{th} degree polynomials are chosen to fit vectors $\boldsymbol{a}$ and $\boldsymbol{b}$, respectively. There will now be $p + q + 2$ coefficients that describe the polynomials and thus the entire transition function. The coefficients are

concatenated into a vector and denoted by $\boldsymbol{\theta}$. The initial estimate of these parameters, using the windowing technique and polynomial fitting, is $\boldsymbol{\theta}_{init}$.

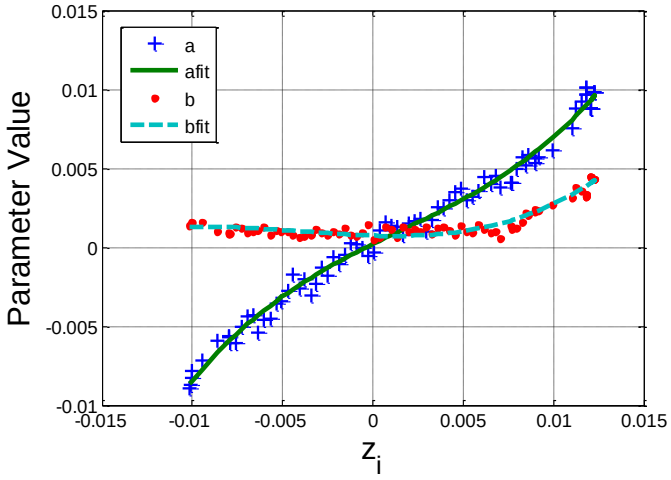

Figure 3-2. Least square parameter fit using cubic polynomials.

MLE is used to optimize the parameters, $\boldsymbol{\theta}$, with an initial estimate $\boldsymbol{\theta}_{init}$. Specifically, the negative of the log-likelihood function of the transition density is minimized, where

$$-l(\boldsymbol{\theta}|\boldsymbol{z}) = -\sum_{i=1}^{m-1} \ln f(z_{i+1}; a(z_i), b(z_i)) \ , \qquad \text{Equation 3.14}$$
$$a = \theta_1 z_i^p + \theta_2 z_i^{p-1} + \cdots + \theta_p z_i + \theta_{p+1} \ ,$$
$$b = \theta_{p+2} z_i^q + \theta_{p+3} z_i^{q-1} + \cdots + \theta_{p+q+1} z_i + \theta_{p+q+2} \ .$$

The parameter set that achieves this optimization is $\boldsymbol{\theta}_{MLE}$, which gives the maximum likelihood for a particular realization ($\boldsymbol{z}$) from the transition density function $f(z_{i+1}; a(z_i), b(z_i))$.

Once $\boldsymbol{\theta}_{MLE}$ is obtained, a synthetic profile can be created. The transition function (CDF) is rearranged into an inverse-CDF (quantile function). Sampling for each transition (future state) is done by considering the current state, coefficient vector, and a uniformly distributed random number on the interval (0,1). The entire process is summarized with the flowchart in Figure 3-3.

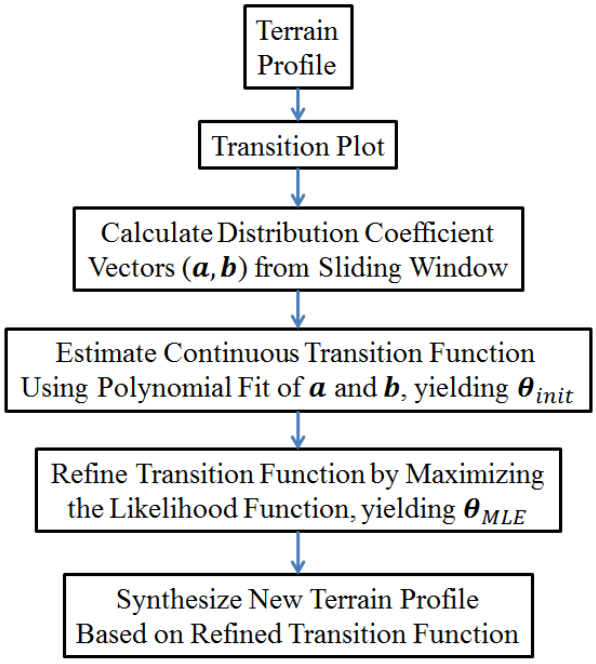

Figure 3-3. CMC creation flowchart

3.4 Example

The following example demonstrates the development of a compact continuous-state Markov chain (CMC) representation of a terrain profile. Consider a terrain profile whose transitions are plotted as shown in Figure 3-1. It should be noted that the longer wavelength content has been filtered from this terrain profile to help illustrate the model. For this particular example, 100 uniformly spaced window locations are used to create an initial estimate of a and b, as shown in Figure 3-2. Next, the functions $a(z_i)$ and $b(z_i)$ are estimated using cubic polynomials. Therefore, there are a total of 8 parameters that will describe this particular Markov transition function. For many profiles, they can be accurately estimated with a linear or quadratic fit.

After a reasonable estimate for the location and scale parameters (polynomials that are functions of the current state, z_i), MLE can be applied to the distribution. The parameter vector that achieves this optimization is $\boldsymbol{\theta}_{MLE}$, which gives the maximum likelihood for the particular realization from the assumed distribution. The number of parameters that characterize the Markov transition function is dependent on the degree of the polynomials used to estimate a and b. If quadratic or linear fits were used instead, the Markov process would be characterized by 6 and 4 parameters, respectively. The values for $\boldsymbol{\theta}_{init}$ and $\boldsymbol{\theta}_{MLE}$ are shown in Table 3-1. The transition function can be visualized as a collection of CDF's (i.e., a CDF manifold) as shown in Figure 3-4.

Table 3-1. Parameterization of CMC

$\boldsymbol{\theta}_{init}$	$\boldsymbol{\theta}_{MLE}$
2.100E+03	1.649E+01
-9.220E+00	-2.837E+00
5.626E-01	1.100E+00
1.861E-04	5.684E-04
1.083E+03	1.227E+01
1.253E+01	-1.391E+00
-3.442E-02	2.527E-02
7.431E-04	1.031E-03

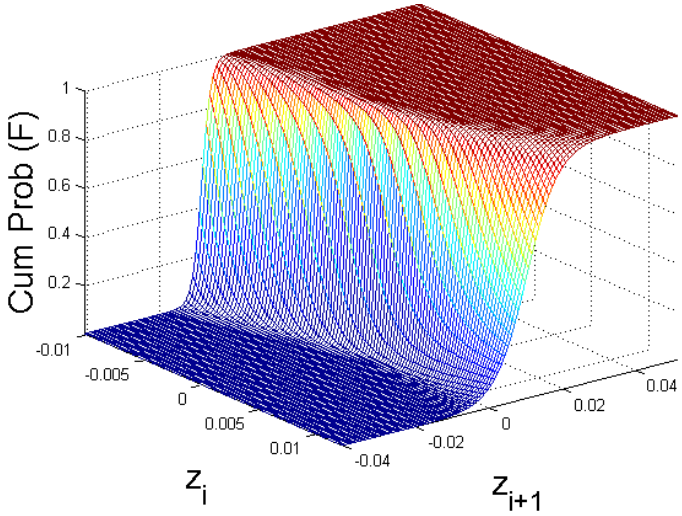

Figure 3-4. CDF manifold for the example profile fit with a logistic distribution and MLE.

At each particular value of z_i, there is an associated CDF where the cumulative probability (F) is a function of the next state (z_{i+1}). Sampling can be visualized on the manifold by choosing any value for the current state and randomly selecting a number from 0 to 1 for the cumulative probability. The next state will be where the intersection occurs on the x-axis (z_{i+1}). This is achieved mathematically by rearranging the transition function (CDF) from Equation 3.12 so that the quantile function (inverse CDF) is obtained

$$z_{i+1} = a(z_i, \theta) + b(z_i, \theta) \ln \frac{F_{logistic}}{1 - F_{logistic}}, \qquad \text{Equation 3.15}$$

where a and b are polynomial functions of the current state (z_i) and coefficient vector ($\boldsymbol{\theta}$) and z_{i+1} is the next state. For synthesis, $F_{logistic}$ is substituted with a uniformly distributed random number on the interval (0,1). The first 150 points of the original and synthesized terrain profiles are shown in Figure 3-5. The longitudinal location of the profile is indexed by i. For this particular example, the longitudinal spacing is 0.05 meters.

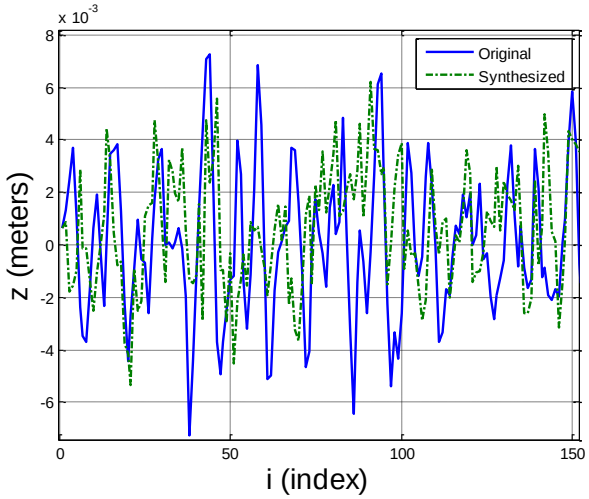

Figure 3-5. Original and synthetic profiles.

The CDF of the transitions for each of the two profiles can be compared as well. For example, the distribution of transitions from $z_i \approx 0$ can be estimated using a small window (± 1 mm) for the original and synthetic profiles. This is shown in Figure 3-6. As expected, they are very similar and should be regardless of the initial state. This similarity in transitions is the exact property that the Markov chain enforces. It will be shown that enforcing this property creates other statistical similarities as well.

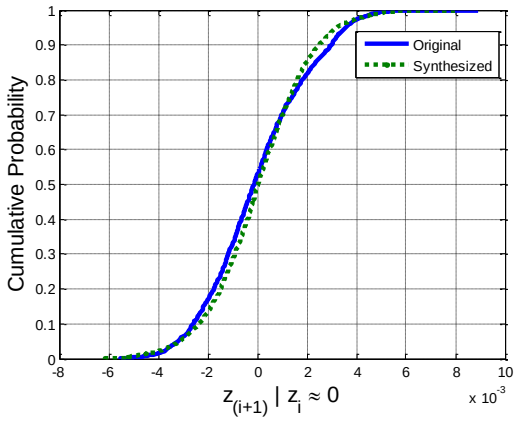

Figure 3-6. Transition distribution of original and synthetic profiles given initial state of 0.

The primary goal of modeling terrain is to create synthetic terrain that is unique but statistically similar to the original terrain. It is assumed that if the content of the vehicle excitations (terrain profiles) are statistically similar, than the vehicle responses will be as well. There are many ways to compare the statistical properties between the original and synthetic terrain profiles. For simplicity, only the root mean square (RMS) distribution will be shown.

The distribution of RMS is compared using a bootstrap method. That is, RMS values are calculated at many different locations along the profile using a fixed window width. For this example, a 30 meter window is used and 100 samples are taken. The CDF of the RMS distribution for the original and synthetic profiles is shown in Figure 3-7. One can clearly see the similarities between the original and synthetic profiles' RMS values. The median RMS for both profiles is about 2.4 mm. The synthesized profile appears to have less variability in RMS, as shown by the slightly tighter CDF.

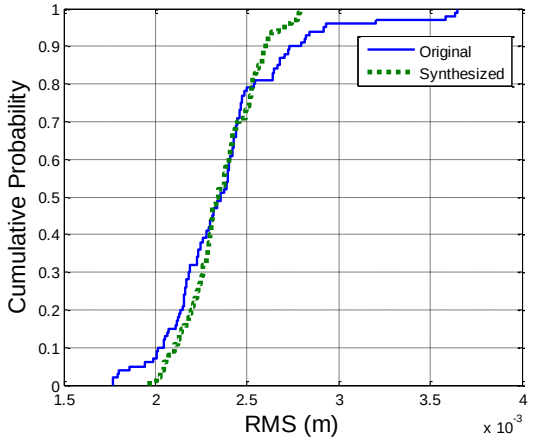

Figure 3-7. RMS distribution of original and synthetic profiles.

3.5 Distribution Comparison

The preceding example can be extended to other types of models. The logistic distribution is one of many admissible distributions where the above process can be applied. For admissibility, the distribution must be part of the location-scale family and be defined for positive and negative location values. They may also include an additional parameter for shape. Some admissible distributions are shown in Table 3-2.

Table 3-2. Admissible distributions.

Distribution	**Parameters**
Cauchy	Location, Scale
Generalized Extreme Value	Location, Scale, Shape
Laplace	Location, Scale
t Location-Scale	Location, Scale, Shape
Logistic	Location, Scale
Gaussian	Location, Scale

A small test is performed to find the most appropriate distribution for modeling a "rough" and "smooth" road with a continuous-state Markov chain. The original road profiles are shown in Figure 3-8 and Figure 3-9. The "rough" road is a gravel loop about 130 m long with relatively

large elevation changes. The “smooth” road is from a paved highway in Minnesota that is about 160 m long.

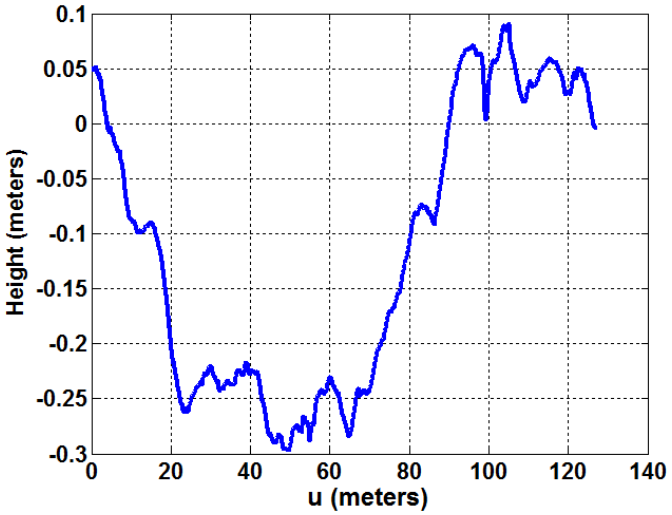

Figure 3-8. Rough road profile, original.

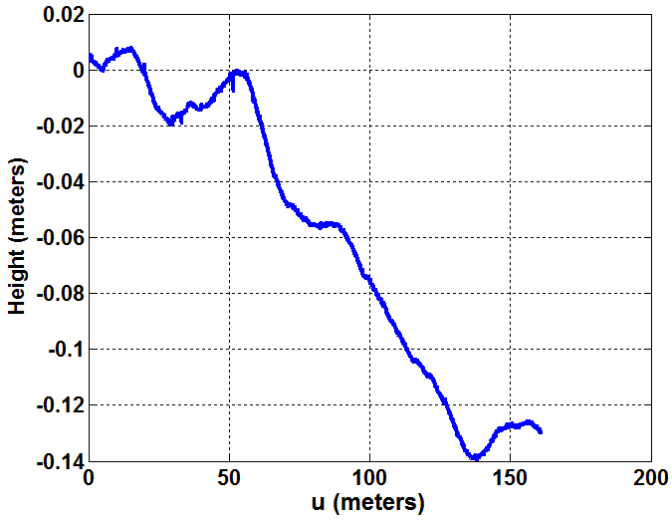

Figure 3-9. Smooth road profile, original.

RMS distributions are calculated and compared for original and synthetic road profiles with a 2-sample Kolmogorov-Smirnov test and bootstrapping (see Section 4.5: Statistical Analysis of Principal Terrain Components). Synthetic profiles are created with each of the admissible distributions. For the sake of simplicity, the parameter distribution of each model is fit with a 3rd degree polynomial. The results are shown in Table 3-3.

Table 3-3. Distribution comparison for continuous-state Markov chain.

Distribution	P-Value Smooth	P-Value Rough
Cauchy	1.55E-45	3.65E-06
Generalized Extreme Value	2.22E-02	1.55E-45
Laplace	9.24E-05	1.55E-45
t Location-Scale	5.81E-02	1.55E-45
Logistic	9.74E-07	1.55E-45
Gaussian	8.42E-02	1.55E-45

The smooth road was modeled best with a Gaussian based continuous-state Markov chain and modeled worst with a Cauchy based continuous-state Markov chain. If $\alpha = .05$, the null hypothesis of the 2-sample KS test (that the two profiles came from the same underlying distribution) would be rejected in all cases except the Gaussian and t Location-Scale models. The Cauchy based chain, however, did the best job modeling the rough road. All p-values would indicate a rejection of the null hypothesis, though. In fact, the number 1.55E-45 indicates a maximum KS statistic, meaning no overlap of original and synthetic profile RMS distributions. Clearly, a rough road could not be effectively be modeled with these results.

3.6 Future Work

A further exploration of modeling types and choices would benefit the application of continuous-state Markov chains to terrain road profiles. The distribution comparison performed in the previous section showed that a continuous-state Markov chain can probably not effectively model a rough road profile. This may be due to the broad range of frequency content present. Perhaps introducing frequency decomposition to profiles such as this would improve the quality of the synthesized profile. Also, additional statistical tests can be used to determine the model quality.

Furthermore, bivariate distributions may prove to be an effective model for terrain. For example, a bivariate Gaussian can be described with five parameters (mean-x, mean-y, variance-x, variance-y, and correlation coefficient). Any bivariate distribution can be viewed as a conditional distribution and subsequently model a Markov chain.

Various windowing methods can be explored to improve the initial values for optimization. In this work, the parameter set $\boldsymbol{\theta}_{MLE}$ is not absolutely guaranteed to globally maximize the likelihood function because the optimization is a local search about the initial parameter set $\boldsymbol{\theta}_{init}$. An adaptive rectangular window, based on the number of transitions held within its bounds, may be appropriate. Alternatively, the transitions could be weighted by their distance from the center of the window. It is possible these other techniques will not alter the initial values for optimization enough to change the end result, but they may still increase

efficiency. If higher degree polynomials are chosen to fit the parameter variation across the state space, the initial parameter estimate for optimization is critical.

Even though the final model created from the above method has the highest likelihood of creating the original profile, some MLE's can be vulnerable to instability. This scenario can occur when the data are very dense and the transition probabilities near the edges of the original profile become insignificant. The MLE of the transition function becomes primarily influenced by the transitions occurring most often (e.g. 5^{th} to 95^{th} percentiles). The result can be large variance transition probabilities when the synthesized profile reaches the boundaries of the original data, causing instability. This problem can be avoided by increasing the degree of the polynomial in the model; however, optimization time may suffer. Other solutions are currently being investigated.

A continuous-state Markov chain may also be applied to surface decompositions to help model three-dimensional terrain. That is, the principal components of terrain (elevation, banking, crowing, etc.) can be represented by a collection traditional two-dimensional longitudinal profiles [3]. These principal component profiles are obtained by projecting the entire surface onto a set of basis vectors. Each component could then be characterized by a continuous-state Markov chain. The synthetic surface would be reconstructed from the collection of synthesized components.

3.7 Conclusions

This work develops a process to estimate a continuous-state Markov process for application with terrain profiles. Current Markov chain applications to terrain profiles require quantization and are described by dense transition matrices. The results of this work produce a better representation of the underlying process of the terrain by building a model around a continuous state space, described by as few coefficients as possible. This is achieved with a compact, versatile Markov chain model (without the need for quantization) that produces synthetic profiles with similar properties to the measured profiles.

A great deal of research is still required to refine this approach. For example, a sliding window is applied to determine the polynomial parameter estimates across the state space; modifications to this window may improve the initial parameter estimates. Numerous admissible distributions can be used to represent the cumulative conditional transition probability and numerous types of terrain need to be considered. Although a short study is shown here, a more comprehensive one would be useful. With so many possibilities available for future testing, it is expected that one or many models, characterized by only a few parameters, can accurately describe terrain profiles.

This compact modeling representation will allow measured terrains with similar physical properties to be grouped together and simulated terrain profiles, with similar physical properties as the group of measured terrain, can be generated in any desired length. In this way, chassis

designers can make informed decisions regarding which terrain sections should be selected for simulation. Knowledge of this excitation, when applied in conjunction with high fidelity tire and vehicle models, would allow chassis loads to be accurately predicted in vehicle simulations. Therefore, throughout the design process the system response to this consistent excitation can be calculated and compared for each chassis design considered. This will, in turn, shorten vehicle development time and reduce overall development costs.

Chapter 4. Surface Modeling

4.1 Introduction

Accurately predicting ground vehicle performance, such as durability and reliability, through modeling and simulation requires accurate vehicle models and excitation of these models. The ability to analyze and simulate terrain will serve as a valuable tool to excite vehicle models, improving the ability to predict durability, reliability, and ride quality through simulation. In turn this will reduce dependence on expensive and time-consuming physical tests for ground vehicle development and allow physical testing to be used for validation and verification of designs.

This work addresses the primary excitation to the ground vehicle, the terrain, for which a modeling and simulation software package is developed. The software, *TerrainSim*, is based on a previous release; however, it is rebuilt from the ground up. The new software package offers major improvements in user interface, visualization, and performance. Additionally, many new concepts have been implemented. These include surface decomposition, frequency decomposition, and new models.

The software decomposes the terrain (three dimensional road surfaces) into its principal components, identifies the optimal parameters for a variety of models based on the projections, and generates synthetic terrain having similar statistical properties. Many options are included for importing terrain, exporting terrain, and model customization. Additionally, there are extensive plotting tools for visualizing terrain, models, and statistics.

The appropriateness of the models created in *TerrainSim* is evaluated in terms of the ability of the synthetic data to match the important statistical properties of the empirical data. Because the empirical and synthetic data are three dimensional surfaces, it is proposed to compare and analyze the empirical and synthetic principal components of terrain. This helps remove the strong correlation among the many longitudinal profiles present in each surface.

The chapter is organized as follows. First, background information is presented on a variety of models, surface principal component decomposition, and statistical comparison testing. A method to model and synthesize a three dimensional surface is developed, followed by a discussion of improvements from strategic frequency decomposition and synthesis. A new method to compare three dimensional surfaces is then proposed. The chapter concludes with a discussion of future work for comparison testing and a comprehensive model study, followed by conclusions.

4.2 Background

4.2.1 Autoregressive Modeling

An autoregressive (AR) model consists of a set of coefficients, $\boldsymbol{\phi}$, and a residual process, $\boldsymbol{a}$, that drives the model. Each point of an AR process is defined by a linear combination of its previous points plus a residual value

$$z_i = \phi_1 z_{i-1} + \cdots + \phi_p z_{i-p} + a_i \,, \qquad \text{Equation 4.1}$$

where the current location is i and the model order is p. If the profile is known, the coefficients can be derived (e.g. via the Yule-Walker method [21]), and the realization of the residual process is calculated. If it can be shown that the residual process is independent and identically distributed (i.i.d.), then the residual process must be strictly stationary and the AR model can be characterized solely by the probability distribution of the stationary residual process. Terrain profiles of typical U.S. highways can be solely modeled this way [8]. Sampling from the i.i.d. residual process may be done using interpolation of its quantile (inverse CDF) function, or the CDF may be described with a known distribution. Maximum likelihood estimation (MLE) is a common method for parameterizing one of these distributions.

4.2.2 Markov Chains

Consider a discrete-time stochastic process

$$\{Z_i, i = 0, 1, 2, \ldots\}, \qquad \text{Equation 4.2}$$

where Z_i are a family of continuous random variables defined on a common probability space. Each measurement (representing a realization of the process) is taken at a discrete moment in time, i. Let S represent the state space where all z_i are elements of S. It should be clear that z_i can take on any value within the continuous state space, *S*. Throughout the development of this technique, the distinction is explicitly made between the general case where all possible realizations (all possible collections of z_i), and the specific case of a particular realization (a particular measured terrain) is being considered.

The continuous-state Markov property can be written as

$$f\left\{Z_{i+1} = z_{i+1} \middle| \begin{matrix} Z_0 = z_0, \ldots, \\ Z_{i-1} = z_{i-1}, Z_i = z_i \end{matrix}\right\} = f\{Z_{i+1} = z_{i+1} | Z_i = z_i\} \,. \qquad \text{Equation 4.3}$$

where f denotes probability density and z_i represents the general case in which any z_i can take on any value within the continuous state space, *S*. That is, if a signal possesses the first order Markov property then, conditioned on the present, the future and past are independent. Of course the conditional probability must satisfy the axioms of probability, including

$$f\{Z_{i+1} = z_{i+1} | Z_i = z_i\} \geq 0, \forall z_i, z_{i+1} \in S, \qquad \text{Equation 4.4}$$

$$\lim_{z_{i+1}\to\infty} P\{Z_{i+1} < z_{i+1} | Z_i = z_i\} = 1 \ , \qquad \text{Equation 4.5}$$

$$\lim_{z_{i+1}\to-\infty} P\{Z_{i+1} < z_{i+1} | Z_i = z_i\} = 0 \ . \qquad \text{Equation 4.6}$$

Oftentimes, the state space is discrete and finite, and the transition properties are time invariant, in which case the process can be fully characterized by a transition matrix [12]. The issue with this representation is that the number of parameters necessary to characterize a transition matrix is equal to the square of the number of states, which becomes cumbersome for more than a few states. There is also error introduced in the quantization process by which the states are defined. The effect of various binning techniques applied to terrain profiles has been researched previously [13, 14]. The purpose of this work is to expand the application of Markov chains on terrain road profiles from discrete space [11, 13, 14] to continuous space.

$$\mathrm{P}\{Z_{i+1} \leq z_{i+1} | Z_i = z_i\} = F(z_{i+1}|z_i) \ \forall z_i, z_{i+1} \in S, \forall i \ . \qquad \text{Equation 4.7}$$

The transition function can be represented as a cumulative distribution function (CDF) for any current state z_i Therefore, a Markov transition function can be visualized as a "CDF Manifold", or a collection of CDF's that span the Cartesian product of the state space, $S \times S \rightarrow F$. Differentiating the transition function with respect to z_{i+1} yields the Markov probability density function (PDF), or transition density, $f(z_{i+1}|z_i)$. More information on the development of a continuous-state Markov chain can be found in Chapter 3: Developing a Compact Continuous-State Markov Chain for Terrain Road Profiles.

4.2.3 Stochastic Models of Deterministic Terrain

Although the terrain itself is clearly deterministic, terrain measurements are dependent on one of infinitely many paths. The measured profile, therefore, is stochastic and varies according to the path chosen. If deterministic patterns are added to the measurement, however, stochastic modeling may not be appropriate.

Consider a bump-and-pothole course that is commonly found on vehicle proving grounds. The potholes and speed bumps that make up the course are randomly arranged but have fixed heights and widths. Stochastic models may be created from this profile, but deterministic properties, such as the height and width of the events, cannot be consistently recreated. The random component of a stochastic model prevents this. An example of this type of course with AR and Markov chain models applied is shown in Figure 4-1 [22].

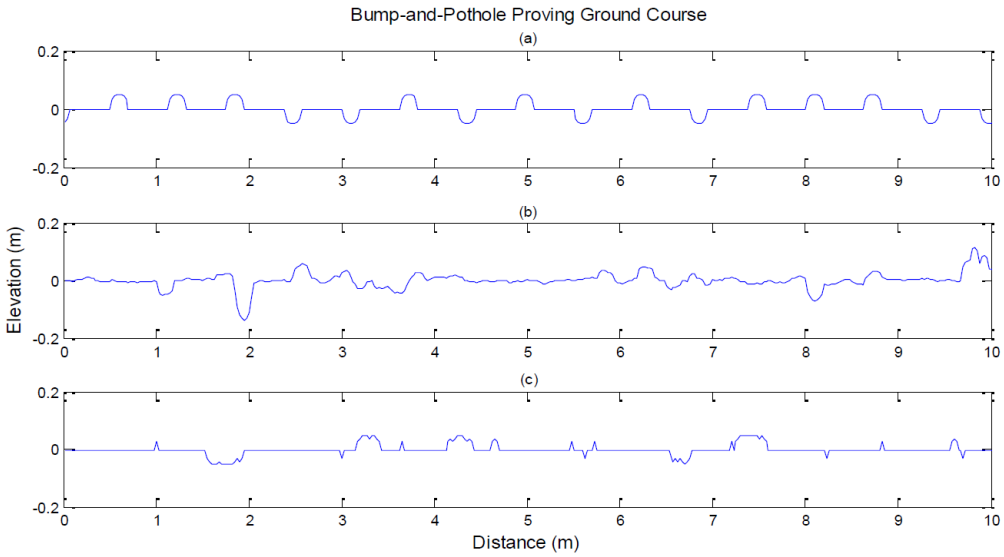

Figure 4-1. (a) Representation of typical bump-and-pothole proving ground course, (b) AR synthesized profile, (c) Markov chain synthesized profile.

The synthesized profiles exhibit many of the same characteristics as the original bump-and-pothole profile. Neither synthesized profile, however, can accurately recreate the constant height and width of the events. The Markov chain based profile contains distinct bumps and holes of varying size and shape. The AR based profile comprises some distinct bumps and holes, but it also has extra rough characteristics, such as spikes.

Alternatively, consider a profile containing periodic square waves (cleat test). This profile could be exactly represented by a linear combination of previous points. Therefore, an AR model could be applied. This would require, however, removal of the residual term in the AR model. Without a residual component dependent on a random process, the AR model would no longer classify as stochastic. A Markov chain could also be applied to this type of profile but with some problems. Similar to the bump-and-pothole test, the length of the square waves would not be consistent. Only the amount of time spent in each state would be the same.

Depending on the application, a profile that contains deterministic components or patterns could be modeled stochastically. If one wishes to introduce some randomness into a pattern enforced profile, a stochastic model would certainly do this. The stochastic model may also create a profile with very similar frequency content. Nevertheless, if the exact pattern (frequency and phase) is vital for simulation or testing, a stochastic model is probably not suitable.

4.2.4 Surface Creation and Decomposition

Consider a collection of many different surfaces. The k^{th} surface, $\{\boldsymbol{z}\}_k$, represents a collection of vectors of transverse heights formatted as a curved regular grid (CRG). Alternatively, the collection of vectors composing the surface can be viewed in matrix form, $\boldsymbol{Z}$.

The CRG consists of a $\boldsymbol{u}$ vector that defines a path and a $\boldsymbol{v}$ vector perpendicular to the path. These vectors are usually regularly spaced. The coordinate definition for a typical CRG is shown in Figure 4-2. Gridding software determines the height of each grid node based on a search of nearby points taken from a point cloud (Refer to Chapter 2: Gridding the Point Cloud) The weighting of nearby points is determined from the inverse distance between data points and grid nodes as well as the horizontal error of the grid nodes [5].

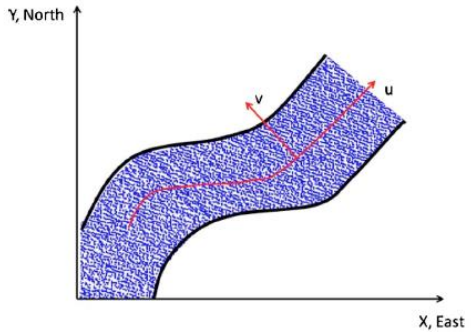

Figure 4-2. Curved regular grid superimposed with a point cloud.

Surfaces can be decomposed into topological components [3]. Each of the transverse profiles that compose a surface is projected on to a set of analytical basis vectors. These basis vectors are based on the Legendre polynomials, shown in Figure 4-3.

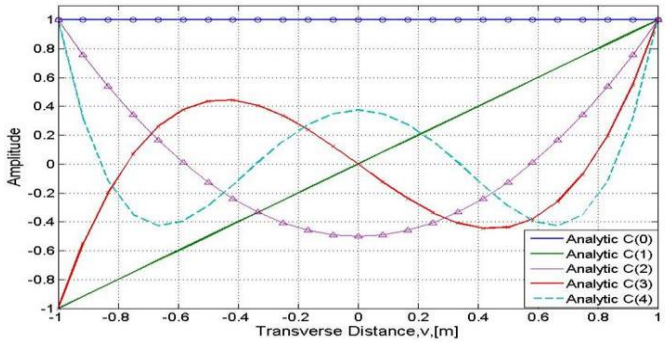

Figure 4-3. First five Legendre Polynomials.

The first five Legendre polynomials can be thought to represent elevation, banking, crowning, asymmetry, and rutting. The Legendre polynomials were chosen after applying SVD on a set of U.S. Highway surfaces and analyzing the empirical basis vectors [3]. They are solutions to the Legendre differential equations and can be expressed by Rodrigues's formula [23]

$$P_n(x) = \frac{1}{2^n n!}\frac{d^n}{dx^n}\left[(x^2-1)^n\right]. \qquad \text{Equation 4.8}$$

The Legendre Polynomials are mapped to the interval [-1, 1] where they are all orthogonal to each other, satisfying

$$\int_{-1}^{1} P_n(x)P_m(x)dx = \frac{2}{2n+1}\delta_{mn}\,, \qquad \text{Equation 4.9}$$

where δ_{mn} is the Kronecker delta function (equal to 1 if $m = n$, equal to 0 otherwise). When applying the Legendre Polynomials to a transverse terrain profiles, it must be discretized based on the number of transverse points in the profile. When discretized, the orthogonality is lost. Although orthogonality may be enforced to simplify some of the calculations, to ensure portability across differently spaced lateral grids, orthogonality is not enforced.

By projecting the original surface on these basis vectors, the surface can be easily represented as a linear combination of the basis vectors. This projection can be described in matrix math by

$$\boldsymbol{B} = \boldsymbol{Z}\boldsymbol{\Omega}^{\dagger}, \qquad \text{Equation 4.10}$$

where † denotes the generalized (pseudo) inverse, $\boldsymbol{\Omega}$ is a matrix of discretized basis vectors (alternately, $\{\boldsymbol{b}\}$), $\boldsymbol{Z}$ is the original surface (alternately, $\{\boldsymbol{z}\}$) in matrix form, and $\boldsymbol{B}$ is a matrix of projections (alternately, $\{\boldsymbol{\beta}\}$). Similarly, the surface can be reconstructed simply with

$$\widehat{\boldsymbol{Z}} = \boldsymbol{B}\boldsymbol{\Omega}\,, \qquad \text{Equation 4.11}$$

where $\widehat{\boldsymbol{Z}}$ is the reconstructed surface. It is the best estimate for the original surface given the set of basis vectors used for the projection.

Because the basis vectors are not orthogonal, they may become ill conditioned. To determine the maximum number of basis vectors (based on the Legendre polynomials) that may be used, the condition number (ratio of largest to smallest singular values) is considered. If the condition number exceeds 10 with a certain number of basis vectors, singular value decomposition (SVD) will be used to create the remaining basis vectors. This number is chosen as a conservative estimate to prevent poor inverse calculations. SVD is applied to the difference of the original surface and a reconstructed surface created from only well-conditioned basis vectors. Therefore, the basis vectors created from SVD are orthogonal to the set based on the Legendre polynomials, as well as each other. An example of how the condition number changes as basis vectors are added is shown in Figure 4-4.

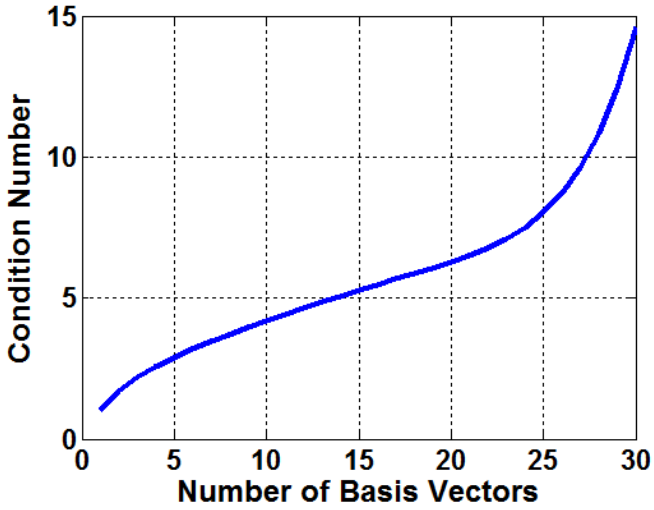

Figure 4-4. Condition number as a function of number of basis vectors for sample road.

For this particular road, there were 89 lateral locations for the grid nodes. Because the condition number exceeds 10 at after 28 basis vectors, the Legendre polynomials would only be used to create the first 27 basis vectors. If more basis vectors were required, SVD would be used for those. The condition number of the set does not change if orthogonal basis vectors are added to the set. As the number of basis vectors increases, the error between the original and reconstructed surface decreases. When the number of basis vectors is equal to the number of lateral points in the surface, this error disappears.

4.3 Modeling a Surface via Principal Components of Terrain

It would be beneficial to characterize terrain as a realization of an underlying stochastic process and to develop a mathematical model of that process (e.g., an autoregressive model or a Markov chain). The model would be parameterized to best fit the measured terrain, preferably with a few parameters. The values for each of the parameters would then indicate the type of terrain being modeled. The resulting stochastic model could then be used to generate as much synthetic terrain of that terrain type as required. It should be clear that the longitudinal profiles that compose a three dimensional road surface are strongly correlated with one another. This correlation makes it very difficult to model the surface stochastically.

Projecting a three dimensional surface on to a set of basis vectors yields a set of principal components of terrain. The first few of these components can be thought of as having a physical meaning (elevation, banking, crowning, asymmetry, and rutting). These components are plainly less correlated with one another than the longitudinal profiles making up the original surface. For example, consider the first 5 projections of gravel (rough) and highway (smooth) roads. Their correlation coefficients are shown in Figure 4-5 and Figure 4-6. Also shown are the correlation coefficients of 5 longitudinal profiles extracted from the same surfaces.

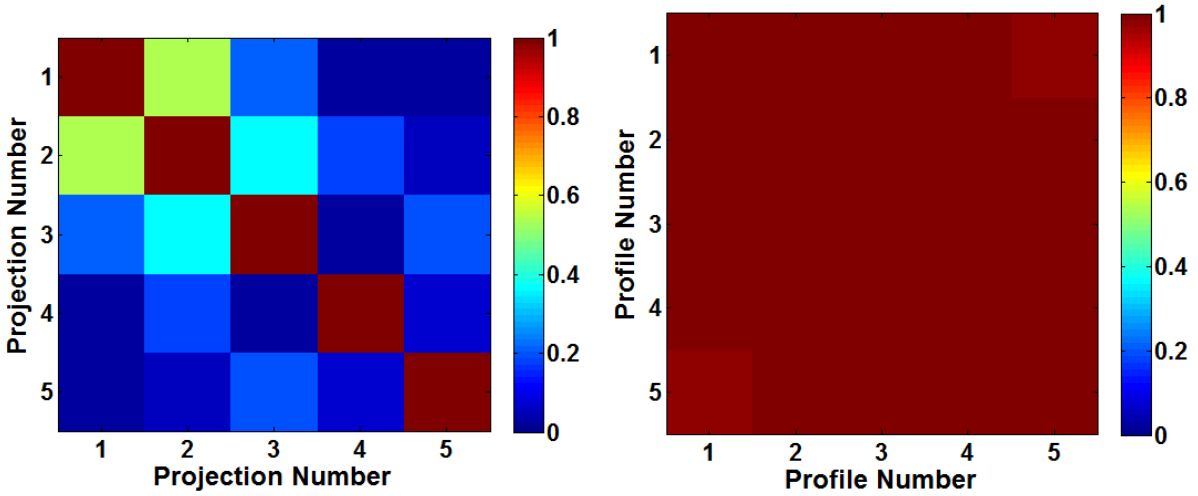

Figure 4-5. Gravel road absolute correlation coefficients, topological components (left) and longitudinal profiles (right).

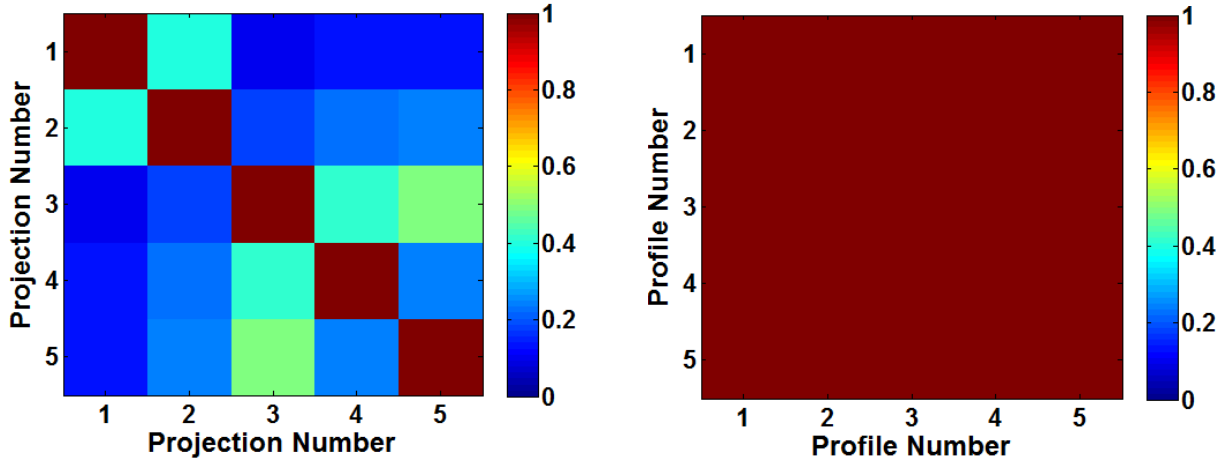

Figure 4-6. Highway road absolute correlation coefficients, topological components (left) and longitudinal profiles (right).

The longitudinal profiles extracted from both roads exhibit strong correlation between each profile. After surface decomposition, the topological components (projections) show much less correlation. For the gravel road, projections 1 and 2 show moderate correlation (about 0.5), and all other projections show low correlation (less than 0.4). For the highway, projections 3 and 5 show moderate correlation, and all others show low correlation. If it is assumed that the components are in fact independent, each component can be modeled individually. This ultimately allows one to create a synthetic surface that is statistically similar to the original.

The synthetic surface can be created as follows. For each terrain component (projection), choose an appropriate stochastic model. Model and synthesize each projection to the desired length of the new surface. As long as each component has the same longitudinal length, the synthesized surface can be constructed from the individual components

$$\widetilde{\boldsymbol{Z}} = \widetilde{\boldsymbol{B}}\boldsymbol{\Omega}\,, \qquad \text{Equation 4.12}$$

where $\boldsymbol{\Omega}$ is the matrix of discretized basis vectors (alternately, $\{\boldsymbol{b}\}$), $\widetilde{\boldsymbol{Z}}$ is the synthetic surface (alternately, $\{\tilde{\boldsymbol{z}}\}$) in matrix form, and $\widetilde{\boldsymbol{B}}$ is a matrix of synthetic projections (alternately, $\{\widetilde{\boldsymbol{\beta}}\}$). An example of an original and synthetic surface is shown in Figure 4-7.

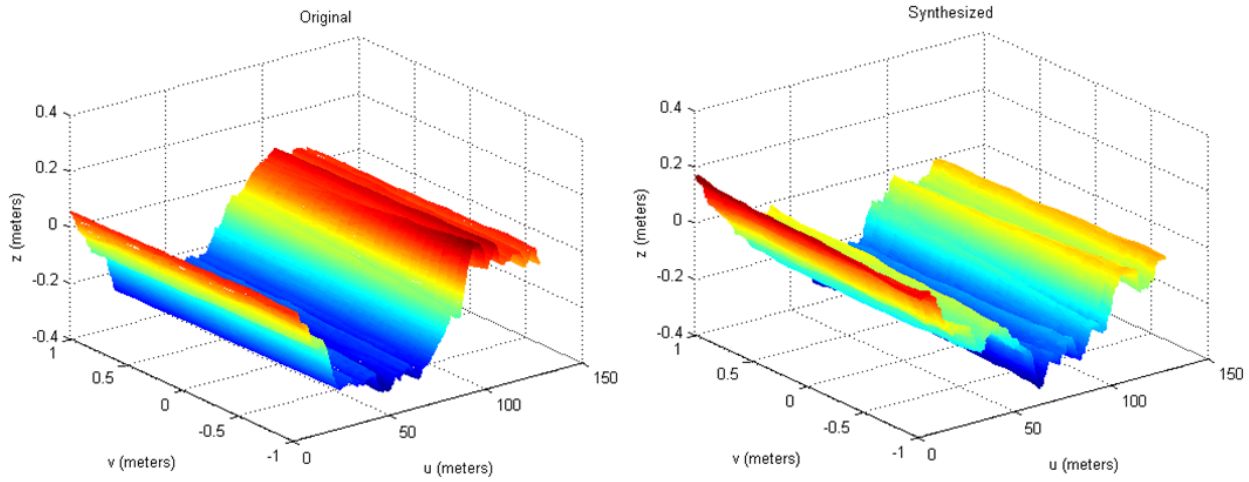

Figure 4-7. Original and synthetic surfaces of a gravel track.

One can clearly see the similarities between the two surfaces. The synthesized surface, although modeled using a collection of two dimensional projections, shows little signs of discontinuity. Hence is the benefit of using principal components of terrain rather than individual longitudinal profiles.

It should also be noted that the number of projections used to model a surface is not limited to those that have a physical meaning. Although the higher order basis vectors do not jump out as a common road characteristic, they can still be used to create synthetic surfaces with higher levels of detail. For example, consider the surface in Figure 4-8.

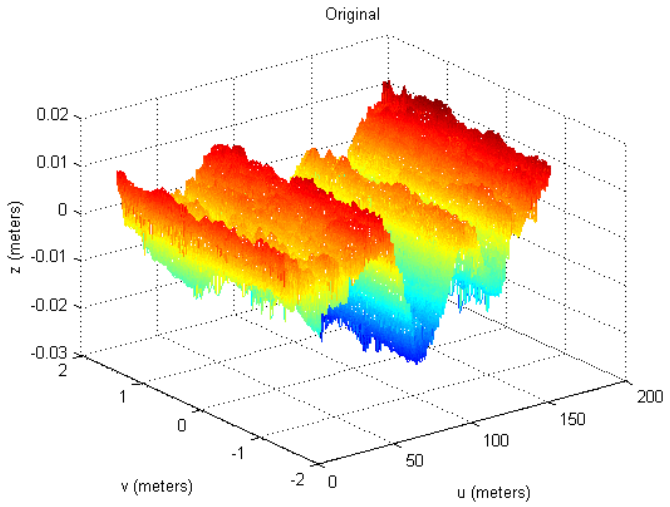

Figure 4-8. Paved surface with high density measurements.

It is clear that there are a diverse set of characteristics present in the surface. They are visible largely because of the density of the grid (about 2.5cm laterally and longitudinally). Projecting and reconstructing this surface on the first five basis vectors produces a surface consisting of only the large scale characteristics. This is shown in Figure 4-9.

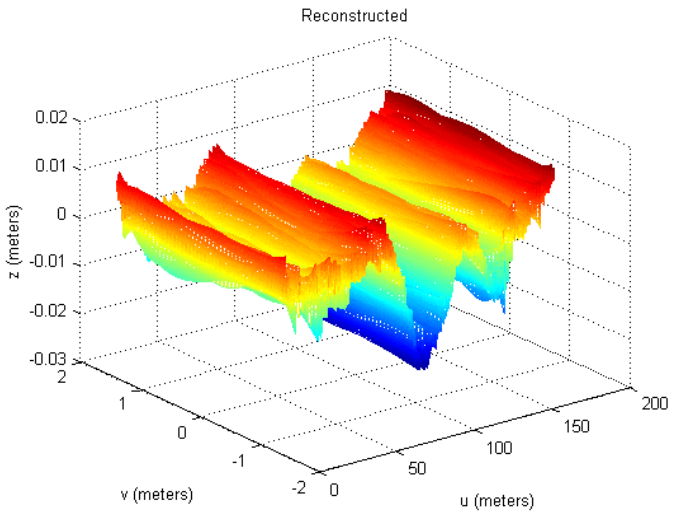

Figure 4-9. Reconstructed surface using first five basis vectors.

The characteristics present in a synthesized surface can only be as good as those available to model. That is, the synthesized surface is ultimately dependent on the reconstructed surface rather than the original, and many of the small events present in some roads can only be described with higher order polynomials. The reconstructed surface approaches the original surface as the number of basis vectors, and thus projections, increases. Because the original surface's lateral profiles consists of 89 points each, the reconstructed surface with 89 basis

vectors is identical to original. An example of these two synthesized surfaces is shown in Figure 4-10.

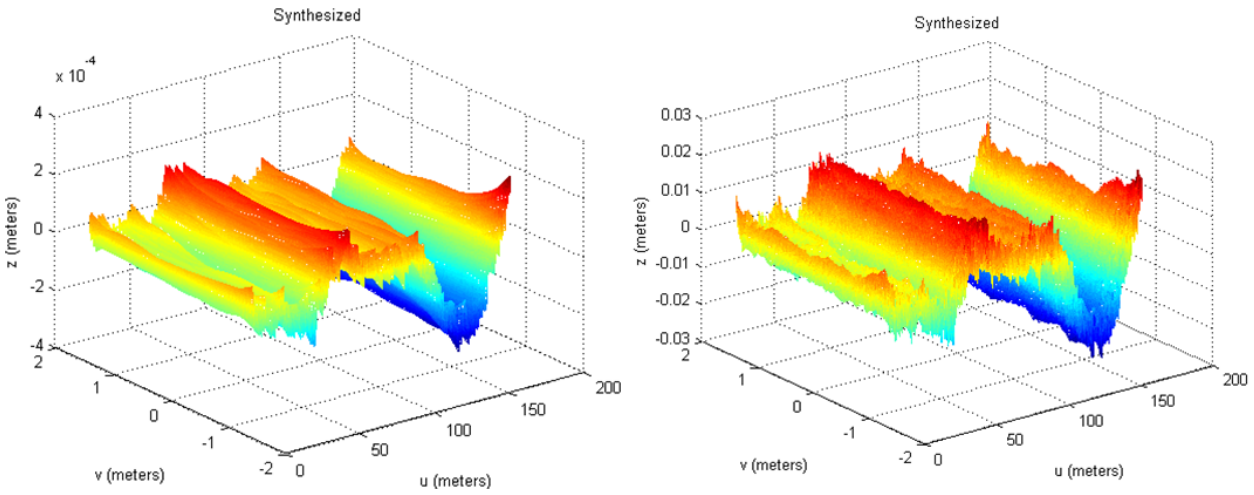

Figure 4-10. Synthesized surfaces using five basis vectors (left) and 89 basis vectors (right).

The two surfaces are reconstructed using the same first five synthetic components representing elevation, banking, crowning, asymmetry, and rutting. The left image reconstructs the surface from solely these projections, while the right surface creates synthetic projections for the remaining 84 basis vectors as well. Therefore, the left surface is essentially a synthesized version of Figure 4-9, and the right surface is a synthesized version of Figure 4-8. Even without a physical interpretation for the higher order basis vectors, the right synthetic surface appears to successfully model many of the small events present in the original surface. Also visible are some spikes in the data, most common on the outer edges of the synthetic road. This is to be expected because the large number of models and synthesized profiles created. Some were likely not perfect models, and the independence among all projections is an ideal assumption. As a whole, however, visual inspection suggests both synthetic surfaces could be used in vehicle simulations.

4.4 Frequency Decomposition of Principal Terrain Components

Decomposing the three dimensional surface into principal terrain components opens many doors for the model types applied to each component. For example, traditional stochastic models such as AR models and Markov chains can be applied to the components. Also, new modeling types, such as continuous-state Markov chains, can also be applied. Each model, however, may have trouble describing too much frequency content at once. It has been shown that the frequency content present in terrain profiles affects the admissibility of various Markov chains [14]. This section develops a method to apply frequency decomposition to terrain components.

Traditionally, frequency is a rate of oscillation as a function of time. Because terrain profiles are measured by location rather than time, it is more intuitive to describe frequency

decomposition in terms of wavelengths. Therefore, this section will discuss wavelength bandwidths, which are in units of meters, instead of frequency bandwidths.

Frequency decomposition is implemented as follows. Given a vector of cutoff wavelengths, $\boldsymbol{c}_w$, each projection, $\boldsymbol{\beta}_l$, is band-pass filtered many times. Each filtered profile contains a distinct set of wavelengths with boundaries specified in $\boldsymbol{c}_w$. The filtered profiles are individually modeled, and synthetic versions of these profiles are created. Each synthetic principal component is constructed by summing the respective synthetic filtered profiles. The synthetic surface can then be formed using the original basis vectors and the synthetic principal components.

For synthesis, the following information must be provided: original principal component profile, model type(s), cutoff wavelengths (c_w), and synthesis length (L). Different models can be applied to different frequency components. The original principal component profile is band-pass filtered based many times. Each filtered profile contains a distinct set of wavelengths with boundaries specified in c_w. Note that the longest and shortest wavelengths in c_w are 0 meters and ∞ meters. Therefore, the first and last filters applied to the original profile are simply high and low pass filters.

The filtered profiles are down-sampled prior to applying any models. This allows the model to "see" further back and improves its quality. Down-sampling rates are strategically chosen such that the filtered profiles are sampled at the smallest rate necessary to contain the entire bandwidth present. According to sampling theorem, this new sample rate (samples/meter) must be

$$s_r = \frac{2\ [\text{samples}]}{w_{short}}, \qquad \text{Equation 4.13}$$

where w_{short} is the shortest wavelength present in a given filtered profile in meters, and s_r is the desired sample rate. Therefore, the down-sample rate necessary to achieve the new sample rate is

$$d_s = s_r u_{inc}\,, \qquad \text{Equation 4.14}$$

where u_{inc} is the gridding increment of the original profile, in meters/sample. The down-sample rate is rounded down if necessary.

Each down-sampled and filtered profile can now be modeled. Any number of models can be used. Each model is synthesized to a distance slightly longer than the desired length of the synthetic surface. That is, if there is a remainder after down-sampling, the up-sampling process will result in extrapolating at the endpoint. To avoid this, the synthesis length is increased by

$$\begin{aligned} \hat{L} &= L + u_{inc}\left(d_{s_{end}} - r\right), \\ r &= \left(\frac{L}{u_{inc}} - 1\right) \left(\text{mod}\ d_{s_{end}}\right), \end{aligned} \qquad \text{Equation 4.15}$$

where L is the requested synthesis length (meters), $\hat{L}$ is the new synthesis length, and $d_{s_{end}}$ is the down-sampling rate of the final filtered profile (longest wavelength content). This ensures no extrapolation, and the final synthesized profile can be truncated to the originally requested length.

Every synthesized signal that has a sample rate less than the original profile must be up-sampled so that it can be added to the other signals. Up-sampling is accomplished via a cubic spline interpolation; however, use of a cubic spline interpolation may introduce shorter wavelength content in the up-sampled signal. This wavelength restriction is enforced in the synthesized interpolated signal so that no unwanted wavelength content arises through additional band-pass filtering. Once every wavelength/frequency component has been modeled, synthesized, and interpolated, each piece is summed together to form the complete synthesized profile.

4.5 Statistical Analysis of Principal Terrain Components

To analyze the statistical similarities between the original and synthesized data, a number of comparison calculations are implemented. The comparisons are done by bootstrapping. That is, many calculations of a specified window width are done at random locations for each profile. These calculations are combined to form a distribution, and the two-sample Komlogorv-Smirnov (KS) test is used to determine a p-value for each comparison [24]. Every statistical test results in a distribution.

There are a variety of statistical tests applied to these projections. Tests for Gaussianity, linearity, and stationarity have been shown to be useful when applied to road profiles [25]. For this reason, these tests have also been implemented for analyzing terrain components. Additionally, statistical tests implemented in previous versions of (two dimensional) *TerrainSim* have been implemented for terrain components. These include: international roughness index (IRI), mean value, filtered root mean square (RMS), standard deviation, and rainflow count. More information on the statistical tests can be found in Appendix A: *TerrainSim* Statistical Tests. Each test statistic is determined using the two-sample KS test. This test calculates the likelihood of two samples having different underlying probability distributions. Therefore, the null hypothesis is that the two samples are from the same underlying population. The critical value for the two-sample KS test is calculated by

$$C = \sqrt{\frac{N_1 N_2}{N_1 + N_2}}\, D\,, \qquad \text{Equation 4.16}$$

where N_1 and N_2 are the number of samples in each set. D is the furthest absolute deviation from the two cumulative distribution functions (CDF's). This is shown in Figure 4-11.

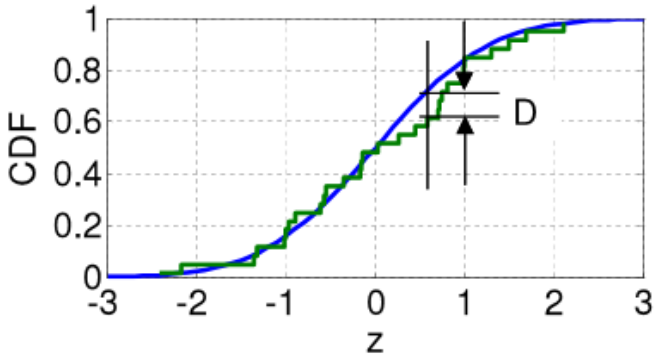

Figure 4-11. Deviation between two CDF's.

After finding the critical value, the null hypothesis can only be rejected if $\alpha > K_a$, where K_α is the desired significance level, and α is calculated from [26]

$$\alpha = 2\sum_{j=1}^{\infty}(-1)^{j-1}e^{-2j^2C^2}\,, \qquad \text{Equation 4.17}$$

If $\alpha > K_a$, then the null hypothesis is rejected with confidence level of α.

A goodness-of-fit (GOF) value is determined by simply doing a weighted average of each of the statistical test results ($p = 1 - \alpha$). Whichever statistical tests are most important can be weighted the highest. Additionally, the quality of the overall synthetic surface can be determined using these GOF's. The GOF for each terrain component can be weighted based on importance, and the overall synthetic surface's GOF can be calculated from the weighted average of each individual terrain component's GOF.

4.6 Physical Interpretation of Roughness Distributions

Some statistical tests used to determine the GOF of a road profile or projection are roughness measures. These include IRI, RMS, standard deviation, and rainflow. Consider the variation of the roughness distribution. A small variation, or tight distribution, may indicate a road that has consistent roughness throughout. Therefore, the loads on a vehicle traveling this road would not fluctuate much. A large variation of the roughness distribution, however, would signify a very diverse road. If a vehicle were to drive over this road, its loads may vary significantly.

The scenario where the variation in roughness is high would certainly concern the designer of a vehicle chassis. The damage on a vehicle may be considerably more on a small rough stretch of road than many miles of relatively smooth road. In this sense, the distribution of a roughness measure contains quite a bit more information than a roughness measure that was simply calculated for the road as a whole.

The distribution of roughness measures may still be impacted by their inherent limitations. For example, RMS and IRI are normalized measures that can be greatly affected by large events or outliers. If a road has a small number of events that each create an excessive amount of impact on the vehicle (compared to the rest of the road), the normalized roughness measure would not explicitly show this. Additionally, if the frequency content of a road excites the primary modes of the quarter-car model, the IRI distribution may be completely different than the other roughness measures. Determining which measure to use must be based on the application (i.e. vehicle type, tire type). One should always take caution with any measure of roughness.

4.7 Software Implementation

The many new techniques developed here have been implemented into a user-friendly software package, *TerrainSim*. The software offers an interface to explore and apply an infinite number of model combinations to a gridded road surface. The user interface is shown in Figure 4-12.

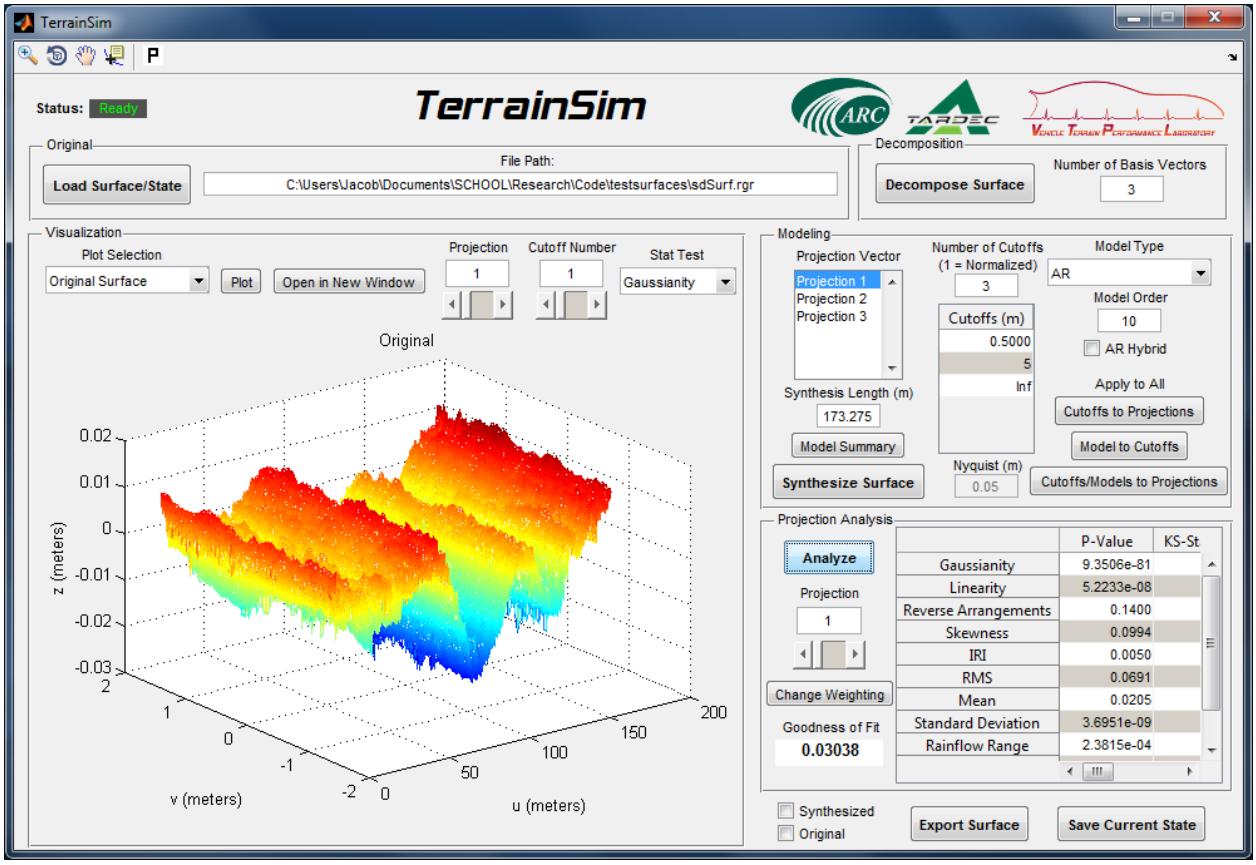

Figure 4-12. *TerrainSim* user interface.

TerrainSim is compatible with a variety of surface formats. After loading a surface, the user can choose the number of basis vectors used to decompose the surface into principal components. Additionally, the software may be used on individual terrain profiles. After decomposing the surface, each projection (terrain component) can be broken into frequency

components and modeled. There are many options for model type and model order, and the synthetic surface can be created to any desired length. Each projection can then be statistically analyzed and compared.

Every step of this process can be examined in the visualization section of the user interface. Finally, the synthetic surface can be exported to a variety of formats (RGR, CRG, Surf). A complete walkthrough of the software can be found in Appendix C: *TerrainSim* Walkthrough.

4.8 Future Work

Although there has been substantial progress in modeling surfaces from this work, there are many opportunities for future research. Because of the infinite number of model combinations available, determining what type of model to use can be a daunting task. A comprehensive analysis of modeling choices and terrain types can be performed to better understand how to best model a particular surface. One may be able to determine the best model types and model orders for each frequency component of each principal terrain component. The cutoff frequencies may be found to be more/less important than the particular model used. Finally, each conclusion may be influenced by the surface type. For example, the cutoff frequencies and model types necessary to describe a gravel road will likely by different than those necessary to describe a paved highway.

The method used to determine the quality of the model(s) may be further explored. There has been some study on which statistics are most important for two dimensional terrain profiles. For example, IRI and RMS are quite popular and have been tuned to measure elevation. Analyzing the banking or crowning projections, however, may require much more research to determine which/if the statistical tests available here are useful. One must also choose how important the higher order projections are with respect to elevation. From the work developed here, there are many tools available to analyze and compare these projections; however, determining how best to use these tools is still an open question.

Perhaps, it may be shown that analyzing the projections is not the best way to compare surfaces. Clearly, analyzing individual longitudinal profiles would be a step backwards because of the strong correlation among them. Simulation software, such as CarSim or Adams, may prove to be a more reliable alternative for determining the similarities between two surfaces. Unfortunately, one would have to perform simulations with a variety of vehicle types to effectively describe the terrains effect on different vehicles.

4.9 Conclusions

This work addresses the primary excitation to the ground vehicle, the terrain, for which a modeling and simulation software package is developed. The software, *TerrainSim*, implements a number of new techniques to model and analyze three dimensional surfaces. Additionally, the

software offers many tools for visualizing each step of the modeling process to better understand the effects of various modeling decisions.

It is shown that three dimensional road surfaces can be modeled using principal terrain component decomposition. By decomposing the surface into its principal components, models can be applied to each individual component and a synthetic version of that component can be generated. The synthetic surface is then created by simply multiplying the synthetic components by the original basis vectors.

The models applied to each component are improved through strategic frequency decomposition. Each terrain component can be filtered into various frequency components, and each frequency component can be modeled individually. The frequency components are downsampled to allow the models to "see" further back, while preserving all the necessary frequency content.

Creating synthetic surfaces also poses a new problem of how to determine the quality of the model. Currently, a method is developed where each principal terrain component is compared to its respective synthetic component with statistical tests. The statistical tests are applied using distributions created from many randomly located windows, and the CDF's of each statistic are compared via the two-sample KS test. The overall GOF can be determined with a weighted average of the many p-values as well as a weighted average of the principal terrain components' GOF.

A comprehensive analysis of various modeling decisions on different terrain types is proposed as future work. Additionally, it is suggested that more research be done in surface comparison, either by furthering the understanding of comparison tests on terrain components, or by introducing multi-body dynamic simulation software.

Accurately predicting ground vehicle performance, such as durability and reliability, through modeling and simulation requires accurate vehicle models and excitation of these models. This work develops a method to model three dimensional surfaces using various decompositions to create statistically similar synthetic surfaces. This is compiled into an easy to use software package. The ability to analyze and simulate terrain serves as a valuable tool to excite vehicle models, improving the ability to predict durability, reliability, and ride quality through simulation. In turn this will reduce dependence on expensive and time-consuming physical tests for ground vehicle development and allow physical testing to be used for validation and verification of designs.

Chapter 5. Compact Terrain Characterization

5.1 Introduction

Engineers from many disciplines who work with terrain surfaces need to describe the overall physical characteristics compactly and consistently. Well established scalar characteristics (IRI and RMS) are the most compact representation, providing insight into the surface character, but limited because they are a single number and do not provide a means by which synthetic surfaces with the same statistical properties can be generated. Alternatively, surfaces can be represented precisely by mathematical models defined by many parameters. Greater insight is gained and synthetic surfaces can be generated, but the representation is not compact. A long standing goal, therefore, is pursued in this chapter.

Currently, surfaces can be decomposed into topological components (elevation, banking, crowning and rutting) and each component can be further decomposed by wavelength content (e.g. long vs. short wavelengths). A mathematical model is applied to each bandwidth of each component; autoregressive models are chosen for the example. Several hundred parameters may be required to accurately describe this complete surface decomposition (reduced from the billion data points that may have defined the surface). For the k^{th} surface, this set of parameters can be written as a single vector, $\boldsymbol{p}_k$. An example is summarized in the flowchart shown in Figure 5-1. For this example, the surface is decomposed into components elevation and bank angle, which are then split into three bandwidths a piece.

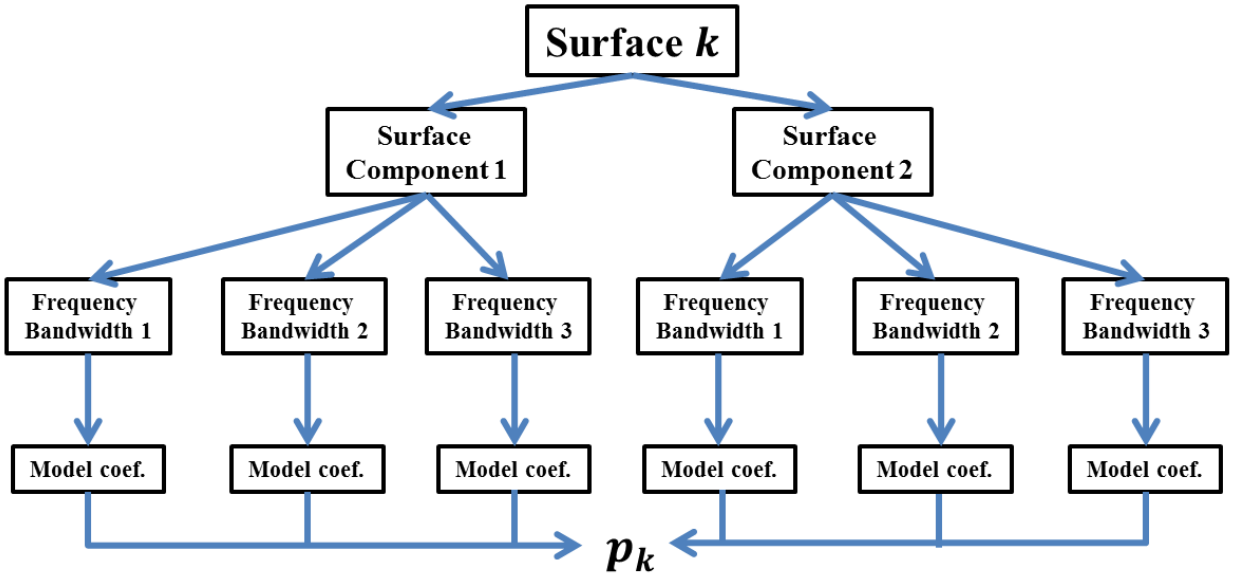

Figure 5-1. Process overview of terrain characterization.

Presently, a method to estimate $\boldsymbol{p}_k$ using a few coefficients is developed; three coefficients are used in the proof of concept. A collection of surfaces is gathered and modeled, producing a

set of parameter vectors. The surfaces used should represent a diverse and complete set to allow characterization to be applied accurately to new surfaces from outside the set. As shown in Figure 5-1, the parameter vectors contain information to model many bandwidths of multiple surface components.

Singular value decomposition is used to identify the most important aspects of the parameter vectors and condense the parameter space while retaining an accurate model of the surface. For the proof of concept, three orthonormal basis parameter vectors are developed: $\boldsymbol{q}_1$, $\boldsymbol{q}_2$, $\boldsymbol{q}_3$. It is shown that this is a sufficient number to model the original collection of surfaces with reasonably accurate results.

The best estimate (in the least-squared error sense) for any $\boldsymbol{p}_k$ is a linear combination of these orthonormal basis vectors: $\boldsymbol{p}_k \approx a_{1k}\boldsymbol{q}_1 + a_{2k}\boldsymbol{q}_2 + a_{3k}\boldsymbol{q}_3$. The resulting set of characteristic coefficients, $\{a\}_k$, is the projection of the parameter vector onto the three basis vectors, is the best estimate of the model parameters, and is proposed as the best compact characterization of terrain surfaces.

The chapter is organized as follows. First, background information is presented on autoregressive models, surface principal component decomposition, and strategic frequency decomposition. This is followed by the development of a method to characterize a collection of surfaces. A proof of concept is performed next, followed by a discussion, proposed future research, and conclusions. Several modeling choices are made in this process, these choices led to results that were promising, but limited in scope. It is strongly believed that further exploration of these modeling choices will lead to a means to accurately characterize the principal physical characteristics of a terrain surface with as few coefficients as possible.

5.2 Background

5.2.1 Autoregressive Modeling

An autoregressive (AR) model is composed of a set of coefficients, $\boldsymbol{\phi}$, and a residual process, $\boldsymbol{a}$. The points of an AR process is then defined by a linear combination of its previous points plus a residual value

$$z_i = \phi_1 z_{i-1} + \cdots + \phi_p z_{i-p} + a_i \,, \qquad \text{Equation 5.1}$$

where the current location is i and the model order is p. If the profile/signal is known, the coefficients can be analytically derived (e.g. via the Yule-Walker method [21]). If it can be shown that the residual process is independent and identically distributed (i.i.d.), then it must be strictly stationary and can be characterized solely by its probability distribution. Terrain measurements of typical U.S. highways can be modeled this way [8].

5.2.2 Surface Creation and Decomposition

Consider a group of many different surfaces. The k^{th} surface, $\{\boldsymbol{z}\}_k$, signifies a collection of vectors of transverse heights formatted as a curved regular grid (CRG). The weighting of nearby points is determined from the inverse distance between data points and grid nodes as well as the horizontal error of the grid nodes [5]. Gridded surfaces can then be decomposed into topological components [3].

Each of the transverse profiles that compose a surface is projected on to a set of analytical basis vectors (sampled discretely). The first five basis vectors can be thought to represent elevation, banking, crowning, asymmetry, and rutting. For more information, refer to Section 4.2.4: Surface Creation and Decomposition.

5.2.3 Frequency Decomposition and Synthesis

It is useful to decompose each terrain surface component (elevation, banking, etc.) into several frequency bands because different modeling techniques may be more effective for different bandwidths. Traditionally, frequency is a rate of oscillation as a function of time. Because terrain profiles are measured by location rather than time, it is more intuitive to describe frequency decomposition in terms of wavelengths. Therefore, this chapter will mostly discuss wavelength bandwidths, which are in units of meters, instead of frequency bandwidths.

Frequency decomposition is implemented as follows. Given a vector of cutoff wavelengths, $\boldsymbol{c}_w$, each principal component, $\boldsymbol{\beta}_{kl}$, is band-pass filtered many times. Each filtered profile contains a distinct set of wavelengths with boundaries specified in $\boldsymbol{c}_w$. The filtered profiles are individually modeled, and synthetic versions of these profiles are created. Each synthetic principal component is constructed by summing the respective synthetic filtered profiles. The synthetic surface can then be formed using the original basis vectors and the synthetic principal components. Frequency decomposition is discussed in more detail in Section 4.4: Frequency Decomposition of Principal Terrain Components.

5.3 Singular Value Decomposition of Parameter Space

It should be clear that a number of models are required to capture the physical characteristics of the surface and that these models must be properly parameterized. This set of parameters can become rather large because of the many models it must describe. Compared to compact characteristics such as IRI and RMS, this parameter set contains much more information about the surface and even allows one to synthesize a similar, unique surface. A compact characteristic, however, is much simpler to represent, transport, and discuss. Therefore, this section uses singular value decomposition to create a new parameter space for characterization that is substantially more compact than the original. It will be shown that this new characterization may be described by as few as three coefficients.

Terrain surfaces can be decomposed into its principal topological components (elevation, banking, etc.) and by wavelength content (e.g. short and long). Any number of components (up

to the number of transverse locations of the surface) and any number of wavelength ranges can be used in the representation. Each vector can be modeled using any number of models, including autoregressive models (AR), Markov chains (MC), and continuous-state Markov chains (CMC).

The individual vector of longitudinal data representing the first principal component (elevation) of the k^{th} surface along the longitudinal direction is $\boldsymbol{\beta}_{k1}$. Similarly, the l^{th} principal component of the k^{th} surface is $\boldsymbol{\beta}_{kl}$.

Consider an individual surface, $\{\boldsymbol{z}\}_k$, that is decomposed into n_b principal components. The l^{th} principal component is decomposed into n_{fl} frequency components. Therefore, the total number of longitudinal vectors of data that must be modeled is

$$n_c = \sum_{l=1}^{n_b} n_{fl} \, . \qquad \text{Equation 5.2}$$

The parameters defining the k^{th} surface are contained in a vector, $\boldsymbol{p}_k$, and the length of the parameter vector is n_p. That is, the model parameters that describe each frequency component are concatenated into one vector. This can be calculated as

$$n_p = \sum_{c=1}^{n_c} o_c \, , \qquad \text{Equation 5.3}$$

where o_c is the number of parameters necessary to describe the model of the c^{th} longitudinal vector. If an AR model were chosen for the c^{th} longitudinal vector, for example, o_c would simply be the order of the AR model.

The vector $\boldsymbol{p}_k$ defines the model of the entire surface. Note that the definition of this parameterization vector is general and applicable to a variety of models (AR, MC, CMC, etc.) and wavelength cutoff locations. Therefore, the parameters representing the m^{th} model for the k^{th} surface is $\boldsymbol{p}_k^m$. In this context, the "model" represents the combination of all modeling choices made for a set of surfaces. This includes the number of basis vectors used in the surface decomposition, the cutoff wavelengths used for frequency decomposition of each projection on to the basis vectors, and the stochastic model type/order chosen for each frequency component. Note there are an infinite number of these combinations.

The set of vectors for all the surfaces, using the m^{th} model, is concatenated into a matrix, $\boldsymbol{P}^m$. That is,

$$\begin{aligned} \boldsymbol{P}^1 &= \left[\boldsymbol{p}_1^1 \, \boldsymbol{p}_2^1 \ldots \boldsymbol{p}_{n_s}^1\right] \\ \boldsymbol{P}^2 &= \left[\boldsymbol{p}_1^2 \, \boldsymbol{p}_2^2 \ldots \boldsymbol{p}_{n_s}^2\right], \end{aligned} \qquad \text{Equation 5.4}$$

where n_s is the total number of surfaces. The number of rows for $\boldsymbol{P}^1$ and $\boldsymbol{P}^2$ differs depending on the required number of parameters for each model (that is, n_p varies with the model being considered).

For each model, a principal component analysis is conducted via singular value decomposition (SVD) yielding sets of singular values and basis vectors specific to each model,

$$\boldsymbol{P}^m \xrightarrow{SVD} \{\sigma_1^m, \boldsymbol{q}_1^m\}, \{\sigma_2^m, \boldsymbol{q}_2^m\} \dots, \quad \text{Equation 5.5}$$

where σ's are singular values and $\boldsymbol{q}$'s are orthonormal basis vectors. Each row of $\boldsymbol{P}^m$ is normalized or standardized so that each parameter has a similar weighting during the SVD. The coefficients necessary to normalize or standardize each row are saved to transform the estimated $\boldsymbol{P}^m$ from projections.

The singular values are arranged in descending magnitude and the parameter vector can be written exactly as

$$\boldsymbol{p}_k^m = \sum_{i=1}^{n_p} a_{ik}^m \, \boldsymbol{q}_i^m \,, \quad \text{Equation 5.6}$$

where n_p is the total number of parameters for the particular model (i.e., n_p will differ depending on the model chosen) and a_{ik}^m is the characterization coefficient for a particular model (indexed by m), basis vector (indexed by i), and surface (indexed by k). Note this basis vector is not the same as the basis vectors used for surface decomposition. The particular value for any a_{jk}^m is determined from the inner-product

$$\langle \boldsymbol{p}_k^m, \boldsymbol{q}_j^m \rangle = \langle \sum_{i=1}^{n_p} a_{ik}^m \, \boldsymbol{q}_i^m \,, \boldsymbol{q}_j^m \rangle = \sum_{i=1}^{n_p} a_{ik}^m \, \langle \boldsymbol{q}_i^m, \boldsymbol{q}_j^m \rangle = a_{jk}^m, \quad \text{Equation 5.7}$$

A matrix of these orthonormal basis vectors is written as

$$\boldsymbol{Q}^m = \left[\boldsymbol{q}_1^m \, \boldsymbol{q}_2^m \dots \boldsymbol{q}_{n_p}^m \right], \quad \text{Equation 5.8}$$

and since the $\boldsymbol{Q}^m$ matrix is orthonormal then $(\boldsymbol{Q}^m)^T \boldsymbol{Q}^m = \boldsymbol{I}$ (the identity matrix) and the matrix of coefficients is written as

$$\boldsymbol{A}^m = (\boldsymbol{Q}^m)^T \boldsymbol{P}^m \,. \quad \text{Equation 5.9}$$

5.4 Developing a truncated set of orthonormal basis vectors for the parameter space

Now consider the case when the number of basis vectors is truncated and only the first n_b basis vectors (corresponding to the largest singular values) are retained ($n_b < n_p$). The

parameter vector for the k^{th} surface, $\boldsymbol{p}_k^m$, can be estimated (in the least-squared-error Galerkin sense), as

$$\boldsymbol{p}_k^m \approx \sum_{i=1}^{n_b} a_{ik}^m \, \boldsymbol{q}_i^m \, . \qquad \text{Equation 5.10}$$

It should be clear that the case when the number of basis vectors is truncated, the values for the coefficients remain unchanged, that is

$$a_{jk}^m = \langle \boldsymbol{p}_k^m, \boldsymbol{q}_j^m \rangle$$
$$\boldsymbol{A}^m = (\boldsymbol{Q}^m)^T \boldsymbol{P}^m \, , \qquad \text{Equation 5.11}$$

however, there will be fewer of these coefficients because the number of basis vectors has decreased to some $n_b < n_p$. That is, $\boldsymbol{Q}^m$ will have n_p rows and n_b columns in the truncated case. The truncated set of orthonormal basis vectors are concatenated and rearranged such that a vector of parameters for a given model and a given surface, $\boldsymbol{p}_k^m$, is estimated in matrix form as

$$\boldsymbol{Q}^m = \left[\boldsymbol{q}_1^m \, \boldsymbol{q}_2^m \, \ldots \boldsymbol{q}_{n_b}^m \right]$$

$$\boldsymbol{a_k^m} = \begin{Bmatrix} a_{1k}^m \\ a_{2k}^m \\ \vdots \\ a_{(n_b)k}^m \end{Bmatrix} \qquad \text{Equation 5.12}$$

$$\boldsymbol{p}_k^m \approx \boldsymbol{Q}^m \boldsymbol{a}_k^m \, ,$$

A matrix of estimated parameters for all the surfaces is the concatenation of the individual parameter vectors, $\boldsymbol{p}_k^m$. For a given model, the matrix of model parameters for all the surfaces is estimated as

$$\boldsymbol{P}^m \approx \boldsymbol{Q}^m \boldsymbol{A}^m \, , \qquad \text{Equation 5.13}$$

where

$$\boldsymbol{P}^m = \left\{ \boldsymbol{p}_1^m \, \boldsymbol{p}_2^m \, \ldots \boldsymbol{p}_{n_s}^m \right\}$$
$$\boldsymbol{A}^m = \left\{ \boldsymbol{a}_1^m \, \boldsymbol{a}_2^m \, \ldots \boldsymbol{a}_{n_s}^m \right\}. \qquad \text{Equation 5.14}$$

Note that the number of rows in the $\boldsymbol{P}^m$ matrix corresponds to the number of parameters required for the chosen model, n_p, but the number of rows in the characterization coefficient matrix, $\boldsymbol{A}^m$, is n_b, a much smaller number (perhaps only three).

The parameters for any model can be estimated by the same number of characterization coefficients. This is accomplished by construction when the number of basis vectors is limited to n_b for all models. Next, it is shown that is it possible not only to have the same *number* of

coefficients for different types of models but that the *same coefficients* can be used for different types of models.

5.5 Model Portability

It should be clear that using a few coefficients, perhaps three, to sufficiently characterize terrain has been a long-standing goal. It would also be a tremendous benefit if the *same coefficients* (i.e., the same $\boldsymbol{a}_k$ vector), could characterize a surface *regardless of the model chosen*.

Assume that one model is determined to be the best and is denoted with an asterisk ($m = *$) and a truncated set of basis vectors is used with some $n_b < n_p$, then $\boldsymbol{Q}^*$ is formed from the SVD of $\boldsymbol{P}^*$, and since $\boldsymbol{Q}^*$ is orthonormal

$$\boldsymbol{A}^* = (\boldsymbol{Q}^*)^T \boldsymbol{P}^* \qquad \text{Equation 5.15}$$
$$\boldsymbol{P}^* \approx \boldsymbol{Q}^* \boldsymbol{A}^*$$

where $\boldsymbol{Q}^*$ is the concatenation of the truncated set of orthonormal basis vectors derived from the SVD of the $\boldsymbol{P}^*$ set of parameters for the "best" model. For any model parameters, $\boldsymbol{P}^m$, such that $m \neq *$, we can define

$$\boldsymbol{Q}^m \triangleq \boldsymbol{P}^m \boldsymbol{A}^{*+}, \qquad \text{Equation 5.16}$$

where $\boldsymbol{A}^{*+}$ is the generalized inverse, giving us the least squared error projection. The generalized inverse (or pseudo inverse) is defined as

$$\boldsymbol{A}^{*+} = \begin{Bmatrix} \boldsymbol{A}^{*T}(\boldsymbol{A}^* \boldsymbol{A}^{*T})^{-1} \text{ for } n_b < n_s \\ (\boldsymbol{A}^{*T} \boldsymbol{A}^*)^{-1} \boldsymbol{A}^{*T} \text{ for } n_b > n_s \\ \boldsymbol{A}^{*-1} \text{ for } n_b = n_s \end{Bmatrix} \qquad \text{Equation 5.17}$$

Therefore, the parameters for any model where $m \neq *$, are estimated as

$$\boldsymbol{P}^m \approx \boldsymbol{Q}^m \boldsymbol{A}^* . \qquad \text{Equation 5.18}$$

In this way the coefficients are model-portable.

5.6 Determining the Best Model

Ultimately, the value of the characterization lies mostly in the ability to capture the important physical characteristics of the terrain. These physical characteristics of each terrain surface are described quantitatively via a set of statistics (RMS, IRI, PSD, etc.). The quality of the characterization can be judged by its ability to create synthetic terrain with similar statistical characteristics to the original. With this quantitative approach, *TerrainSim* can be used to determine the "best" model (and thus the best characterization) by comparing the distributions of various statistics.

Realizations for any set of coefficients (corresponding to the characterization of a surface) are constructed as follows. First a model type is selected so that the proper $\boldsymbol{Q}^m$ is used to estimate the model parameters for the k^{th} surface.

$$\boldsymbol{p}_k^m \approx \widetilde{\boldsymbol{p}}_k^m = \boldsymbol{Q}^m \boldsymbol{a}_k \qquad \text{Equation 5.19}$$

These estimated parameters, $\widetilde{\boldsymbol{p}}_k^m$, are used in the model to generate a synthetic realization, $\tilde{\boldsymbol{z}}_k^m$. Any synthetic realization should have very similar physical characteristics to the true (measured) surface, $\boldsymbol{z}_k$. Identical statistical tests (with *TerrainSim*) are applied to both the true and synthesized surfaces. The best model is then defined as the one that produces statistical distributions of the synthetic surface that are closest to those of the true surface.

5.7 Proof of Concept

A case study of six courses provided from TARDEC is presented to demonstrate the concept developed in this work. These courses consist of two terrain profiles (wheel paths) at a longitudinal spacing of 5mm. There are many types of models that can be applied to a surface. An AR model was selected for all the possible components for the proof of concept presented in this work. Future research should explore other options as well. The following table details the settings chosen for the proof of concept case study.

Table 5-1. Proof of concept modeling choices.

Model Type	AR
Residual Distribution	Logistic
Model Order	10
Cutoff Wavelengths	4m, 40m
Principal Components	Elevation, Banking
Number of Basis Vectors, n_b	3

More details about the autoregressive model can be found in 5.2.1: Autoregressive Modeling. Each road surface is first decomposed into its principal components, elevation and banking. These components are separated into three frequency bandwidths (less than 4m, 4m-40m, 40m and greater). Down-sampling is performed as discussed in Section 5.2.3: Frequency Decomposition and Synthesis

For each course, there are now six longitudinal data sets. Each longitudinal data set is modeled using a 10^{th} order AR model. Because the residual distribution for each AR model is characterized with two parameters (location and scale of a logistic distribution), there are 12 total parameters for each longitudinal data set. Therefore, a set of 72 parameters describes the entire surface.

All 6 courses (indexed by *k*) are modeled and the parameter sets, $\boldsymbol{p}_k$, are calculated. A principal component analysis (via SVD) is performed on the resulting [72 x 6] parameter matrix, $\boldsymbol{P}$. The $n_b = 3$ basis vectors, $[\boldsymbol{q}_1\ \boldsymbol{q}_2\ \boldsymbol{q}_3]$, corresponding to the largest singular values $[\sigma_1\ \sigma_2\ \sigma_3]$ are retained in the [72 x 3] matrix, $\boldsymbol{Q}$.

The courses contained in this study are of varied type and roughness levels. It is assumed that for this proof of concept that these six courses adequately describe the full space of possible parameter vectors. In the future, this technique should be applied to a broader collection of surfaces.

The individual parameter sets for each TARDEC course, $\boldsymbol{P}$, are projected onto the basis vectors, $\boldsymbol{Q}$, resulting in three characterization coefficients for each course, $\boldsymbol{a}_k$. To approximate the full parameter set for a given course, the three element coefficient vector is multiplied by the basis vectors. The approximate parameter set is then used to synthesize a new profile. Table 5-2 shows the characteristic coefficients for each TARDEC course. Each row in the table defines a course's correlation coefficients written as the transpose of the characterization vector (that is, each row is $\boldsymbol{a}_k^T$).

Table 5-2. Characteristic coefficients for proof of concept.

Course	Coefficient 1	Coefficient 2	Coefficient 3
Bears Run	-2.023	0.094	-0.871
Grassy Mogul Bypass	-3.016	1.009	-1.546
Gravel Road Loop	-2.166	1.318	2.621
Korean Loop South	-2.682	0.985	-0.548
Raptor Course	-2.365	-0.938	0.813
Virgin Grade	-1.943	-3.350	0.152

The synthesized and original wheel path profiles are analyzed using statistics and *TerrainSim.* Each course consists of two wheel paths with a longitudinal spacing of 5 mm. The lengths of the courses range from 0.8 to 8 km.

The probability density function (PDF) of each statistic, as well as the real and synthesized profiles, are plotted in Appendix B: Terrain Characterization Test Case Results. Each course is decomposed into its principal components of elevation and banking. The longitudinal data that represent these components, $\boldsymbol{\beta}$, are modeled and synthesized using frequency decomposition and AR models. The statistics being considered are IRI and RMS which are calculated with 100 randomly selected 50m windows (bootstrapping). The distribution of these statistics is calculated, providing much greater insight into the similarities and differences of each synthesis than simply calculating the overall statistic.

Only the original and synthesized *right* wheel paths are shown in the figures; very similar results are obtained by comparing the original and synthesized left wheel paths as well. It should be noted that the difference in the original and the synthetic profiles are attributed to the modeling technique (AR modeling) and the compression of the parameter space to form the characteristic coefficients (that is, some of the difference is strictly attributed to the modeling technique, even without the compression of the parameter space to three coefficients).

Results for one of the courses (Raptor Course) are shown in this section. For this particular course, each profile (left and right wheel path) is about 3.5km long with longitudinal spacing of 5mm (total of 700,000 points). The synthesized profiles are chosen to be the same length as the original, solely for comparison. One advantage of using this method is that synthetic terrain of any length can be generated and the resulting synthetic surface will have very similar properties as the original, finite length, surface. Figure 5-2 shows the original and synthesized right wheel path of the Raptor Course from a complete and zoomed view.

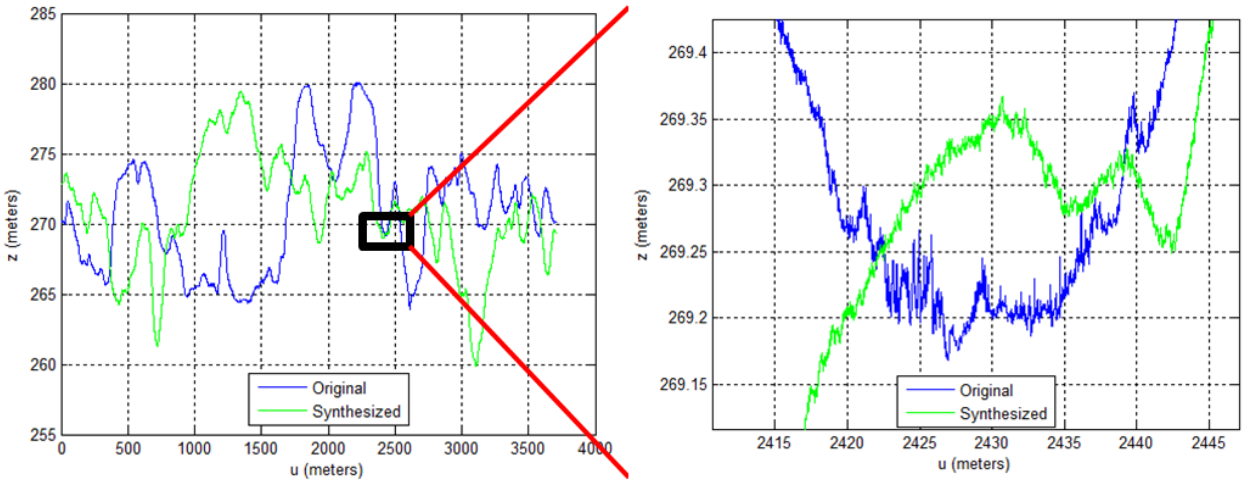

Figure 5-2. Raptor Course right wheel path original and synthesized profiles

Similar results are developed for the remaining five courses and are presented in Appendix B: Terrain Characterization Test Case Results. The wheel path profiles are finely spaced with broad frequency content, yet the similarities between the original and synthetic profiles are consistent at different scales (for brevity, only the complete view of the original and synthesized profiles are provided).

Figure 5-3 and Figure 5-4 show that the statistical distributions for IRI and RMS exhibit less variance for the synthetic profiles than the corresponding original profiles. They do, however, have similar medians. The distributions of the probability density for the synthetic profiles fall within the distribution of the original PDF.

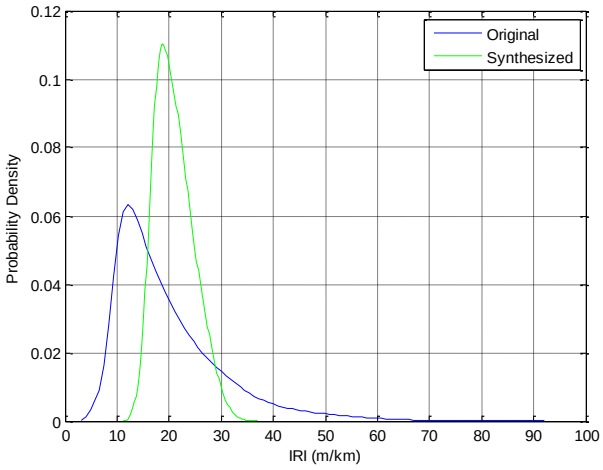

Figure 5-3. Raptor Course IRI distribution original and synthesized right wheel path

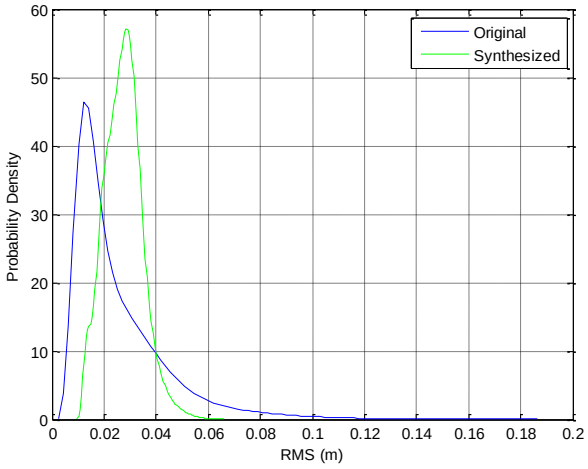

Figure 5-4. Raptor Course RMS distribution original and synthesized right wheel path

5.8 Discussion

The results of this case study demonstrate the great potential for this technique. The similarities in each of the profile comparisons, IRI and RMS distributions, and median statistic values are clear. As expected, the characterization method developed in this work is better able to fit some courses than others, yet some common properties are exhibited. The statistical distributions for IRI and RMS show less variance for the synthetic profiles than the corresponding original profiles. Due to the compactness of the models, this is to be expected. Many of the distributions have similar median points. The bounds of the PDF for the synthetic profiles fall within the bounds of the original PDF for most of the original profiles (the PDF of the RMS of Bears Run and Grassy Mogul Bypass are the two exceptions). In this way, there are no unreasonably rough or unreasonably smooth segments in the synthetic profiles according to the distribution of the IRI and RMS statistics. This is quite encouraging.

The longitudinal data vectors, $\boldsymbol{\beta}$, that are synthesized are simply multiplied by the basis vectors (first two Legendre polynomials) and added together to obtain the surface. In this particular case, the "surface" is two wheel path profiles. Comparing the original and synthesized $\boldsymbol{\beta}$ profiles is another way to determine the validity of the model, while plotting a mesh of the surface is another way to view the results. Statistical analysis of the $\boldsymbol{\beta}$ vectors may also be considered when determining the quality of the characterization technique. For simplicity in this status report, the statistical tests are only applied to the wheel paths rather than the $\boldsymbol{\beta}$ vectors.

As a side note, if the surface can be characterized by three coefficients, it would be possible to map these three characterization coefficients to an 8-bit RGB color scale and represent a road surface with a 24-bit (3-byte) color. In this case, the terrain roughness could be identified by a specific color.

5.9 Future Considerations

Although the proof of concept shows great promise for this technique, there are many modeling choices made that are in need of further research. Each modeling choice has its own considerations. First, only two surface components (elevation and bank angle) and three frequency ranges are being used to decompose the surface. The underlying process for the terrain characterization should be applied towards more complicated surfaces. The number of surface components necessary to model a more detailed road surface (greater than two profiles) is likely more than two. Here, components such as crowning, asymmetry, and rutting can be introduced. Additionally, three frequency ranges may prove to be too much, or more than enough, for different surfaces.

Next, an AR model is used to model each frequency component. The success of the underlying model is largely affected by the model type, order, and cutoff frequencies. There are many tradeoffs when choosing these values. For example, the cutoff frequencies should be chosen such that the most important frequencies in vehicle testing are modeled most effectively. Higher numbers of cutoff frequencies and an increased model order often create better models. However, the more parameters present in the model limits the effectiveness of SVD. Model order and model types may be different across separate bandwidths. There are numerous combinations of components that may be used to fine tune the underlying model and creation of basis vectors. These combinations can be further researched to increase the effectiveness of the model.

Additionally, a complete change in model type for one or more of the components should be explored. For the case of the AR model, SVD can sometimes result in a set of AR coefficients that do not produce a stable filter (even though the original filter was stable). Currently, when this occurs, the poles are adjusted to ensure stability. For example, the poles of an unstable AR model are shown below.

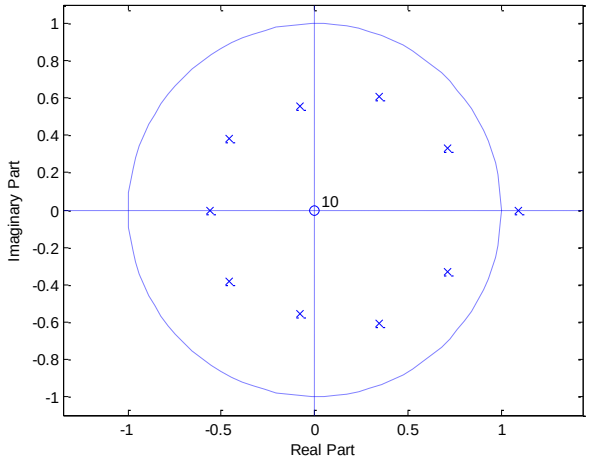

Figure 5-5. Pole zero plot of unstable AR filter

The pole-zero plot is created by finding the roots of the polynomial described by the AR coefficients (which can be cast as an IIR filter). Clearly one pole is outside the unit circle, causing instability. The current solution is to move the pole back within the unit circle to a radius of 0.95 whenever this occurs. The angle (in this case, 0 deg) is maintained. The rest of the poles remain unchanged and the coefficients of the AR model are recreated. This ad hoc solution may be improved through more research.

Because the AR model may not be the best choice to characterize many components of a terrain surface, it may be replaced with a continuous-state Markov chain (CMC). The CMC is defined by a similar number of parameters as an AR model and may provide a better model for some surface components. The CMC has many of its own model specifications that can be fine-tuned for particular types of profiles. Both the AR and CMC models take advantage of the logistic distribution to estimate the distribution of residuals (AR) or transitions (CMC). Other distributions need to be explored to determine the "best" for any particular scenario. Hybrid modeling techniques should also be explored.

While the Galerkin reduction produces a least-squared-error solution to the order reduction problem, there are other metrics that may be considered. For example, if minimizing outliers is of particular interest, a minimax reduction may be appropriate. Alternatively an intermediate metric, such as minimizing the error vector raised to the fourth power (instead of the second) may be appropriate. Ultimately, this method should be applicable to describe the excitation it provides to vehicles. Reduction techniques that emphasize the important excitations to a vehicle should also be explored.

In the proof of concept, the IRI and RMS values were used to demonstrate the quality of the model and reduction technique that results in the characterization coefficients. However, it is clear that these two statistics are almost certainly insufficient to develop a robust technique for

characterization. Other statistics that need to be evaluated include the PSD, Wave Number Spectrum, and tests for linearity, stationarity, and normality. The *TerrainSim* software could be augmented for this purpose.

Multiple models may be applied to a terrain surface, thus creating a model-portable technique. That is, by creating matrices to transfer the characterization coefficients across models, the coefficients describing a particular surface may be used to create multiple parameter sets for different models. It was assumed that a least-squared-error projection would be best, however other metrics should also be considered other than minimized the squared error.

The courses contained in this study are of varied type and roughness levels. It is assumed that for this proof of concept that these six courses adequately describe the full space of possible parameter vectors. In the future, this technique should be applied to a broader collection of surfaces. The courses used to create the basis vectors of the model were also used to create the three coefficients describing each course. Ultimately, there must be a diverse and complete set of data used to create the basis vectors outside of the profiles used for testing. If this can be done, the basis vectors resulting from the SVD of the parameter space can be finalized and *standardized*. In this way, only the three characterization coefficients are needed to completely synthesize a new surface. Standardized basis vectors for each modeling configuration would define the parameterization of each model and synthetic surfaces could then be generated. These synthetic surfaces generated from the same set of characteristic coefficients would all share similar properties.

5.10 Conclusions

Engineers from many disciplines who work with terrain surfaces need to describe the overall physical characteristics compactly and consistently. This chapter establishes the link between the compactness of scalar characteristics (e.g., statistics like IRI and RMS that provide insight into the surface character, but are limited because they are a single number and do not provide a means by which synthetic surfaces with the same statistical properties can be generated) and mathematical models defined by many parameters where greater insight is gained and synthetic surfaces can be generated.

The case study developed in this chapter showed that the distribution of two statistics (RMS and IRI) for a set of six pairs of wheel paths could be emulated after a reduction of the characterization of those wheel paths to three characterization coefficients. The technique developed in this work is quite encouraging (the PDF's of the statistics for the synthesized surfaces are within the variation of the original surfaces and their median values are similar) but required numerous modeling choices to be made. These choices led to results that were promising, but limited in scope. The method developed in this chapter is preliminary and many aspects of the method should evolve with continued research. It is strongly believed that further exploration of these modeling choices will lead to a broadly applicable, standardized means to characterize terrain surfaces with a few (perhaps three) characterization coefficients.

Chapter 6. Conclusions

This thesis aims to make many improvements in the terrain modeling field by addressing the needs associated with gridding, modeling, and characterization. *A collection of novel methods can be developed to aid in the study and application of 3D terrain measurements, which are dense and non-uniform, including efficient gridding, stochastic modeling, and compact characterization*.

This work focuses on measured terrain, primarily taken from a 3D terrain measurement system. The terrain is assumed to be non-deformable and anisotropic in nature. For example, open fields, beaches, mud, or soft soil measurements are outside the scope. This work, however, can be applied to paved asphalt and concrete roads, gravel roads, or rough trails. Any modeling, synthesis, or characterization is performed on terrain that has been gridded into a curved regular grid. Although a point cloud can be reconstructed from synthetic data, the necessary modeling and decompositions cannot be applied to the original, non-uniform, point cloud.

The main contributions of this thesis are:

1) Multiple techniques to effectively and efficiently grid 3D terrain, including automatic center and alternate (random) vehicle path generation, application of sorted gridding methods, and software implementation.
2) A process to create a compact continuous-state Markov chain to be applied to terrain road profiles.
3) Methods to model and synthesize 3D terrain, determine the quality of a synthetic surface, and a software package to explore 3D terrain modeling.
4) A technique to characterize 3D terrain with only a few coefficients.

Accurate terrain models provide the chassis designer with a powerful tool to make informed design decisions early in the design process. During this stage, engineers are challenged with predicting vehicle loads through modeling and simulation. The accuracy of these simulation results depends not only on the fidelity of the model, but also on the excitation to the model. These models are often based directly on physical measurements; therefore, the terrain measurements must be as accurate as possible.

Terrain measurement systems are an enabling technology, creating a new level of fidelity and resolution in terrain measurement. However, these terrain measurements are not collected with uniform spacing, which is necessary for efficient data storage and simulation. The process of accurately gridding the data requires extensive search algorithms that can be computationally inefficient. The grid is also largely dependent on a coordinate transformation known as a curved regular grid, where a path must be chosen to represent the center of the road. By developing and implementing methods to automate and streamline the gridding process, engineers can more efficiently transition from measurement to simulation.

Once the data have been gridded, the relevant terrain points used for simulations can quickly be extracted from the data. Depending on the simulation type, this may be one 2D profile, a 3D wheel-path strip, or the entire 3D grid. Regardless of the format of the terrain data used for simulation, it is beneficial to characterize the terrain as a realization of an underlying stochastic process and to develop a mathematical model of that process (e.g., an autoregressive model or a Markov chain). The model would be parameterized to best fit the measured terrain, preferably with a few parameters. The values for each of the parameters would then indicate the type of terrain being modeled. The resulting stochastic model could then be used to generate as much synthetic terrain of that terrain type as required. The advantage to using synthetic terrain with the same physical properties as the original measured terrain is that some variation in the simulation results can be achieved, thus improving the reliability of the simulation results and decreasing the need for measured terrain.

In addition to having the ability to create unique, synthetic terrain, engineers from many disciplines who work with terrain surfaces need to describe the overall physical characteristics compactly and consistently. Well established scalar characteristics, such as International Roughness Index (IRI) and Root-Mean-Square (RMS), are the most compact representation, providing insight into the surface character, but limited because they are a single number and do not provide a means by which synthetic surfaces with the same statistical properties can be generated. Alternatively, surfaces can be represented precisely by mathematical models defined by many parameters. Greater insight is gained and synthetic surfaces can be generated, but the representation is not compact. Therefore, a long standing goal would be achieved by accurately characterizing the principal physical characteristics of a terrain surface with as few coefficients as possible.

Chapter 7. References

1. Aurell, J. and S. Edlund. *Operating severity distribution - a base for vehicle optimization*. in *Proceedings of the 11th International Association of Vehicle System Dynamics Symposium (IAVSD 1989)*. 1989. Kingston, Ontario, Canada.
2. Kern, J.V. and J.B. Ferris, *Development of a 3-D Vehicle-Terrain Measurement System Part I: Equipment Setup*, in *ISTVS: Innovations in Terrain and Vehicle Systems*2007, ISTVS: Fairbanks, AK.
3. Chemistruck, H.M., J.B. Ferris, and D. Gorsich, *Using a Galerkin Approach to Define Terrain Surfaces.* Journal of Dynamic Systems, Measurement, and Control, 2012. **134**(2): p. 021017.
4. Detweiler, Z.R. and J.B. Ferris, *Interpolation methods for High-fidelity three dimensional terrain surfaces.* Journal of Terramechanics, 2009.
5. Rui Ma, J.B.F., *Terrain Gridding Using a Stochastic Weighting Function.* DSCC, 2011.
6. Wong, J.Y., *Theory of Ground Vehicles*. 2008: John Wiley & Sons.
7. *Classification Using Nearest Neighbors*. 2012 [cited 2012 November 30]; 2012b:[KD Tree Image]. Available from: http://www.mathworks.com/help/stats/classification-using-nearest-neighbors.html#bsehylk.
8. Wagner S. M., F.J.B., *Residual Analysis of Autoregressive Models of Terrain Topology. Submitted to the Journal of Probabilistic Engineering Mechanics*, 2010.
9. Kern, J.V. and J.B. Ferris. *Characterizing 2-D topographic mappings of roads*. 2006. Chicago, IL, United States: American Society of Mechanical Engineers, New York, NY 10016-5990, United States.
10. Wagner, S. and J.B. Ferris, *Stability and Interpretation of Autoregressive Models of Terrain Topology*. Journal of Dynamic Systems, Measurement, and Control, 2011. **133**(2): p. 021003.
11. Ferris, J.B., *Characterising road profiles as Markov Chains.* International Journal of Vehicle Design 2004: p. 103-115.
12. Taylor, H.M. and S. Karlin, *An Introduction to Stochastic Modeling*. 1998, San Diego: Academic Press.
13. Chin, P.A., J.B. Ferris, and A.A. Reid. *Improving Markov Chain models for road profiles simulation via definition of states*. in *American Control Conference*. 2012. Montreal.
14. Chin, P.A., J.B. Ferris, and A.A. Reid. *Methodology for Optimizing First Order Markov Chains of Spectrally Decomposed Terrain Profiles*. in *DSCC*. 2012. Fort Lauderdale.
15. Rao, P., *Maximum likelihood estimation for Markov processes.* Annals of the Institute of Statistical Mathematics, 1972. **24**: p. 333-345.
16. Jiang, G.J. and J.L. Knight, *ECF estimation of Markov models where the transition density is unknown.* Econometrics Journal, 2010. **13**(2): p. 245-270.
17. Hansen, L.P. and J.A. Scheinkman, *Back to the Future: Generating Moment Implications for Continuous-Time Markov Processes.* Econometrica, 1995. **63**(4): p. 767-804.
18. Aït-Sahalia, Y., *Transition Densities for Interest Rate and Other Nonlinear Diffusions.* The Journal of Finance, 1999. **54**(4): p. 1361-1395.
19. Sørensen, M., *Estimating Functions for Discretely Observed Diffusions: A Review.* Lecture Notes-Monograph Series, 1997. **32**(ArticleType: research-article / Issue Title: Selected Proceedings of the Symposium on Estimating Functions / Full publication date: 1997 / Copyright © 1997 Institute of Mathematical Statistics): p. 305-325.

20. Liporace, L., *Maximum likelihood estimation for multivariate observations of Markov sources.* Information Theory, IEEE Transactions on, 1982. **28**(5): p. 729-734.
21. Box, G.E.P., G.M. Jenkins, and G.C. Reinsel, *Time Series Analysis*. 1994, Upper Saddle River, NJ: Prentice-Hall International Inc.
22. S.J., K., *Implication of Terrain Topology Modelling on Ground Vehicle Reliability*, in *Mechanical Engineering*2010, Virginia Tech. p. 97.
23. Agarwal, R. and D. O'Regan, *Legendre Polynomials and Functions*, in *Ordinary and Partial Differential Equations*. 2009, Springer New York. p. 47-56.
24. Frank J. Massey, J., *The Kolmogorov-Smirnov Test for Goodness of Fit.* Journal of the American Statistical Association, 1951. **46**(253): p. 66-78.
25. Chaika, M., D. Gorsich, and T.C. Sun, *Some statistical tests in the study of terrain modelling.* International Journal of Vehicle Design, 2004. **36**(2): p. 132-148.
26. Marsaglia, G., W.W. Tsang, and J. Wang, *Evaluating Kolmogorov's Distribution.* Journal of Statistical Software, 2003. **8**(18): p. 1-4.
27. *US Army Test Operation Command Test Operating Procedure*, 2006.

Appendix A. *TerrainSim* Statistical Tests

A.1 Gaussianity

A Gaussian distribution of data is a normal distribution of values about a mean value (μ), with a standard deviation of σ.

The distribution of the elevation values of the terrain profile is compared to a standard normal distribution in order to obtain a statistic of how closely the terrain data matches a normal (Gaussian) distribution [25]. The statistic in this case is a measure of deviation of the terrain values from the standard normal curve at each data point.

From the terrain data, the mean (μ) and variance (σ^2) are calculated. The terrain data (z) is *normalized* as

$$\hat{\mathrm{Z}} = \frac{x - \mu}{\sigma^2}, \qquad \text{Equation A-1}$$

and then sorted in ascending order. The normal cumulative distribution function (CDF) of the normalized data ($\hat{\mathrm{Z}}$) is then calculated ($\Phi(\hat{\mathrm{Z}})$). The Empirical CDF of $\hat{\mathrm{Z}}$ is calculated as

$$\mathrm{ECDF}\left(\hat{\mathrm{Z}}_i\right) = \frac{n(i)}{N}. \qquad \text{Equation A-2}$$

Here, $n(i)$ is the number of values less than or equal to $\hat{\mathrm{Z}}_i$, and N is the number of data points in the terrain profile. Since $\hat{\mathrm{Z}}$ is ordered, the ECDF becomes a step function that increases by $1/N$ at each data point. The test statistic, D_N, is then calculated as the supremum difference between the ECDF and the Standard Normal CDF of the terrain data,

$$D_N = \left|\mathrm{ECDF}\left(\hat{\mathrm{Z}}\right) - \Phi\left(\hat{\mathrm{Z}}\right)\right|. \qquad \text{Equation A-3}$$

A.2 Linearity

A procedure devised by Keenan is used to test for Linearity of the terrain profile data [25]. Keenan's test statistic, F, will be used as a metric. Keenan's test for Linearity is performed as follows.

Suppose $X_1, X_2, \ldots, X_n$ is a stationary time series. It will be assumed that it is bilinear which means that it can be expressed as an expansion consisting of two parts. That is,

$$X_t = \mu + \sum_{i=-\infty}^{\infty} b_i \varepsilon_{t-i} + \sum_{i,j=-\infty}^{\infty} b_{ij} \varepsilon_{t-i} \varepsilon_{t-j}, \qquad \text{Equation A-4}$$

where ϵ_t is a random series (a series of random shocks), $\{b_i\}$ and $\{b_{ij}\}$ are each a sequence of constants and μ is a constant. In this case X_t has a representation as a linear model, the constants b_{ij} in Equation A-4 would be zero and consequently the data can be approximated by an autoregressive model of a very large order M, written $AR(M)$. That is

$$X_t = a_0 + \sum_{j=1}^{M} a_j X_{j-t} + \varepsilon_t \,, \qquad \text{Equation A-5}$$

where $\{a_j\}$ are constants and M is as described. The test for linearity can be summarized as follows:

The code was developed to calculate the test statistic F for all realizations $\{F_1, F_2, \dots, F_n\}$, where the given profile is divided into segments of a common width, and each segment is considered a realization of the same stochastic process. The code is outlined as below.

Step 1 Regress X_t on $\{1, X_{t-1}, \dots, X_{t-M}\}$. M is a large but fixed integer set as 8, but can be changed. Calculate the predicted values called $\{\hat{X}_t\}$ and let the estimated residuals be called $\{\hat{\varepsilon}_t\}$, for $t = M+1, M+2, \dots, n$. Calculate the residual sum of squares, $\sum_t \hat{\varepsilon}_t^2$.

Step 2 To remove the effects of the correlation of $\{1, X_{t-1}, \dots, X_{t-M}\}$ on $\hat{X}_t^2$, regress $\hat{X}_t^2$ on $\{1, X_{t-1}, \dots, X_{t-M}\}$ and calculate the resulting residuals $\{\hat{\xi}_t\}$ for $t = M, M+1, \dots, n$.

Step 3 Regress $\hat{\varepsilon}_t$ *on* $\hat{\xi}_t$ and calculate the regression coefficient $\hat{\eta}_0$. Set $\hat{\eta} = \hat{\eta}_0 \left(\sum_{t=M+1}^{n} \hat{\xi}_t^2\right)^{1/2}$. Calculate: $F = \frac{\hat{\eta}^2 (n-2M-2)}{\sum_{t=M+1}^{n} \hat{\varepsilon}_t^2 - \hat{\eta}^2}$

Step 4 Repeat steps 1 to 3 for all *n* realizations and calculate $\{F_1, F_2, \dots, F_n\}$.

A.3 Reverse Arrangements

A Reverse Arrangements Test is performed on the profile [25]. In this simple test, each data point is considered individually. The value of that data point is then compared with all other points that follow it, and the number of times that its value exceeds the following points is calculated. This number is called Reverse Arrangements.

A test statistic (ζ) is then calculated according to the following formula:

$$\zeta = \frac{A - \left[\frac{N(N-1)}{4}\right]}{\sqrt{\frac{2N^3 + 3N^2 - 5N}{72}}}, \qquad \text{Equation A-6}$$

where A is the total number of Reverse Arrangements in the profile, and N is the total number of data points in the terrain profile (or projection).

A.4 Skewness

The sample skewness of each segment of the profile is also calculated. Similar to every other test, these values are held to form a distribution, and a p-value is calculated using a two-sample KS test.

A.5 International Roughness Index (IRI)

The International Roughness Index (IRI) is a metric that describes pavement roughness in terms of the number of inches per mile (or meters per kilometer) that the suspension of an ideal car model travels in the vertical plane. The lower the IRI number, the smoother the ride is said to be.

In the calculation of the IRI for a road surface, two filters are used:

1. Moving Average filter: to simulate the enveloping behavior of pneumatic tires and to reduce the sensitivity of the IRI calculation, to the data interval Δ (250 mm).

2. Quarter Car filter: to simulate the dynamic effects that determine how road roughness causes vibrations in a vehicle.

Golden Car parameters are used in the IRI calculations, assuming a vehicle velocity of 80 km/h. These parameters (normalized by the sprung mass) are given as:

a. $c = c_s/m_s = 6.0$

b. $k_1 = k_t/m_s = 653$

c. $k_2 = k_s/m_s = 63.3$

d. $\mu = m_u/m_s = 0.15$

Where
- m_s – sprung mass
- m_u – unsprung mass
- c_s – damping coefficient of the damper
- k_t – stiffness of the tire
- k_s – stiffness of the spring
- μ - ratio of unsprung to sprung mass

The IRI is calculated as:

$$IRI = \frac{1}{L}\int_0^{L/V} \dot{z}_s - \dot{z}_u \; dt \qquad \text{Equation A-7}$$

Where $\dot{z_s}$ – vertical velocity of sprung mass

$\dot{z_u}$ – vertical velocity of unsprung mass

L – length of the profile

V – forward speed

The vertical velocities of the masses are calculated using the method of solving a 2 degree-of-freedom vibrations problem. To improve efficiency, the equations of motion are modeled in state space form and converted to a digital filter in *TerrainSim*.

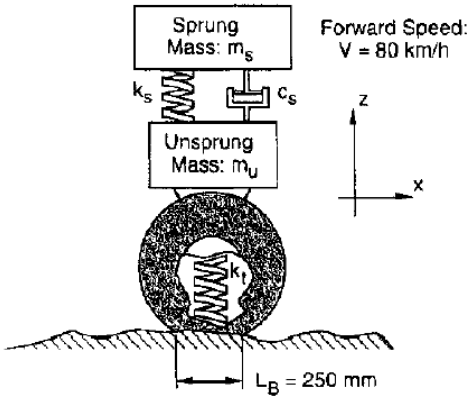

Figure A-1. Quarter car vehicle model used to calculate IRI.

A.6 RMS

Root Mean Square (RMS) calculations are done for many different segments of the profile [27]. First the profile is high pass filtered to detrend the data and remove long wavelength content. This is done using the following two-sided double exponential filter

$$y_n(x) = \frac{\sum_{l=0}^{E}\{y(x+l\delta x) + y(x-l\delta x)\}e^{-\frac{l\delta x}{y}}}{2\sum_{l=0}^{E} e^{-\frac{l\delta x}{y}}}, \qquad \text{Equation A-8}$$

where $y(x)$ is the elevation at point x, $y_n(x)$ is the correction factor, l is the step number, δx is the measurement interval (0.25ft), γ is the weighting constant, and E is the limit of summation. The detrended data is thus.

$$y_d(x) = y(x) - y_n(x) \qquad \text{Equation A-9}$$

This filtering process does not discriminate between low frequency data created as an artifact of the integration process (due to offsets in amplifiers and digitizers, etc.) and legitimate long wavelength data such as hills. It is generally accepted among the terrain roughness community that wavelengths beyond 18 m (60 ft) have little effect on vehicle dynamics, and are ignored. The frequency response of the filter is shown in Figure A-2.

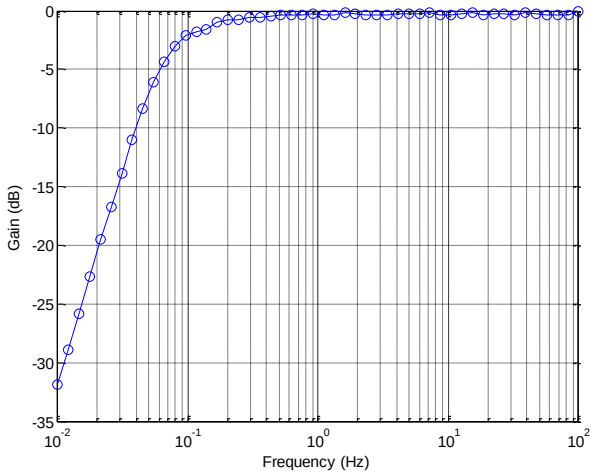

Figure A-2. Frequency response of filter.

After filtering the data, it is zero-meaned, and the RMS is calculated as the standard deviation of the new profile.

A.7 Mean

The mean of each segment of the profile is also calculated. Similar to every other test, these values are held to form a distribution, and a p-value is calculated using a two-sample KS test.

A.8 Standard Deviation

The standard deviation of each segment of the profile (without filtering) is also calculated. Similar to every other test, these values are held to form a distribution, and a p-value is calculated using a two-sample KS test.

Appendix B. Terrain Characterization Test Case Results

The following images compare the original and synthesized right wheel path profiles for each course. Additionally, the distributions of two statistics are shown for each profile. These are RMS (as calculated by TARDEC) and IRI. The distributions are created from randomly selecting 100 segments of 50m length for each profile (original and synthesized) and calculating the statistic. The probability distribution functions (PDF's) are created using a non-parametric kernel smoothing density estimate (MATLAB's *ksdensity* function).

For all plots, *blue* represents the original data and *green* represents the synthesized data. The comparisons of original and synthetic profiles only provide a glimpse of the actual similarities. Because the profiles have a resolution of 5 mm, and their lengths are 0.8 to 8 km long, one certainly cannot see the high frequency similarities between the original and synthesized profiles. The high frequency content, however, does greatly affect the statistics which are plotted as well.

B.1 Bears Run

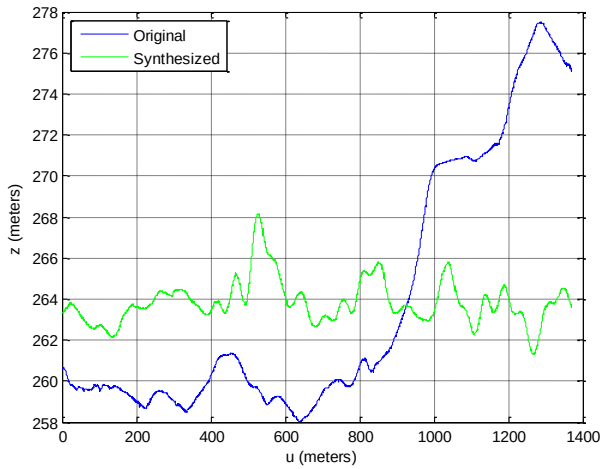

Figure B-1. Bears Run right wheel path original and synthesized profiles.

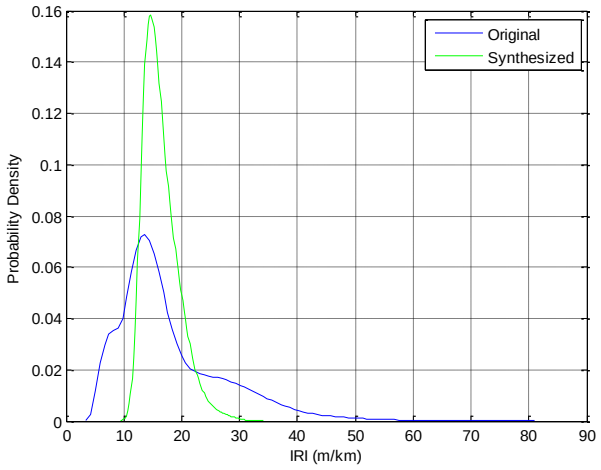

Figure B-2. Bears Run IRI distribution original and synthesized right wheel path.

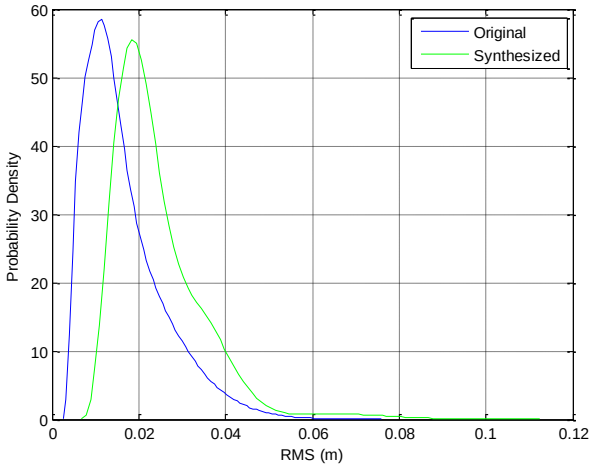

Figure B-3. Bears Run RMS distribution original and synthesized right wheel path

B.2 Grassy Mogul Bypass

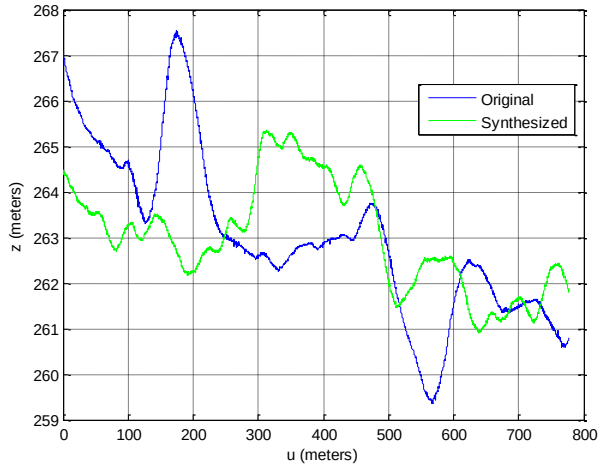

Figure B-4. Grassy Mogul Bypass right wheel path original and synthesized profiles

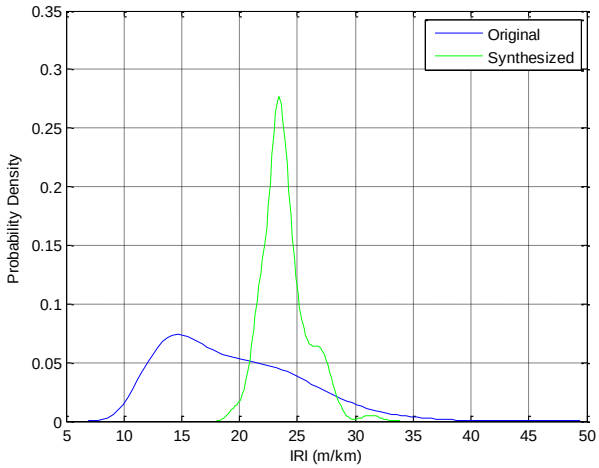

Figure B-5. Grassy Mogul Bypass IRI distribution original and synthesized right wheel path

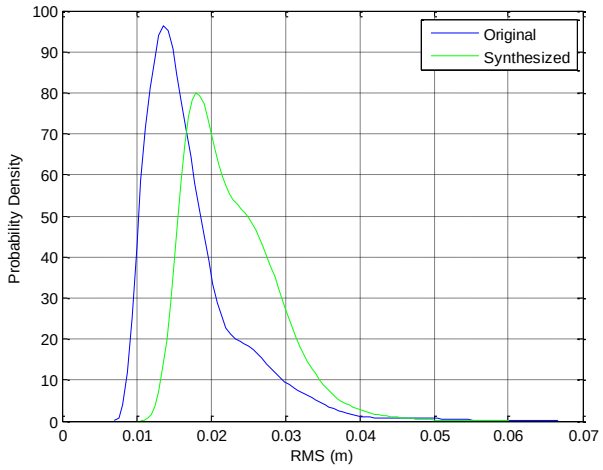

Figure B-6. Grassy Mogul Bypass RMS distribution original and synthesized right wheel path

B.3 Gravel Road Loop

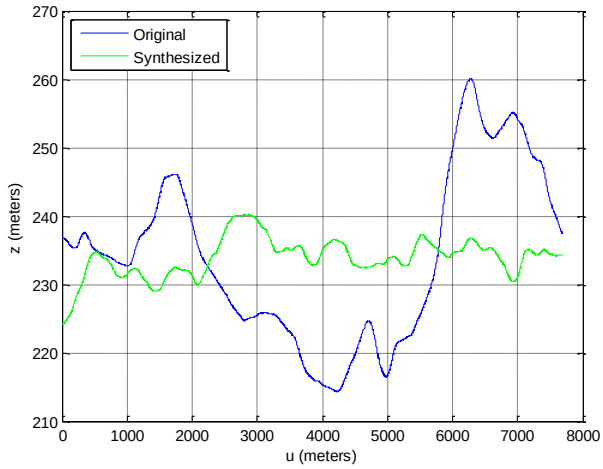

Figure B-7. Gravel Road Loop right wheel path original and synthesized profiles

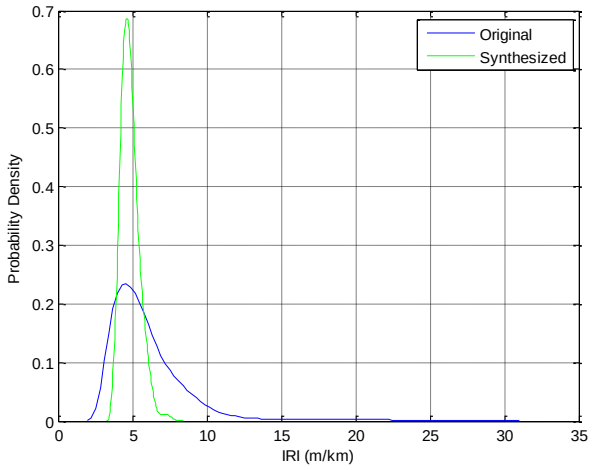

Figure B-8. Gravel Road Loop IRI distribution original and synthesized right wheel path

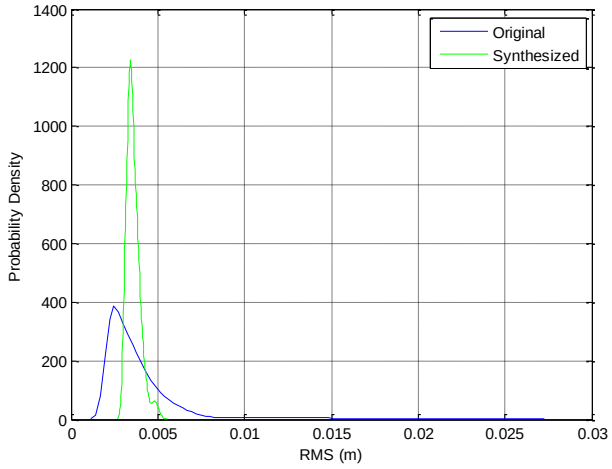

Figure B-9. Gravel Road Loop RMS distribution original and synthesized right wheel path

B.4 Korean Loop South

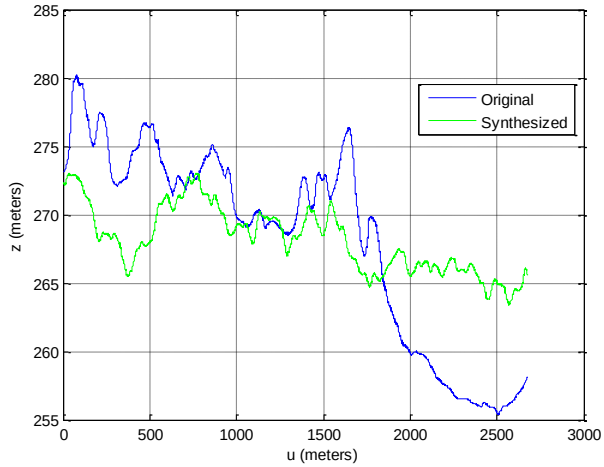

Figure B-10. Korean Loop South right wheel path original and synthesized profiles

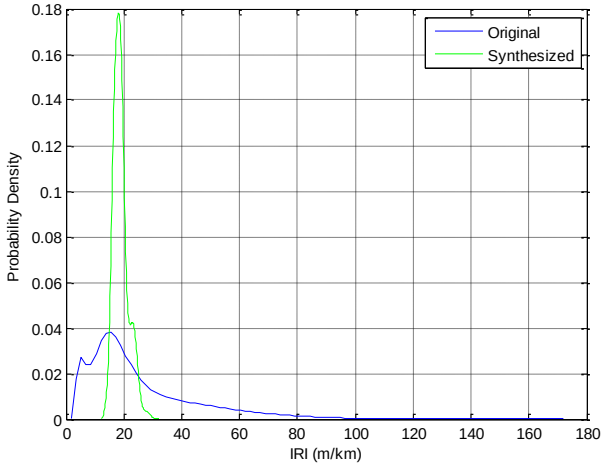

Figure B-11. Korean Loop South IRI distribution original and synthesized right wheel path

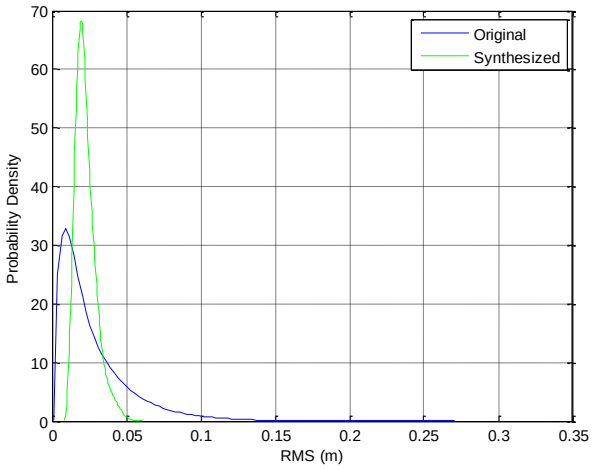

Figure B-12. Korean Loop South RMS distribution original and synthesized right wheel path

B.5 Raptor Course

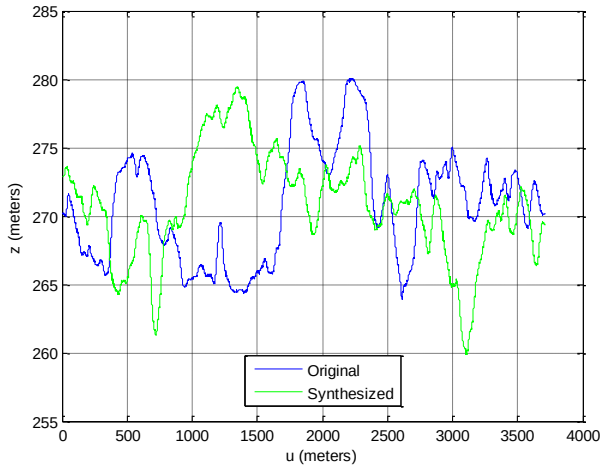

Figure B-13. Raptor Course right wheel path original and synthesized profiles

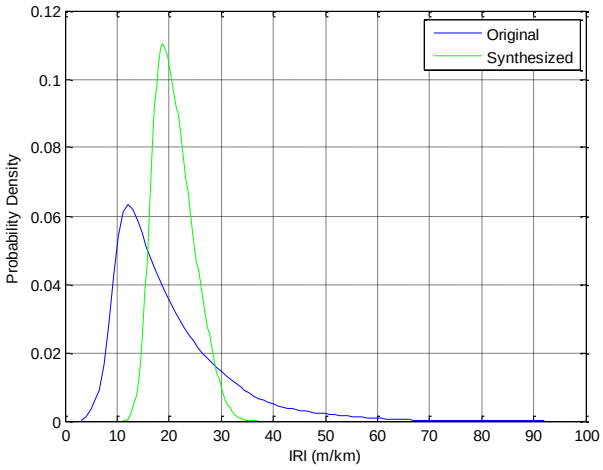

Figure B-14. Raptor Course IRI distribution original and synthesized right wheel path

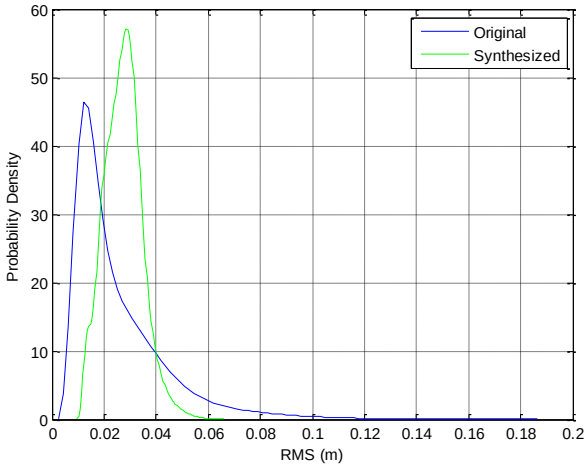

Figure B-15. Raptor Course RMS distribution original and synthesized right wheel path

B.6 Virgin Grade

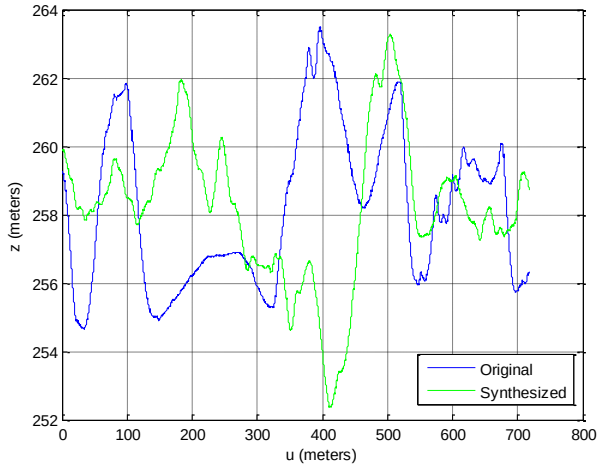

Figure B-16. Virgin Grade right wheel path original and synthesized profiles

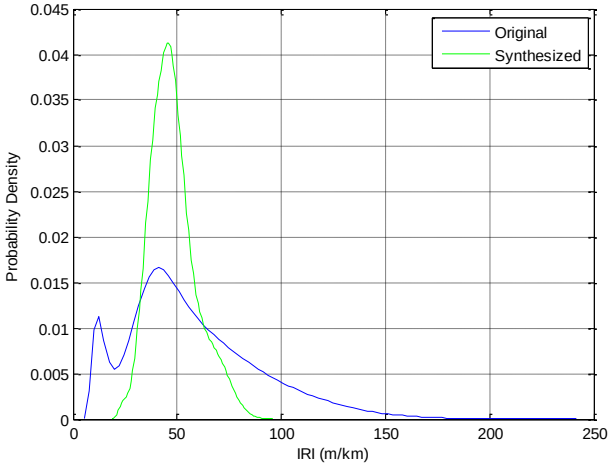

Figure B-17. Virgin Grade IRI distribution original and synthesized right wheel path

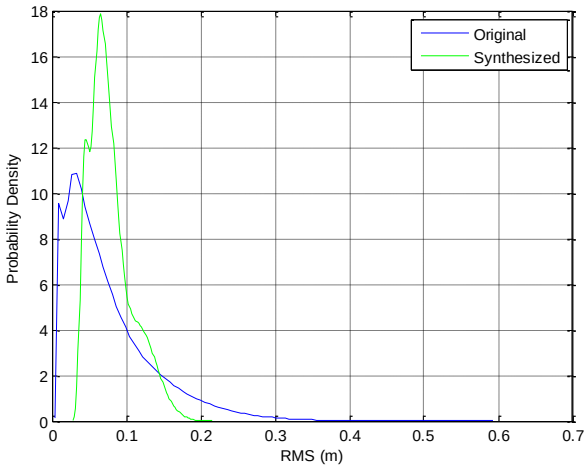

Figure B-18. Virgin Grade RMS distribution original and synthesized right wheel path

Appendix C. *TerrainSim* Walkthrough

C.1 Loading a Surface

To open a road profile/surface, press the "Load Surface/State" button located at the top left of the user interface.

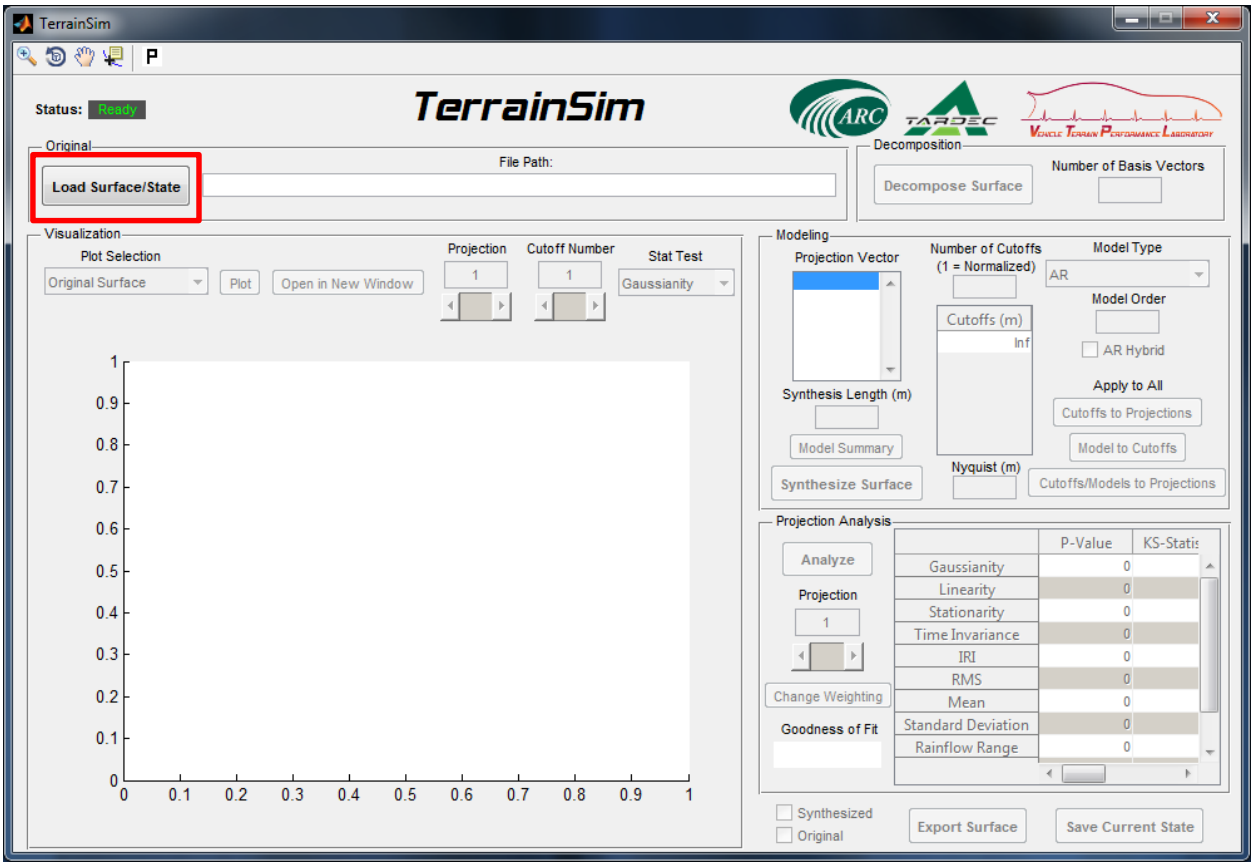

TerrainSim can open 4 file formats. They are: curved regular grid (.crg), regular grid road (.rgr), VTPL CloudSurfer surface structure (.mat), and *TerrainSim* state structure (.tss). If there is a corresponding .rdf file to the .rgr, this will automatically be loaded. More information about the .crg format can be found on the OpenCRG website: http://www.opencrg.org/. More information about the .rgr format can be found on the cosin website: http://www.cosin.eu/. More information about the *TerrainSim* state structure can be found in the section Save Current State.

C.2 Decomposing a Surface

After loading a surface, the next step is to decompose it into its principal components. More information can be found in Section 4.2.4: Surface Creation and Decomposition.

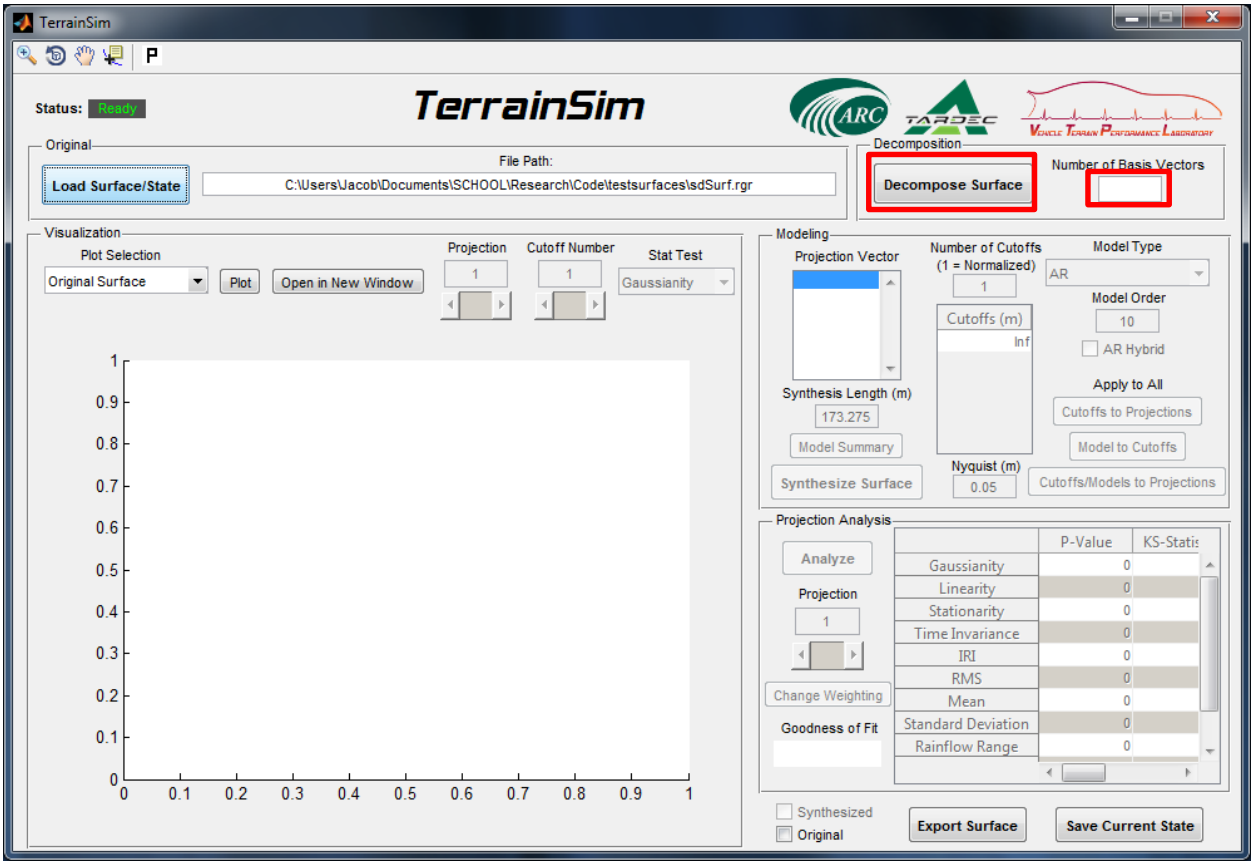

To decompose a surface, simply press the "Decompose Surface" button located in the upper right side of the user interface. If you know exactly how many principal components or basis vectors (elevation, crowning, rutting, etc.) you would like to use, specify this in the box to the right of the button. If this box is left blank or set to "0", a plot showing the error associated with reconstructed surfaces with different number of basis vectors will be shown. Using this, one may easily decide how many basis vectors to use. The number of basis vectors cannot exceed the total number of transverse (lateral) nodes across the grid. By construction, the error drops to zero as the number of basis vectors approaches the total number of transverse locations on the grid.

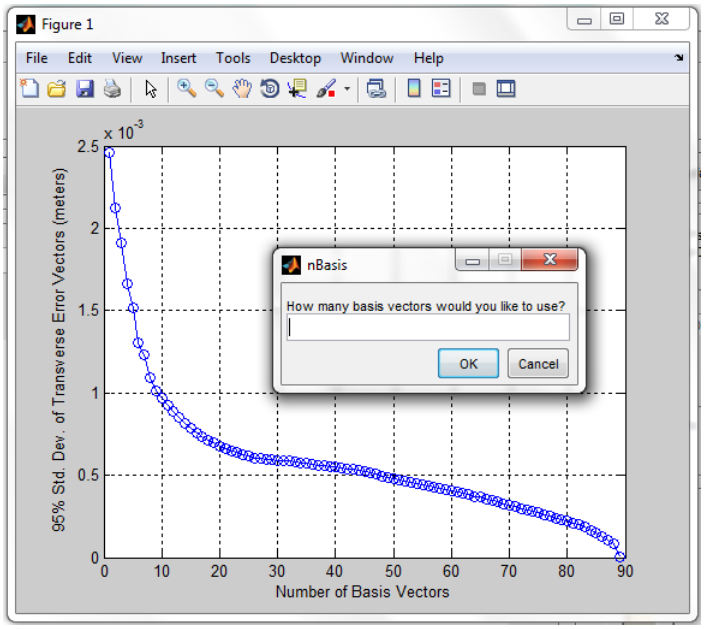

The y-axis shows the 95 % standard deviation of transverse error vectors, while the x-axis shows the number of basis vectors used. The transverse error vectors are obtained by subtracting the original surface from the surface reconstructed from the projections and basis vectors.

If the projection matrix becomes ill conditioned after a certain number of basis vectors, singular value decomposition (SVD) will be used to create the remaining basis vectors. The user will be notified if this occurs. SVD is applied to the difference of the original surface and a reconstructed surface created from only well-conditioned basis vectors.

C.3 Modeling

After decomposing the surface into its principal components, one can model and synthesize a new surface from these projections. The settings for modeling the surface are all located in the “Modeling” section of the user interface.

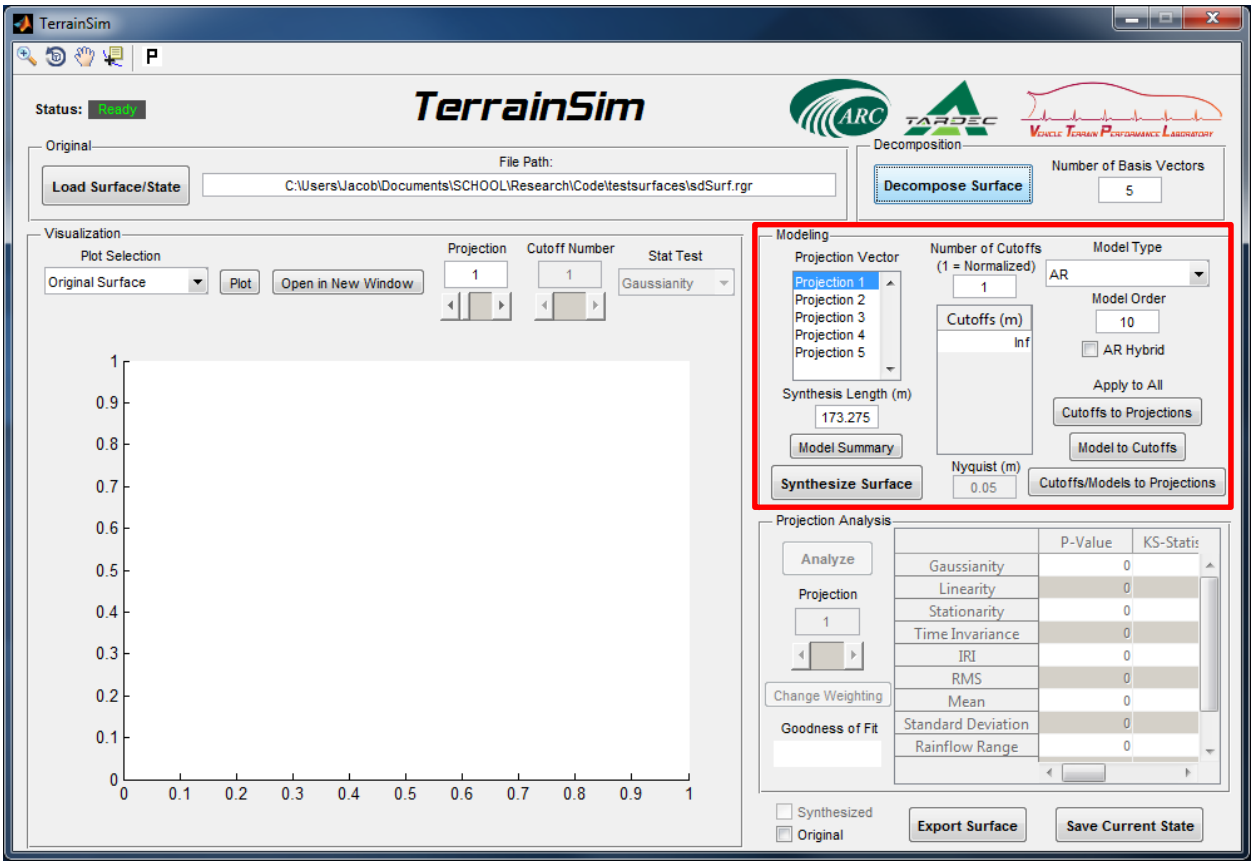

There are many different model settings to choose from before synthesizing data. Remember, rather than modeling the surface directly, *TerrainSim* models and synthesizes the projections of the surface on a set of basis vectors (principal components), which can be reconstructed form a synthesized surface.

C.4 Projection Vector

Projection vector refers to the projections of the true surface on the desired number of basis vectors (elevation, banking, crowning, asymmetry, rutting, etc.). This can be selected from the listbox located on the left side of the modeling section. Any modeling choices will be applied to the selected projection vector.

C.5 Cutoffs

The first option for modeling is to choose is the number of cutoffs. Cutoffs refer to the bandwidths (wavelengths) used to spectrally decompose each signal and model it. More information about spectral decomposition can be found in Section 4.4: Frequency Decomposition of Principal Terrain Components.

The box labeled “Number of Cutoffs” allows the user to change the size of the table located directly below it. In the table you can specify the exact cutoff wavelengths to use for the spectral decomposition, “0” for no spectral decomposition, or one value for a normalized cutoff

wavelength (to apply only one exact cutoff frequency, simply make the second cutoff wavelength "inf"). A normalized cutoff wavelength will automatically be converted to a list of wavelengths (ending when *TerrainSim* determines there will no longer be enough points to model), and can be thought of as the inverse of a normalized frequency.

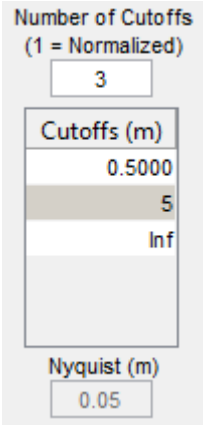

Directly below the cutoff frequency table is a box labeled "Nyquist (m)". This box contains the Nyquist wavelength (inverse of frequency, half the sample rate) of the road profile. This is the shortest wavelength the signal can unambiguously represent. Therefore, it is the shortest wavelength that one can filter the profiles and model separately.

C.6 Model Type

There are many different model types to choose from. These can be accessed from the pull-down menu located below the label "Model Type".

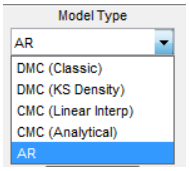

There are 5 model types to choose from. They are:

1. DMC (Classic) – Classic discrete-state Markov chain. "Model Order" specifies the number of bins (states). The bin locations are determined using Kmeans algorithm.
2. DMC (KS Density) – Identical to the classic discrete-state Markov chain except for sampling. Sampling is done by using KS Density (non-parametric empirical distribution estimate) to estimate a continuous distribution for every initial state (specified by "Model Order") using the percentages in each bin.
3. CMC (Linear Interp) – Continuous-state Markov chain using a sliding window and piecewise linear interpolation for all initial states. No continuous functions or MLE's are applied. "Model Order" is not used.

4. CMC (Analytical) – Continuous-state Markov chain as described in Chapter 3: Developing a Compact Continuous-State Markov Chain for Terrain Road Profiles. “Model Order” specifies the degree polynomial used to estimate the parameter fluctuation as a function of the initial state. This field may be left blank or as “0” to allow for plot of the parameter fluctuation and prompts for the model order.

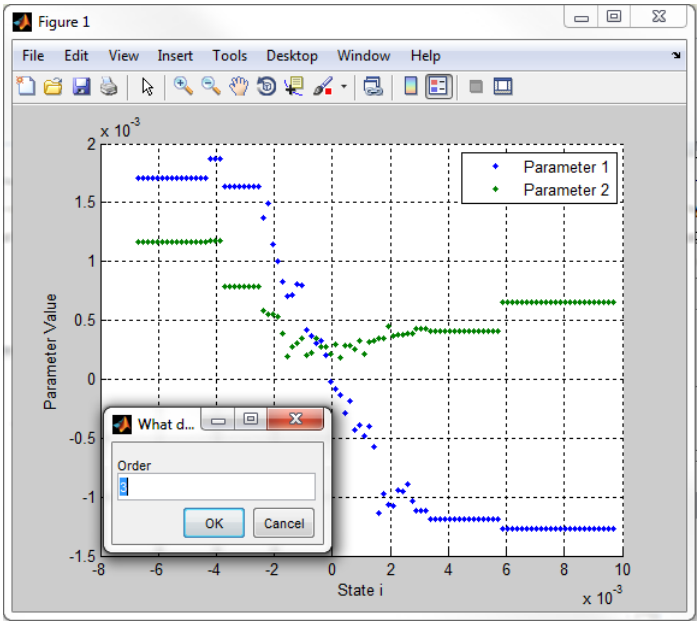

5. AR – Autoregressive (AR) model as described in Section 4.2.1: Autoregressive Modeling. “Model Order” specifies the model order of the AR model. “Model Order” may be left blank or set to “0”. This will allow the user to choose the model order from a plot of the differenced partial autocorrelation.

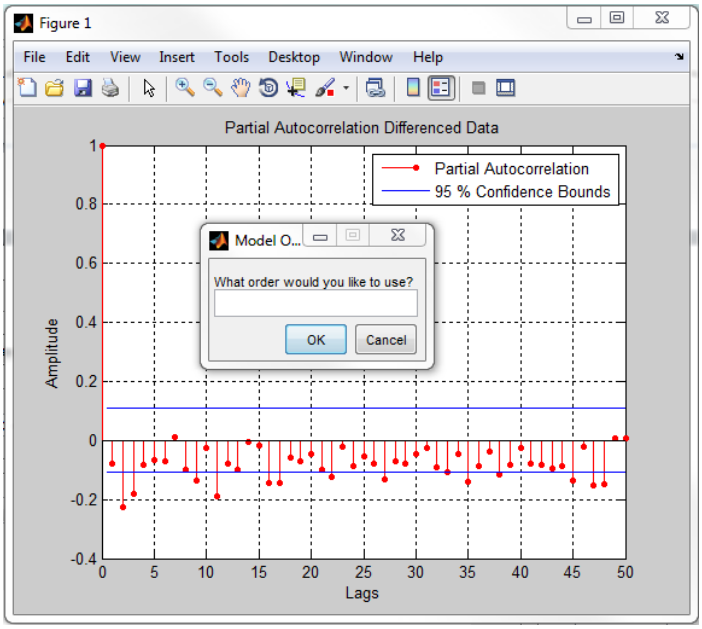

In addition to the model types, there is also an additional model option initiated by selecting the checkbox “AR Hybrid”. This will apply an AR model to the selected projection and use the models/cutoffs specified in the modeling section to model the residuals of this AR model.

C.7 Apply to All

There are 3 buttons located in the “Modeling” section of the user interface that allows quick model type cutoff applications.

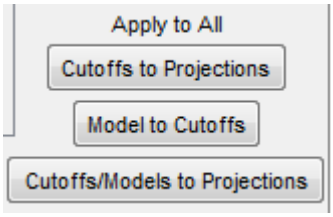

The first button is labeled “Cutoffs to Projections”. This button applies the current cutoff wavelengths configuration to the rest of the projection vectors. The model choices for each projection will remain the same. The second button is labeled “Model to Cutoffs”. This will apply current model type and model order to each cutoff for the currently selection projection vector. The third button is labeled “Cutoffs/Models to Projections”. This button will apply the current projection vector’s cutoff wavelength configuration along with their respective model types/orders to every projection vector. To see a summary of the model information, simply press the button labeled “Model Summary”.

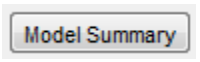

Pressing this will open an HTML file containing a table with all the model information for the current surface.

Modeling Summary

	Cutoff Wavelengths	Model Orders	Model Types	AR Hybrid
Projection 1	0.5 5 Inf	3 10 10	CMC (Analytical) AR AR	no
Projection 2	Inf	10	AR	no
Projection 3	Inf	10	AR	no
Projection 4	Inf	10	AR	no
Projection 5	Inf	10	AR	no

This is a good thing to inspect before synthesizing the surface. The HTML file will also be saved in the current folder for later viewing.

C.8 Synthesize Surface

After selecting all the modeling options, the user may create a synthesized surface. The synthesized surface will be as long as specified in the box labeled “Synthesis Length (m)”.

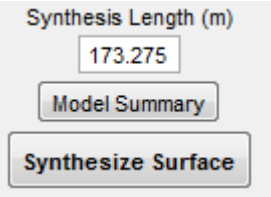

By default, this box is set to the length of the original surface. It may be changed to any value, however. Pressing the button labeled “Synthesize Surface” will start the modeling and synthesizing. Updates regarding the synthesis can be viewed in the command window. Remember, a model is created for each spectral and projection vector specified in the earlier sections.

C.9 Projection Analysis

After synthesizing a surface, the user can compare the original and synthesized projection vectors. This is done using the section in the lower right of the user interface.

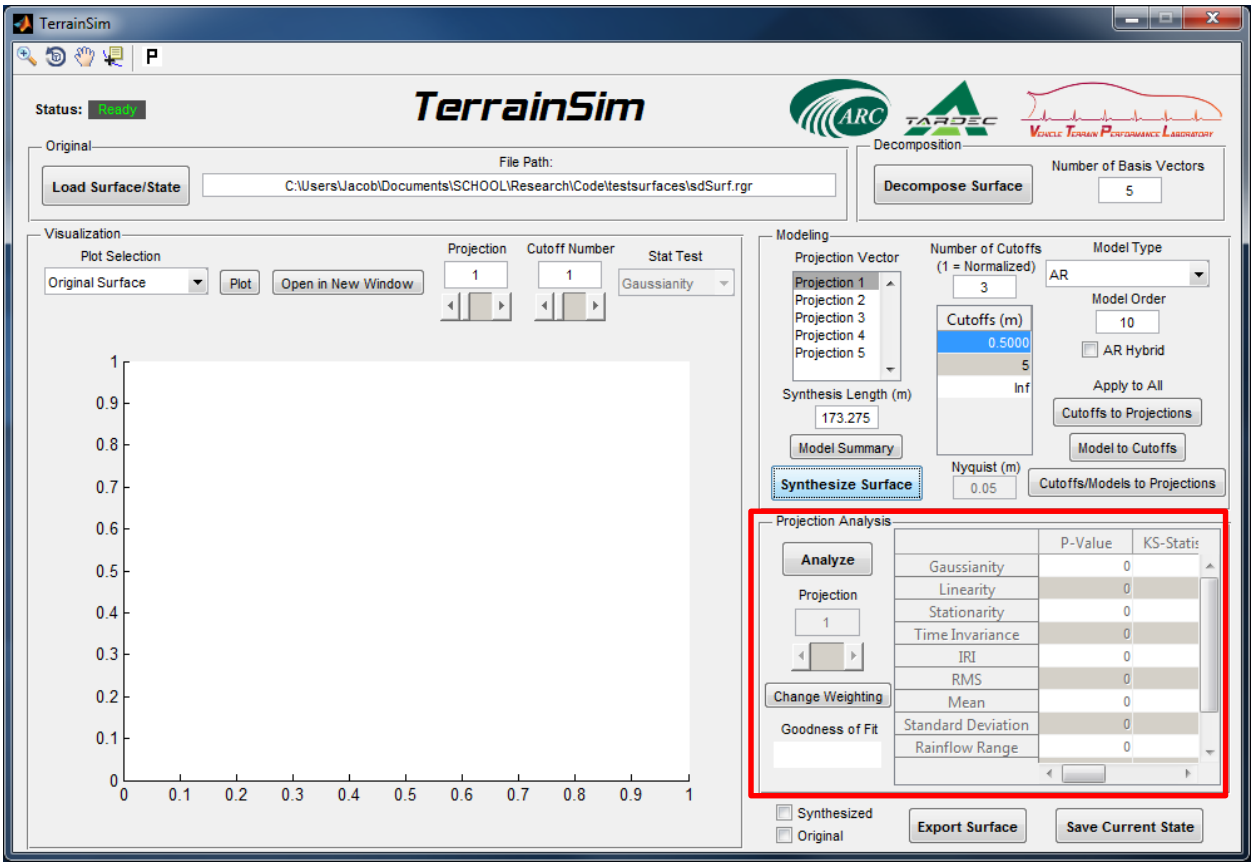

The user may select the button labeled “Analyze” to initiate the analysis. Alternatively, pressing the “Change Weighting” button will allow the user to adjust how each p-value is weighted to obtain the overall goodness-of-fit.

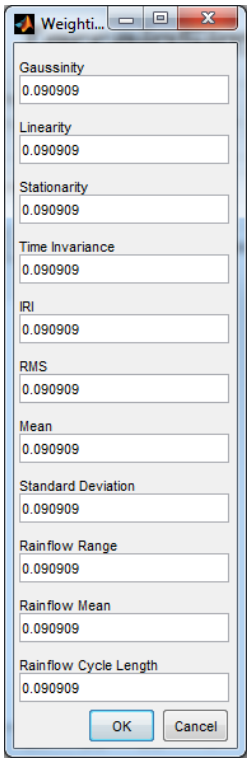

By default, all tests are weighted equally. The user may use any scale they wish to re-weight the tests and it will be normalized prior to analysis. Specifying a weighting of “0” for a particular test will tell *TerrainSim* to skip that test. This can be useful if the user is only interested in a few tests and wishes to save time.

After pressing the “Analyze” button, the command window will show updates of the progress. Analysis is done for every projection vector. The table contains the results of the analysis.

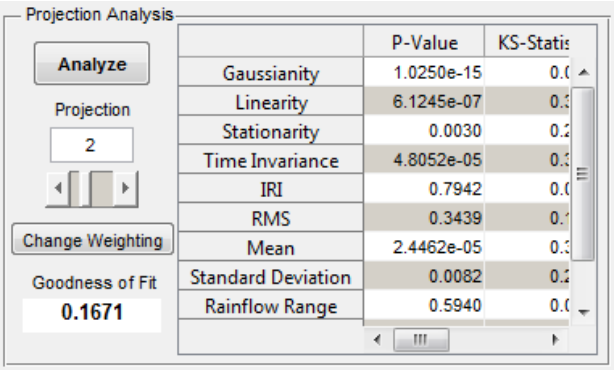

The user may switch between the results of each projection. The following fields are shown in the table:

1. P-Value – P-value from the comparison test used (2-Sample Kolmogorov-Smirnov)
2. Statistic – The statistic used to determine the p-value
3. Value Original – overall value calculated for the full original profile
4. Value Synthetic – overall value calculated for the full synthetic profile

C.10 Visualization

The final section of the user interface allows one to plot a variety of things regarding the original and synthesized surfaces, models, and statistics. The "Visualization" section is located on the lower left of the user interface.

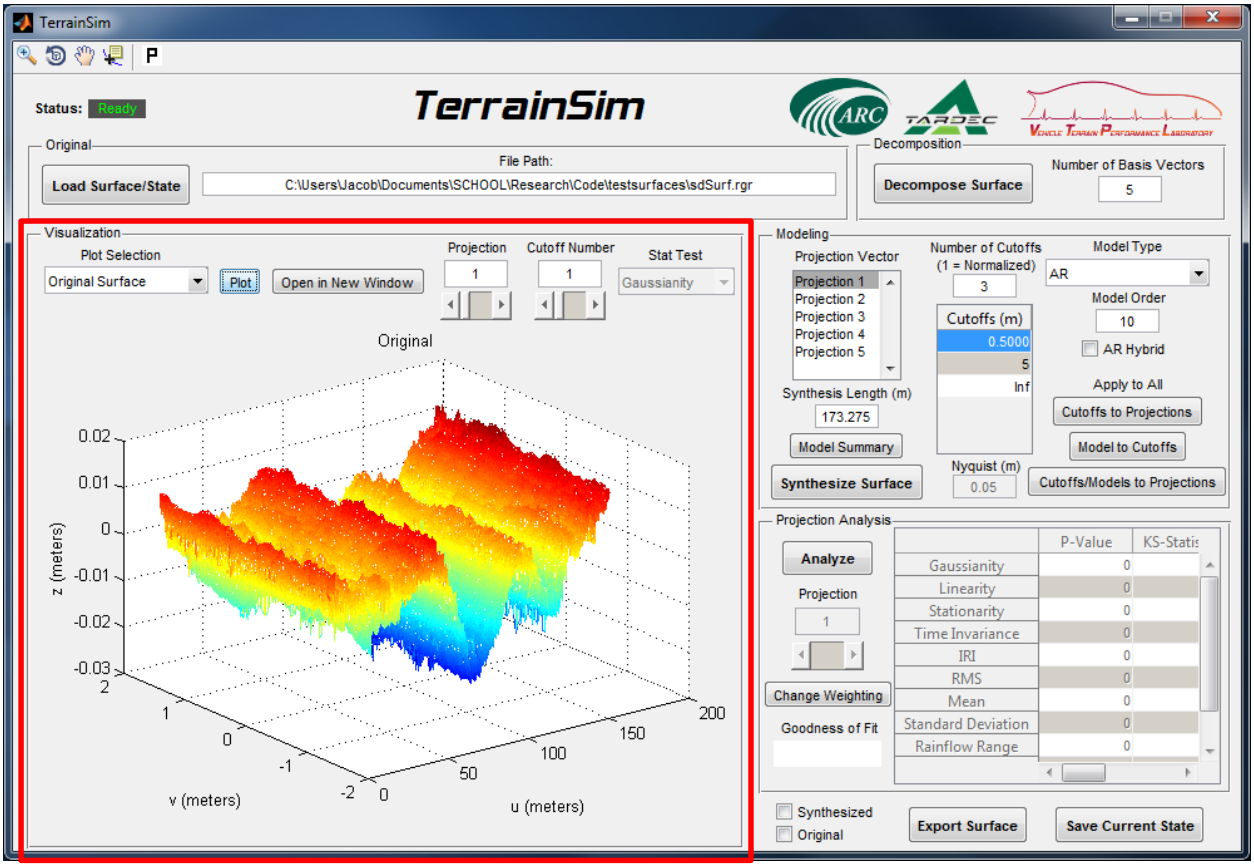

To create a plot, simply choose from the pull down menu located below the label "Plot Selection". There are many options for plotting.

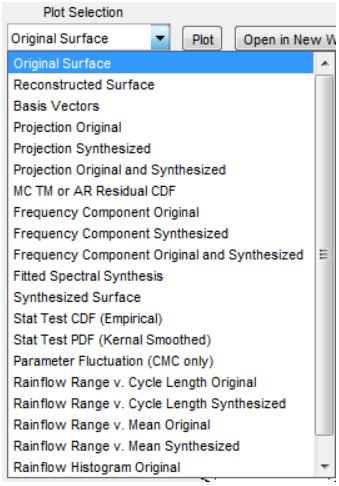

The different plot selections are:

1. Original Surface: The original surface loaded into *TerrainSim* for analysis and modeling. The surface is plotted on the axes z (height), v (lateral location), and u (longitudinal location). The absolute x and y positions of the surface are not plotted. The plot is a 3D mesh.

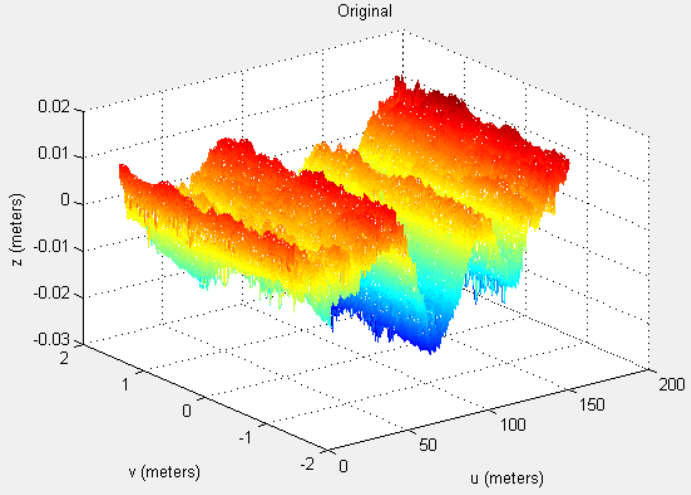

2. Reconstructed Surface – The surface estimate using principal component analysis applied in the "Decompose Surface" section. When the number of basis vectors is equal to the number of lateral points of the original surface, the reconstructed surface is identical.

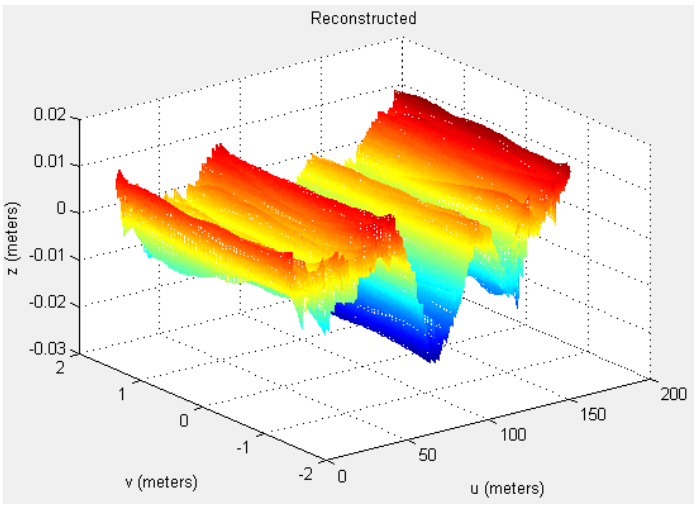

Basis Vectors – The basis vectors used in the principal component analysis. More information can be found in Section 4.2.4: Surface Creation and Decomposition.

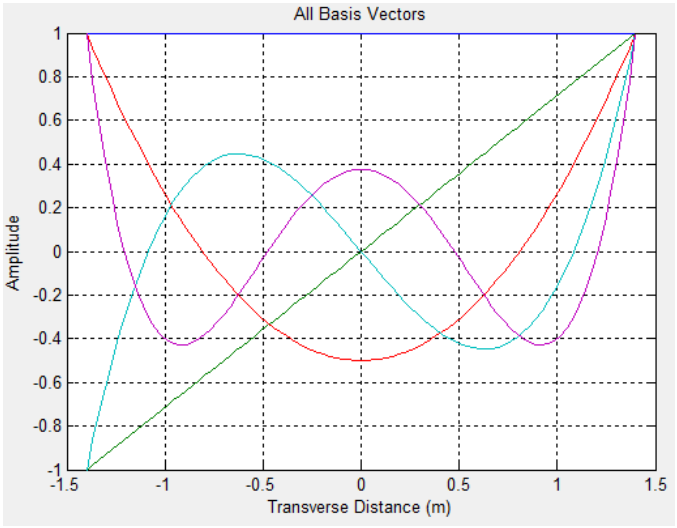

3. Projection Original – Projection vector extracted from the original surface. This is determined by the box labeled “Projection”.

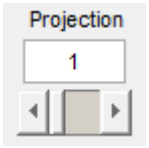

4. Projection Synthesized - Projection vector extracted from the synthesized surface. This is determined by the box labeled “Projection”.
5. Projection Original and Synthesized – Both projection vectors plotted on top of one another. This is determined by the box labeled “Projection”.

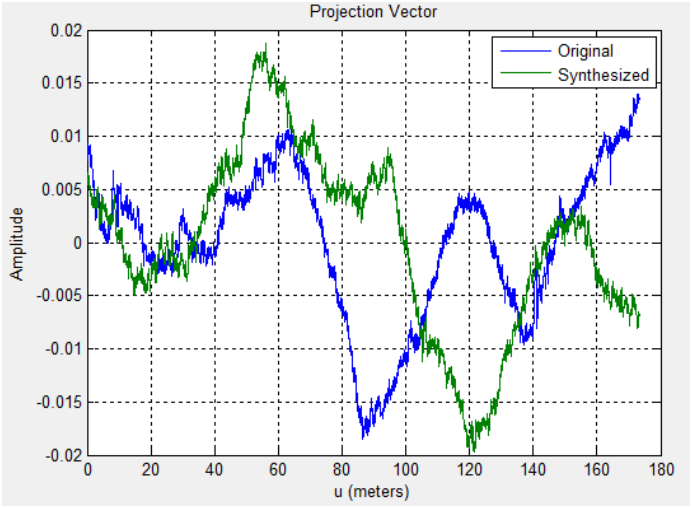

6. MC TM or AR Residual CDF – The characteristic curve of the synthesis method. This can be a number of things and is dependent on the boxes labeled "Projection" and "Cutoff Number".

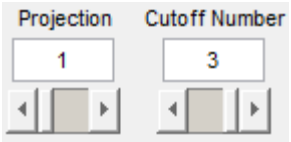

For an AR model, this curve is the empirical CDF of the residuals plotted alongside the continuous distribution fit.

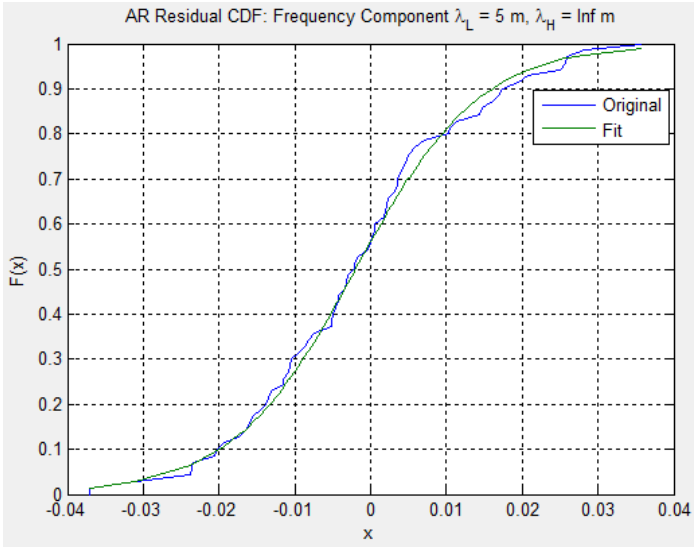

For a discrete-state Markov chain, the plot is a color-scaled image of the transition matrix characterizing the specified projection and cutoff number.

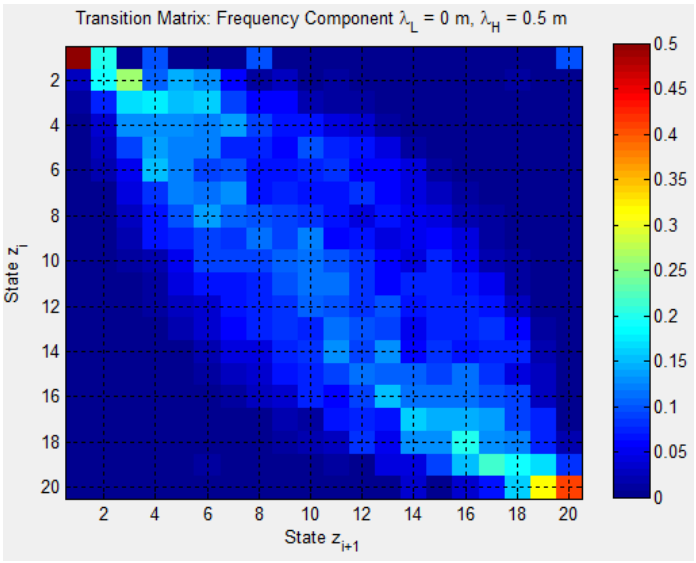

For a continuous-state Markov chain, the plot is a "CDF-Manifold" of the transition function characterizing the specified projection and cutoff number.

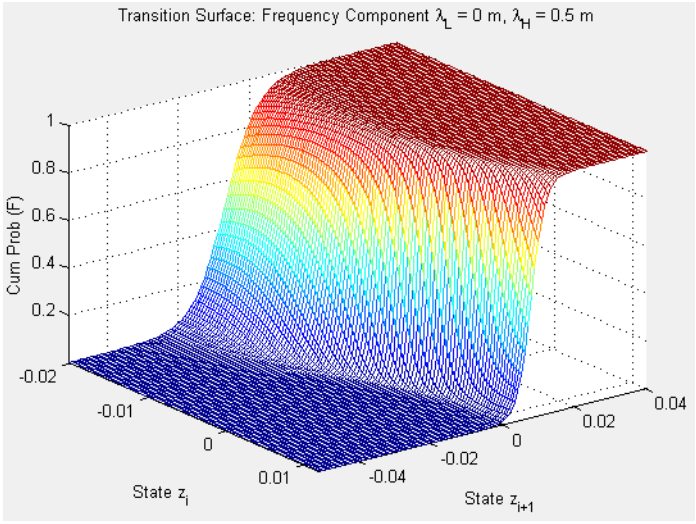

7. Frequency Component Original – The original frequency component signal specified by projection and cutoff number.
8. Frequency Component Synthesized – The synthesized frequency component signal specified by projection and cutoff number.
9. Frequency Component Original and Synthesized – The original and synthesized frequency component signals plotted against each other and specified by projection and cutoff number.

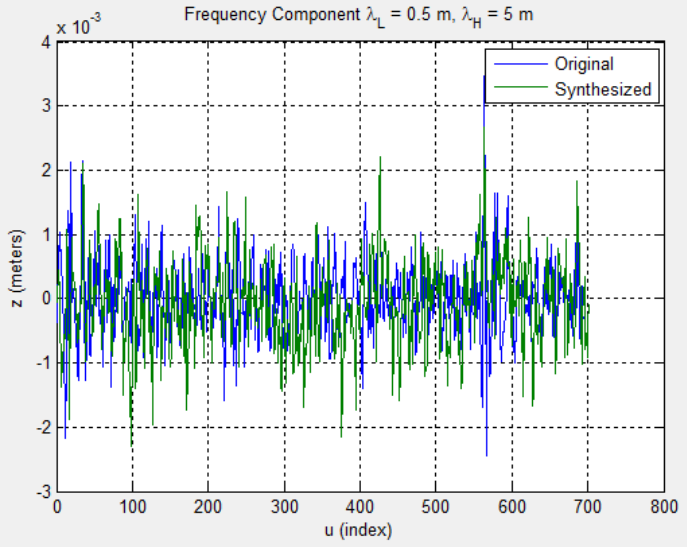

10. Fitted Spectral Synthesis – A collection of synthesized signals for each frequency bandwidth modeled. These signals are fitted using a cubic spline so that they are all at the same sample rate. Summing these signals together yields the full synthesized projection. This plot is dependent solely on projection selection.

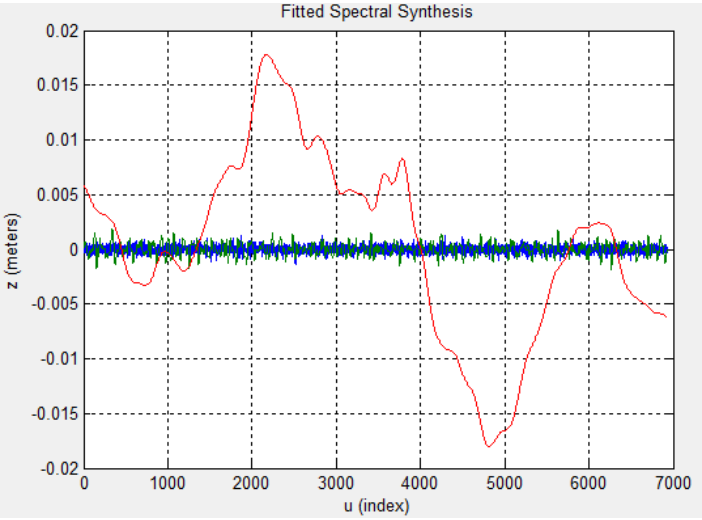

11. Synthesized Surface – The synthesized surface created from multiplying the synthesized projections by their respective basis vectors and summing. This is a 3D mesh.

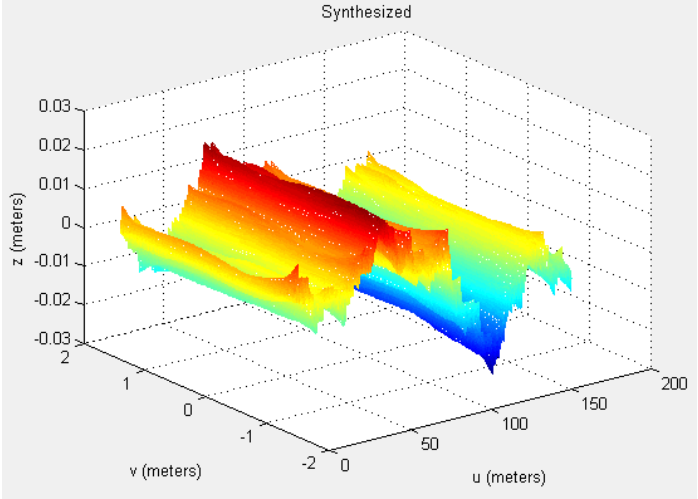

12. Stat Test CDF (Empirical) – Empirical CDF of the synthesized and original statistical test specified from the pull down box labeled “Stat Test”.

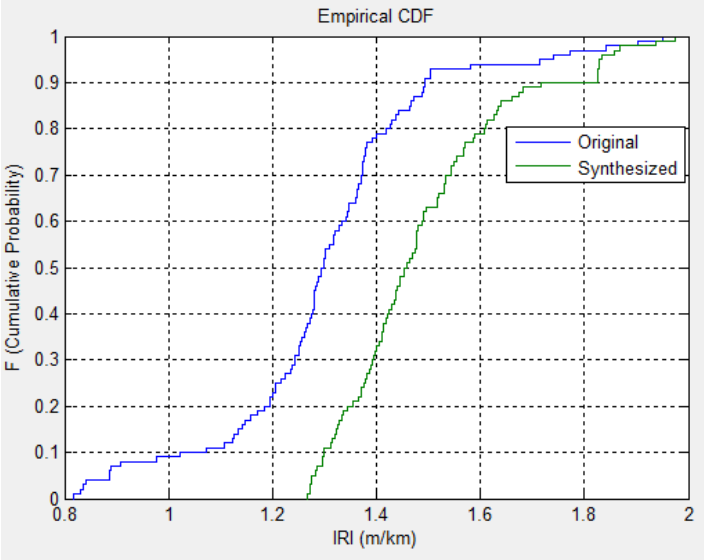

13. Stat Test PDF (Kernal Smoothed) – Empirical PDF estimate of the synthesized and original statistical test specified from the pull down box labeled “Stat Test”. The PDF is created using the non-parametric KS density estimate.

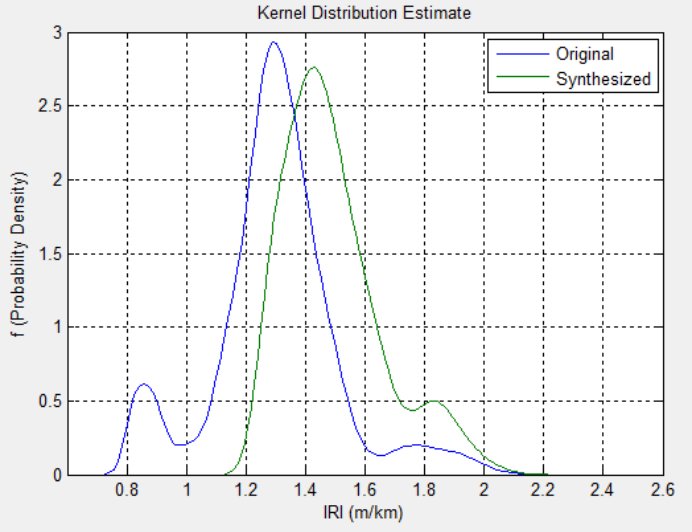

14. Parameter Fluctuation (CMC Only) – Plot of the polynomials used to estimate the location and scale parameters of the continuous-state Markov chain as a function of the initial state. This is dependent on projection and cutoff number.

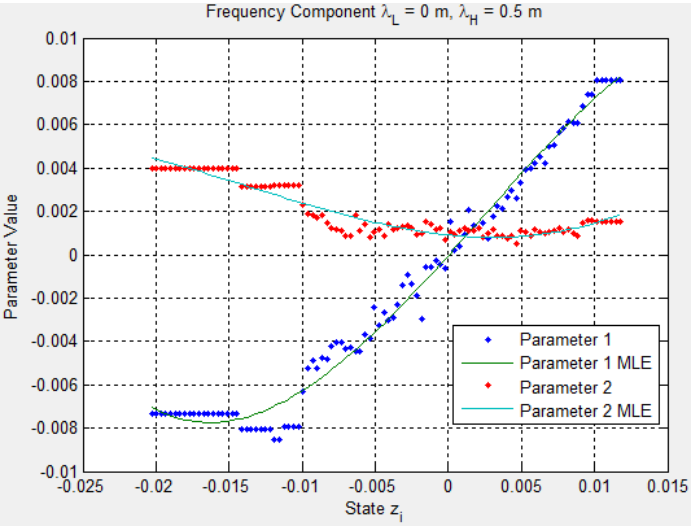

15. Rainflow Range v. Cycle Length Original – Contour plot of the joint probability mass function (PMF) between rainflow range and cycle length of the original profile. This is dependent on projection.

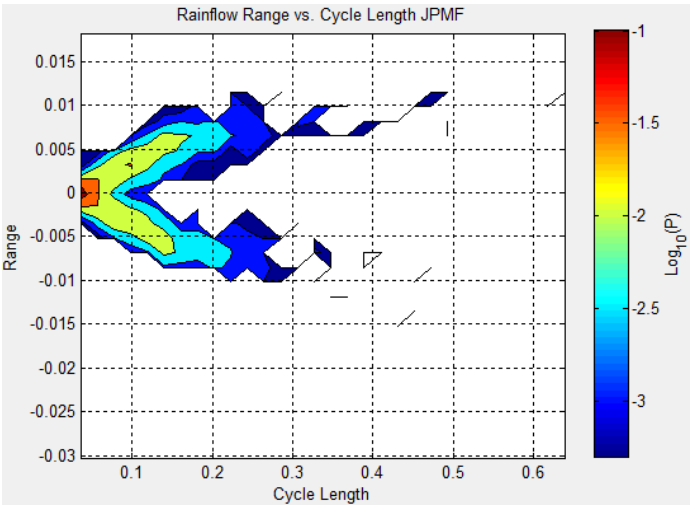

16. Rainflow Range v. Cycle Length Synthesized – Contour plot of the joint probability mass function (PMF) between rainflow range and cycle length of the synthesized profile. This is dependent on projection.
17. Rainflow Range v. Mean Original – Contour plot of the joint probability mass function (PMF) between rainflow range and mean of the original profile. This is dependent on projection.

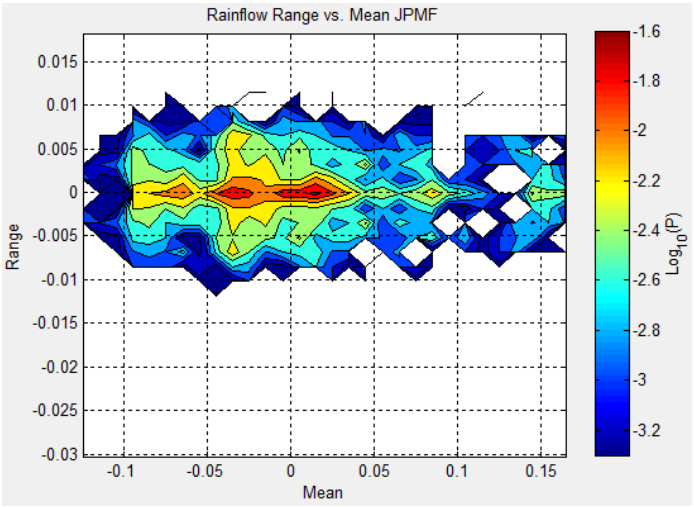

18. Rainflow Range v. Mean Synthesized – Contour plot of the joint probability mass function (PMF) between rainflow range and mean of the synthesized profile. This is dependent on projection.
19. Rainflow Histogram Original – Bar graph of the rainflow number of occurrences at different cycle locations for the original profile. The cycle locations are spaces at the segment length specified in the advanced settings. This is dependent on projection.

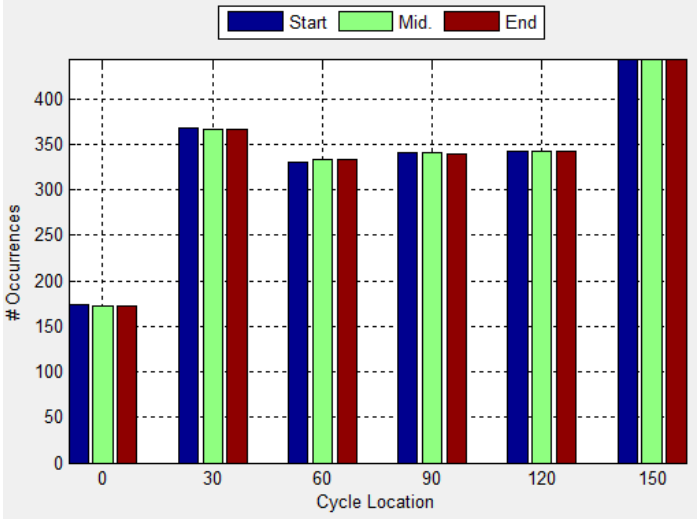

20. Rainflow Histogram Synthetic – Bar graph of the rainflow number of occurrences at different cycle locations for the synthetic profile. The cycle locations are spaces at the segment length specified in the advanced settings. This is dependent on projection.

Pressing the button labeled “Open in New Window” will extract whatever is currently plotted and put it on its own individual window. This is useful to obtain additional options, plot multiple things at once, or save the plot for future use.

Finally, the plots may be modified within the user interface using plot tools located on the far upper left of the user interface.

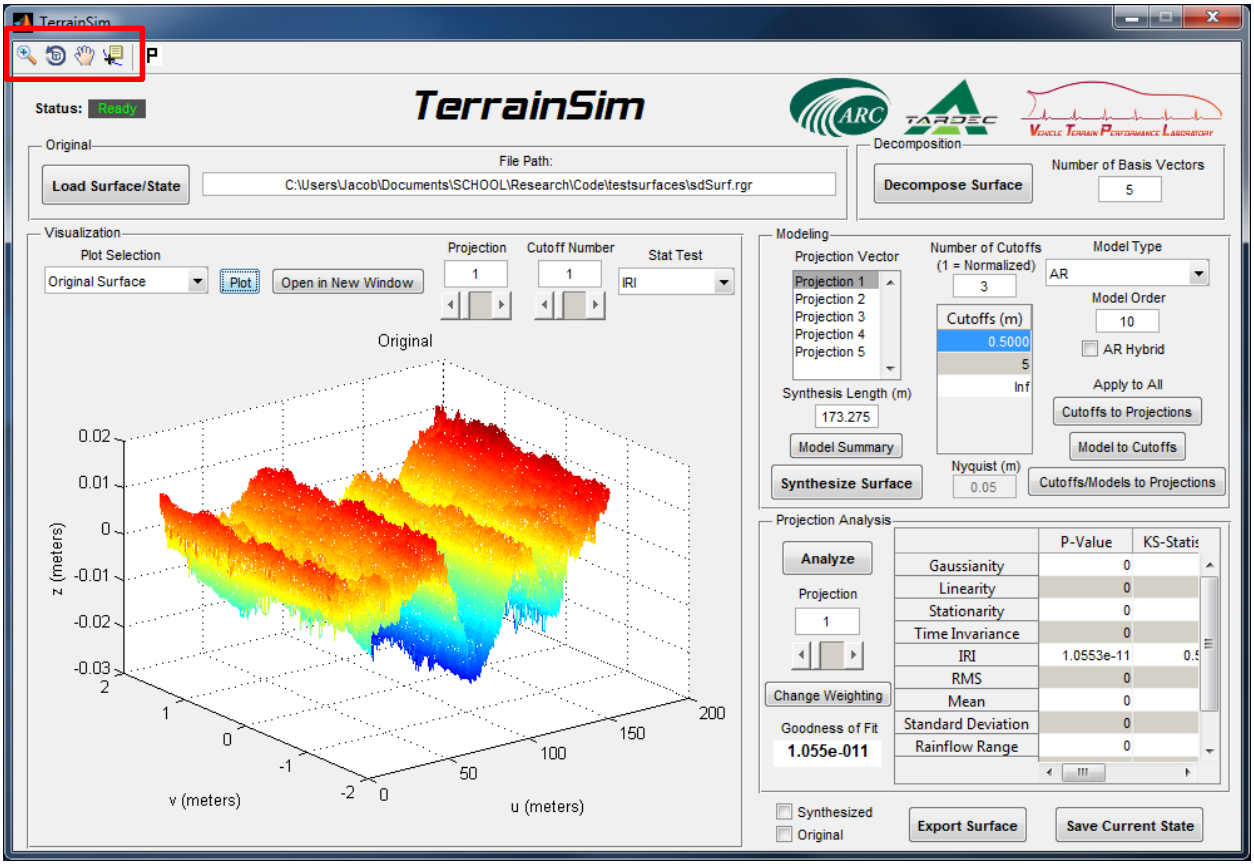

C.11 Advanced Settings

A dialog box containing a list of miscellaneous advanced settings can be modified by pressing the “P” button on the toolbar.

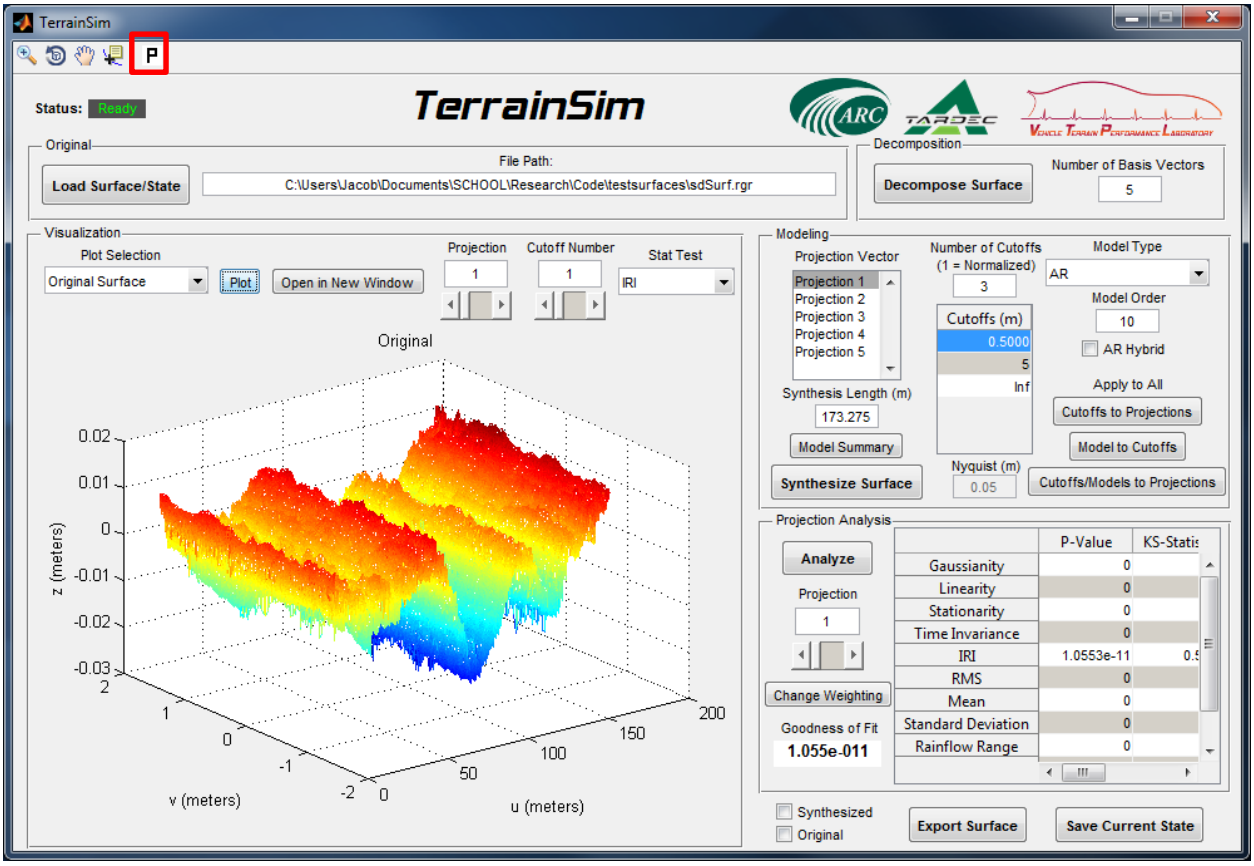

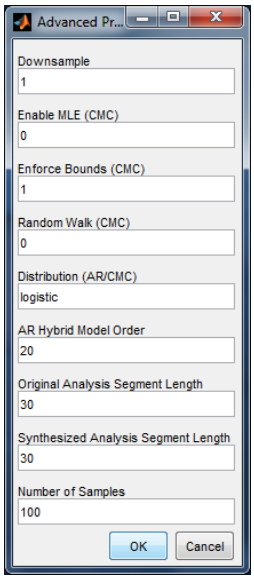

The following properties/settings can be changed:

1. Downsample – A logical specifying whether to strategically downsample during spectral decomposition. By default, this is "1". Skipping downsampling is not recommended; however, it may be useful if the user wishes to avoid any cubic spline fitting. Note: if

"Downsample" is disabled and a normalized cutoff frequency is used, the total number of cutoffs will still be determined using a downsample estimate.

2. Enable MLE (CMC) – A logical specifying whether to refine the coefficients of the continuous state Markov chain with MLE. Disabling this may improve stability and increase modeling speed in some scenarios.
3. Enforce Bounds (CMC) – A logical specifying whether to limit the synthesized results to the maximum and minimum of the measured signals. If enabled and a synthesized point lies outside these bounds, it is replaced with the boundary.
4. Random Walk (CMC) – A logical specifying whether to model the transition function as the probability of the transitions between states given the current state, or the probability of the transitions difference (jump) given the current state. In some scenarios, this may improve stability of the CMC.
5. Distribution (AR/CMC) – A string specifying the distribution used for the CMC or the AR residuals. The following distributions are available for use in *TerrainSim*: "logistic", "normal"/"norm", "laplace", "cauchy", "generalized extreme value"/"gev", and "tlocationscale". Generalized extreme value and t-location scale are 3 parameter distributions (location, scale, and shape). The others are 2 parameter distributions (location and scale).
6. AR Hybrid Model Order – The model order used for the "AR Hybrid" modeling option. This is the model order used for an initial AR model of a projection, while the residuals are modeled using separate model types and spectral decomposition (the residuals are not assumed to be i.i.d.).
7. Original Analysis Segment Length – The segment width used for statistical analysis of original profiles with bootstrapping.
8. Synthesized Analysis Segment Length – The segment width used for statistical analysis of synthesized profiles with bootstrapping.
9. Number of Samples – Number of random segments taken for the statistical analysis of the profiles. A higher number of samples will create a smoother CDF estimate.

C.12 Export Surfaces

Both the original and synthesized surfaces can be exported in a variety of formats. This can be done by using the "Export Surface" section in the lower right of the user interface.

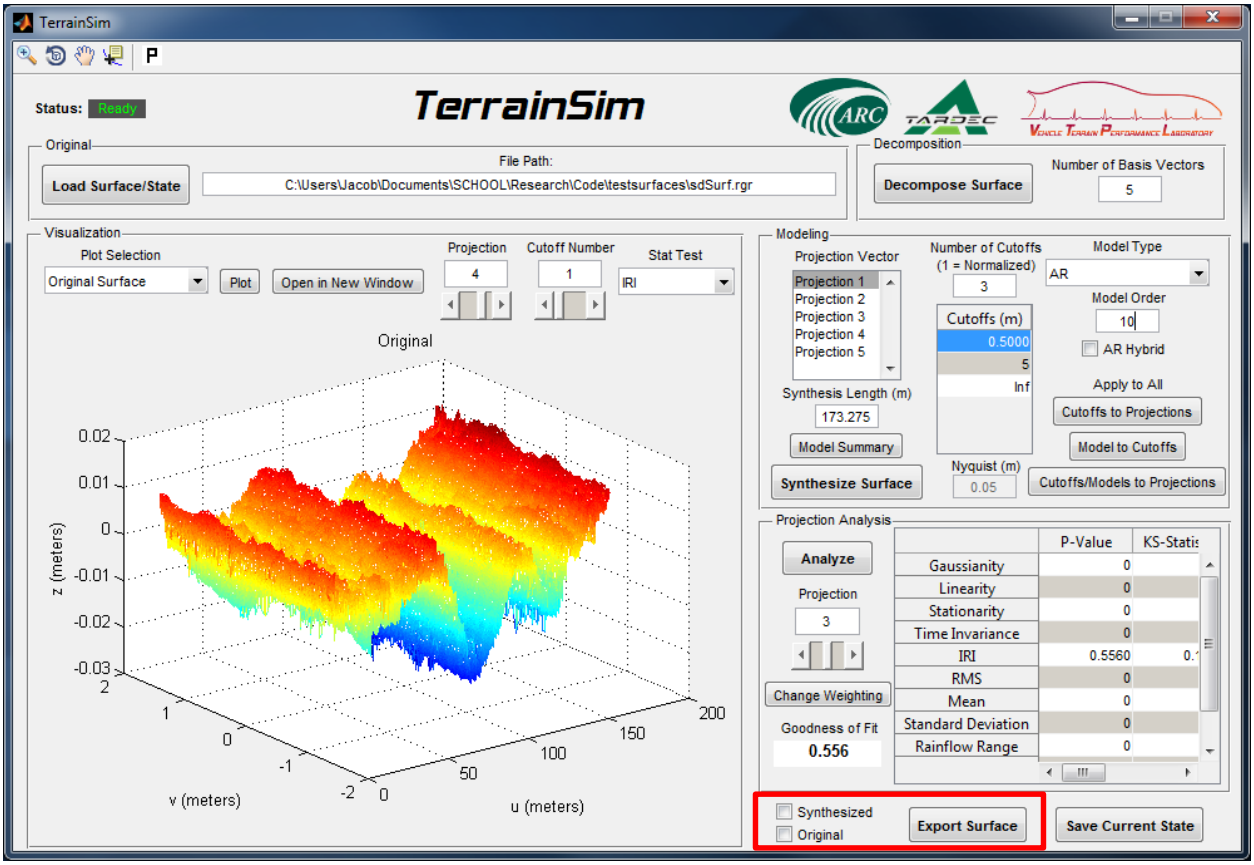

To export a surface, first click the check box of the desired surface to export, either “Original” or “Synthesized”. Next, press the “Export Surface” button to export the surface. A dialog box allowing the user to change the filename will appear, and the exported surface will be saved in the format specified. If .rgr is requested, and there are path points present in the original profile, an accompanying .rdf file will also be creating. The .rdf file contains the global path points of the center of the road. Similarly, a .crg file will only contain path information if it was present in the original surface.

C.13 Save Current State

The user can save the state of the current *TerrainSim* session by pressing the “Save Current State” button located on the bottom right of the user interface.

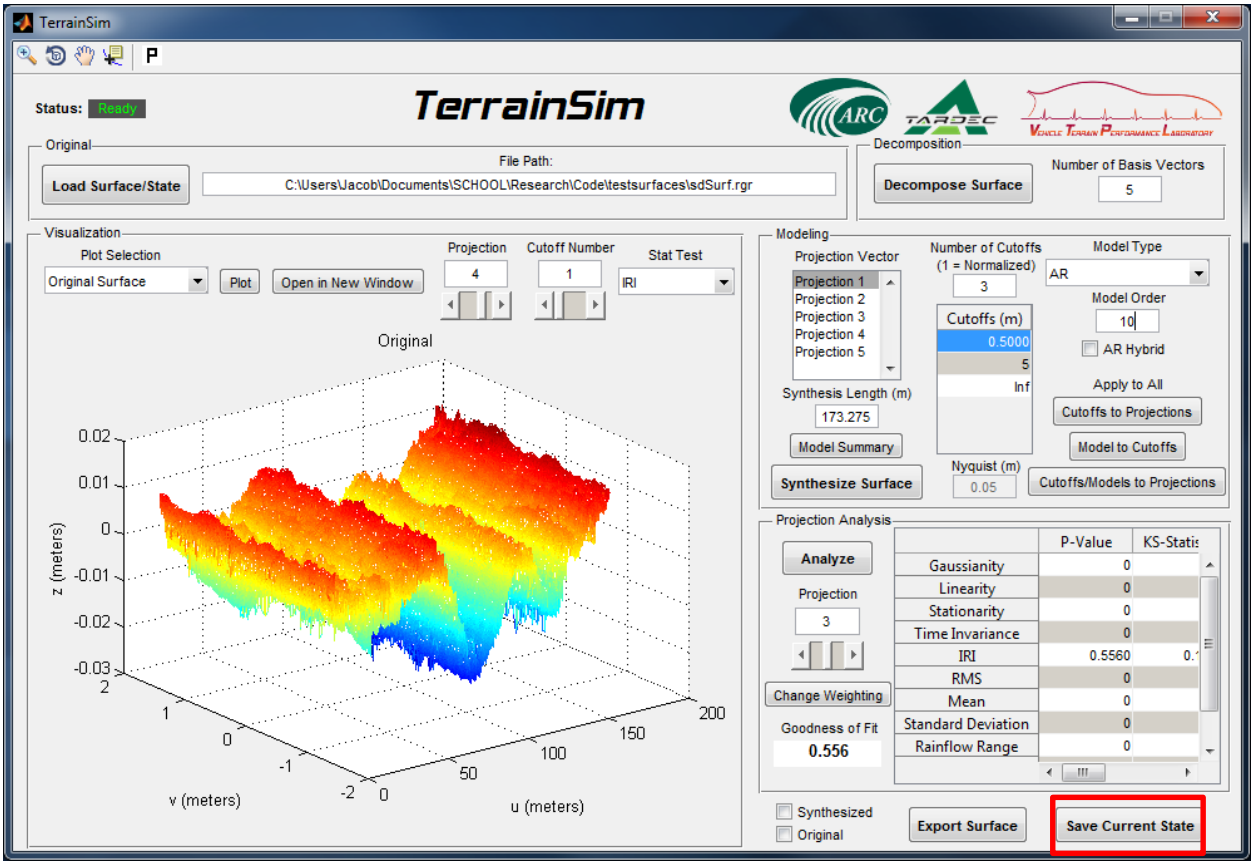

Pressing this button will save a *TerrainSim* state structure as a .tss file containing all of the information from the current session's modeling, synthesis and analysis. Loading this file back into *TerrainSim* will resume the exact state of the current session.